TKK Dissertations 229
Espoo 2010

DATA-BASED FAULT-TOLERANT MODEL PREDICTIVE CONTROLLER: AN APPLICATION TO A COMPLEX DEAROMATIZATION PROCESS

Doctoral Dissertation

Markus Kettunen

Aalto University
School of Science and Technology
Faculty of Chemistry and Materials Sciences
Department of Biotechnology and Chemical Technology

TKK Dissertations 229
Espoo 2010

DATA-BASED FAULT-TOLERANT MODEL PREDICTIVE CONTROLLER: AN APPLICATION TO A COMPLEX DEAROMATIZATION PROCESS

Doctoral Dissertation

Markus Kettunen

Doctoral dissertation for the degree of Doctor of Science in Technology to be presented with due permission of the Faculty of Chemistry and Materials Sciences for public examination and debate in Auditorium KE2 (Komppa Auditorium) at the Aalto University School of Science and Technology (Espoo, Finland) on the 17th of December 2010 at 14 o'clock.

Aalto University
School of Science and Technology
Faculty of Chemistry and Materials Sciences
Department of Biotechnology and Chemical Technology

Aalto-yliopisto
Teknillinen korkeakoulu
Kemian ja materiaalitieteiden tiedekunta
Biotekniikan ja kemian tekniikan laitos

Distribution:
Aalto University
School of Science and Technology
Faculty of Chemistry and Materials Sciences
Department of Biotechnology and Chemical Technology
P.O. Box 16100 (Kemistintie 1)
FI - 00076 Aalto
FINLAND
URL: http://chemtech.tkk.fi/
Tel. +358-9-47001
E-mail: chemat@tkk.fi

ISBN 978-952-60-3200-9
ISBN 978-952-60-3201-6 (PDF)
ISSN 1795-2239
ISSN 1795-4584 (PDF)
URL: http://lib.tkk.fi/Diss/2010/isbn9789526032016/

TKK-DISS-2771

Multiprint Oy
Espoo 2010

Aalto University

ABSTRACT OF DOCTORAL DISSERTATION	AALTO UNIVERSITY SCHOOL OF SCIENCE AND TECHNOLOGY P.O. BOX 11000, FI-00076 AALTO http://www.aalto.fi

Author Markus Kettunen

Name of the dissertation
Data-based fault-tolerant model predictive control: an application to a complex dearomatization process

Manuscript submitted 22.3.2010	Manuscript revised 15.11.2010

Date of the defence 17.12.2010

☒ Monograph ☐ Article dissertation (summary + original articles)

Faculty	Faculty of Chemistry and Material Science
Department	Department of Biotechnology and Chemical Technology
Field of research	Process control
Opponent(s)	Prof. Ruth Bars, Prof. Bernt Lie
Supervisor	Prof. Sirkka-Liisa Jämsä-Jounela
Instructor	Prof. Sirkka-Liisa Jämsä-Jounela

Abstract

The tightening global competition during the last few decades has been the driving force for the optimisation of industrial plant operations through the use of advanced control methods, such as model predictive control (MPC). As the occurrence of faults in the process measurements and actuators has become more common due to the increase in the complexity of the control systems, the need for fault-tolerant control (FTC) to prevent the degradation of the controller performance, and therefore the better optimisation of the plant operations, has increased. Traditionally, the most actively studied fault detection and diagnosis (FDD) components of the FTC strategies have been based on model-based approaches. In the modern process industries, however, there is a need for the data-based FDD components due to the complexity and limited availability of mechanistic models. Recently, active FTC strategies using fault accommodation and controller reconfiguration have become popular due to the increased computation capacity, easier adaptability and lower overall implementation costs of the active FTC strategies.

The main focus of this thesis is on the development of an active data-based fault-tolerant MPC (FTMPC) for an industrial dearomatization process. Three different parallel-running FTC strategies are developed that utilise the data-based FDD methods and the fault accommodation- and controller reconfiguration-based FTC methods. The performances of three data-based FDD methods are first compared within an acknowledged testing environment. Based on the preliminary performance testing, the best FDD method is selected for the final FTMPC. Next, the performance of the FTMPC is validated with the simulation model of the industrial dearomatization process and finally, the profitability of the FTMPC is evaluated based on the results of the evaluation.

According to the testing, the FTMPC performs efficiently and detects and prevents the effects of the most common faults in the analyser, flow and temperature measurements, and the controller actuators. The reliability of the MPC is increased and the profitability of the dearomatization process is enhanced due to the lower off-spec production.

Keywords Fault-tolerant control, model predictive control, oil refining control application, industrial dearomatization process

ISBN (printed) 978-952-60-3200-9	ISSN (printed) 1795-2239
ISBN (pdf) 978-952-60-3201-6	ISSN (pdf) 1795-4584
Language English	Number of pages 180+12

Publisher Aalto University, School of Science and Technology, Department of Biotechnology and Chemical Technology

Print distribution Aalto University, School of Science and Technology, Department of Biotechnology and Chemical Technology

☒ The dissertation can be read at http://lib.tkk.fi/Diss/2010/isbn9789526032016/

Aalto-yliopisto

VÄITÖSKIRJAN TIIVISTELMÄ	AALTO-YLIOPISTO TEKNILLINEN KORKEAKOULU PL 11000, 00076 AALTO http://www.aalto.fi
Tekijä Markus Kettunen	
Väitöskirjan nimi Vikasietoisen säätöstrategian kehittäminen ja käyttö teollisen aromaattienpoistoprosessin ohjauksessa	
Käsikirjoituksen päivämäärä 22.3.2010	Korjatun käsikirjoituksen päivämäärä 15.11.2010
Väitöstilaisuuden ajankohta 17.12.2010	
☒ Monografia	☐ Yhdistelmäväitöskirja (yhteenveto + erillisartikkelit)
Tiedekunta Kemian ja materiaalitekniikan tiedekunta Laitos Biotekniikan ja kemian tekniikan laitos Tutkimusala Prosessien ohjaus Vastaväittäjä(t) Prof. Ruth Bars, Prof. Bernt Lie Työn valvoja Prof. Sirkka-Liisa Jämsä-Jounela Työn ohjaaja Prof. Sirkka-Liisa Jämsä-Jounela	

Tiivistelmä

Maailmanlaajuisen kilpailun kiristyessä teollisten prosessien optimointiin on kiinnitetty yhä enemmän huomiota. Ylemmän tason säädöt, kuten mallipredikti ivinen säätö (MPC) on kasvattanut suosiotaan erityisesti prosesseissa, jossa tarvitaan optimaalista ohjausta. Säätö- ja automaatiojärjestelmien monimutkaisuuden kasvaessa järjestelmien komponentti- ja laiteviat ovat kuitenkin lisääntyneet. Viat ja prosessihäiriöt aiheuttavat säätimien suorituskyvyn laskua, mikä pyritään estämään käyttämällä esimerkiksi vikasietoista säätöä (FTC). Aktiivinen vikasietoinen säätö on perinteisesti toteutettu käyttämällä mallipohjaisia vianhavainnointijärjestelmiä (FDD), mutta yksityiskohtaisten dynaamisten mallien puuttuessa tilastollisten FDD-menetelmien suosio on kasvanut. Aktiivisten viankorjausmenetelmien, kuten vikakompensoinnin ja säätimen uudelleenkonfiguroinnin, käyttö prosessiteollisuudessa onkin lisääntynyt etenkin kasvaneen laskenta- ja tallennuskapasiteetin, paremman soveltuvuuden ja alentuneiden järjestelmien asennuskustannusten myötä.

Väitöskirjan tavoitteena on kehittää tilastollisiin vikahavainnointimenetelmiin perustuva aktiivinen vikasietoinen mallipredikti ivinen säädin teollisen aromaattienpoistoprosessin säätämiseen. Työssä on kehitetty kolme erilaista tilastollisiin FDD-menetelmiin, vikakompensointiin sekä säätimen uudelleenkonfigurointiin perustuvaa strategiaa. Kolmen tilastollisen FDD-menetelmän tehokkuutta on ensin arvioitu tunnetussa testiympäristössä, jonka jälkeen tehokkain FDD-menetelmä on valittu lopulliseen sovellukseen ja kaikkien kolmen FTC-strategian tehokkuutta on testattu teollisen aromaattienpoistoprosessin simulointimallilla. Lopuksi testauksen tulosten perusteella on arvioitu vikasietoisen mallipredikti ivisen säätimen taloudellista kannattavuutta.

Kehitetty vikasietoinen mallipredikti ivinen säädin toimii tehokkaasti ja pystyy selvästi pienentämään vikojen vaikutuksia analysaattoreissa, virtausmittauksissa, lämpötilamittauksissa sekä säätöventtiileissä. Myös teollisen aromaattienpoistoprosessin säädön luotettavuus paranee, hävikkituotteen määrä vähenee sekä prosessin kannattavuus lisääntyy vikojen vaikutusten pienentyessä.

Asiasanat	vikasietoinen säätö, mallipredikti ivinen säätö, öljynjalostusteollisuuden säätösovellus, teollinen aromaattienpoistoprosessi		
ISBN (painettu)	978-952-60-3200-9	ISSN (painettu)	1795-2239
ISBN (pdf)	978-952-60-3201-6	ISSN (pdf)	1795-4584
Kieli	Englanti	Sivumäärä	180+12
Julkaisija	Aalto-yliopiston teknillinen korkeakoulu, Biotekniikan ja kemian tekniikan laitos		
Painetun väitöskirjan jakelu	Aalto-yliopiston teknillinen korkeakoulu, Biotekniikan ja kemian tekniikan laitos		
☒ Luettavissa verkossa osoitteessa http://lib.tkk.fi/Diss/2010/isbn9789526032016/			

Preface

The research work presented in this thesis was carried out at the Laboratory of Process Control and Automation at Aalto University of Science and Technology. The author originally started the research work on the fault-tolerant MPC within the networked control systems tolerant to faults (NeCST, EU IST-2004-004303) project that ended in 2007. The author has worked as a researcher in the laboratory during 2006 - 2007; as a process engineer at the Naantali refinery owned by Neste Oil Oyj during 2007 - 2009; and as a specialist in production planning models at Neste Oil Oyj main offices from 2010. During 04/2006 - 04/2007 and 10/2008 - 12/2008, the research work of the author was funded in a project financed by Academy of Finland, and during 01/2009 - 02/2009 by an Academy of Finland scholarship.

I would like to express my gratitude to my supervisor Professor Sirkka-Liisa Jämsä-Jounela, who has encouraged and guided me, kept the quality of the thesis high and provided me with the opportunity to finish my thesis on time. Her comprehensive academic knowledge has been invaluable both in the research work and in writing the thesis. In addition, thanks also go to Professor Raimo Ylinen for his excellent professional advice and to Alexey Zakharov for his valuable help in the final stages of this thesis.

I would also like to thank the pre-examiners of the thesis: Professor Ruth Bars from the Budapest University of Technology and Economics and D.Sc. (Tech.) Jenő Kovács from the University of Oulu for their thorough pre-examination of this thesis and helpful comments and remarks.

I wish to thank Neste Oil Oyj and Kimmo Koskihaara, my former supervisor and production manager at the Naantali refinery, and Markko Rajatora, my current supervisor and the manager of the decision support model group at the Espoo offices. They and Neste Oil Oyj have made it possible for me to write and finish the thesis during my employment from 2007 - 2010. I would also like to thank Jyri Lindholm, automation division manager at Neste Jacobs Oy and Mikko Vermasvuori, design engineer in the automation division at Neste Jacobs Oy for their expert comments on the empirical part of the thesis. Also thanks go to my former and current colleagues, both in Aalto University and in Neste Oil Oyj, for their excellent support and many encouraging discussions.

I would also like to thank my parents Päivi and Ensio Kettunen for their continuous support over the years.

And finally, my love and greatest gratitude goes to my wife, Heidi Kettunen, who has supported and encouraged me during the entire writing process and, in the end, made it possible for me to finish the thesis.

Espoo, 15.11.2010

Markus Kettunen

Contents

List of abbreviations

AFTCS	Active fault-tolerant control strategy
BP	Bottom product
CA	Control allocation
CSTH	Continuous stirred tank heater
CSTR	Continuous stirred tank reactor
CV	Controlled variable
DCP	Daisy-chaining principle
DISSIM	Monitoring method based on dissimilarity
DMC	Dynamic matrix control
DV	Disturbance variable
FCC	Fluid catalytic cracking
FDD	Fault detection and diagnosis
FDI	Fault detection and isolation/identification
FOPTD	First order plus time delay
FP	Flashpoint
FTC	Fault-tolerant control/controller
FTCS	Fault-tolerant control strategy
FTMPC	Fault-tolerant MPC

GIMC	Generalised internal model control / controller
GLR	Generalised likelihood ratio
GPC	Generalised predictive control / controller
GUI	Graphical user interface
IBP	Initial boiling point
ICA	Independent component analysis
ISS	Input-to-state stability
I/O	Input and output
IMM	Interacting multiple model
LARPO	Solvent dearomatization process, in Finnish ‘Liuottimien aromaattien poisto’
LMI	Linear matrix inequality
LPV	Linear parameter varying
LQG	Linear quadratic gaussian
LTI	Linear time invariant
LV	Latent variable
MIMO	Multi-input and multi-output
MMAE/MMAC	Moving-bank multiple model adaptive estimation and control
MPC	Model predictive control / controller
MV	Manipulated variable

NIPALS	Nonlinear iterative partial least squares
NLP	Nonlinear programming
NMPC	Nonlinear model predictive control /controller
PCA	Principal component analysis
PLS	Partial least squares / projection to latent structures
PWL	Piecewise linear
QDMC	Quadratic dynamic matrix control / controller
RHC	Receding horizon control / controller
RLQR	Robust linear quadratic regulator
RMPC	Robust model predictive control / controller
RMSE	Root mean square error
RMSEP	Root mean square error of prediction
SCP	Shell control problem
SIMPLS	Simple partial least squares
SISO	Single input and single output
SMI	Subspace model identification
SPE	Squared prediction error
SSMPC	State-space MPC

List of symbols

Greek alphabet

α	User-defined confidence level for the Hotelling T^2 calculations
ΔA	Parametric state fault matrix of the state space model
ΔB	Parametric input fault matrix of the state space model
ΔC	Parametric output fault matrix of the state space model
Δd	Residual between the predicted d and the measured d
Δu	Residual between the predicted u and the measured u
Δv	Residual between the predicted v and the measured v
Δy	Residual between the predicted y and the measured y
Λ	Eigenvalue matrix
λ	Eigenvalue
χ	Matrix composed of all the past input and output values and the future input values

Latin alphabet

A	State matrix of the state space model
B	Input matrix of the state space model
C	Output matrix of the state space model
$c_{i,t}$	Value of the fault probability counter for the ith diagonal entry at the time step t
c_α	Value of the normal density distribution

$c_{i,max}$ Maximum limit for the fault probability counter i for engaging the FTC actions

$c_{i,min}$ Minimum limit for the fault probability counter i for engaging the FTC actions

CV Variable determination matrix for the controlled variables

D Feed through matrix of the state space model

D_0 Process disturbance operating point

d Disturbance measurement

d_{est} Estimated value of d

d_f Faulty disturbance measurement

d_{norm} Normalised value of d at the operating point D_0

d_{past} Past values of d

DV Variable determination matrix for the measured disturbances

E Disturbance matrix of the state space model

F Probability on the F distribution / Fault detection index

F_{lim} Fault detection index limit

F_u Input fault matrix of the state space model

F_y Output fault matrix of the state space model

f_i Fault diagnosis information for the FTC strategy i

f_d Disturbance fault

f_u Input fault

f_y Output fault

K Gain matrix

k Number of the selected principal components / Number of the current time step in discrete calculations

L Matrix for controlling the accommodation of v_f

m Number of the measurements / Length of the MPC control horizon / Number of the variables in PCA training data / Number of the inputs in SMI

MV Variable determination matrix for the manipulated variables

N Number of the observations for Hotelling T^2

n Number of the test data set samples / Number of the SMI outputs

P Matrix for controlling the accommodation of u_f / PLS loading vector for the inputs X

p Length of the MPC prediction horizon

P_0 Weight for the predicted output

P_K Selected k first principal components

Q PLS loadings of the outputs Y / Weight for the predicted output

Q_α Detection threshold for the squared prediction error

Q_p Squared prediction error value

R Estimation matrix / Input weighting matrix

R_{PLS} PLS regression matrix

T PLS score vector for the input values of X

t Current *v*alue of the time vector

T^2 Hotelling T^2 index value

U PLS score vector for the outputs Y

U_0 Process input operating point

u Input measurement

u_{est} Estimated value of u

u_f Faulty input

u_{MV} Selected control inputs for an MPC

u_{norm} Normalised value of u at the operating point U_0

u_{past} Past values of u

u_{ref} Reference input from an MPC to a sub-level controller

V Reference signal multiplication matrix

V_0 Auxiliary variable representing Y_0, U_0 or D_0

v Auxiliary variable representing y, u or d

v_{est} Estimated value of y, u or d

$v_{norm,PLS}$ Normalised value of y, u or d for the PLS

W PLS weight matrix of the input matrix X

w Window size for the moving average filter

X FDD input matrix / System state (in the SMI calculations)

X^+ Matrix X without the first row (in the SMI calculations)

X^- Matrix X without the last row (in the SMI calculations)

$\hat{x}$ Predicted measurement values in PCA

x_{scaled} Current autoscaled measurement values in PCA

x_{start} Value of x during the time step $k = 0$

Y_0 Operating point of the process output

Y_t Response between the input u and the output y

y Output of a system

y_{CV+DV} CV and DV measurements in a same vector

y_{CV} Selected controlled variables for MPC

y_{DV} Selected measured disturbance values for MPC

y_f Faulty output

y_{est} Estimated output

y_{norm} Normalised value of y at the operating point Y_0

y_{past} Past values of y

y_r Reference of the controlled variables

Z Future values of the outputs Y

List of figures

List of tables

1 Introduction

1.1 Background

Tightened global competition, higher product quality requirements and environmental and safety regulations have forced the oil refining industry to continuously enhance and optimise the efficiency and profitability of its process plants. Profitability can generally be enhanced through process optimisation, by cutting down costs and by reducing the duration of planned and unplanned shutdowns. Optimisation can further be enhanced by focusing on preventing the off-spec production caused by faults and process disturbances.

The effect of faults and process disturbances on the process can be reduced by using fault-tolerant control (FTC) methods, which are categorised into passive and active approaches. Passive FTC aims at improving the robustness of the controller against faults and disturbances by modelling the effects of the faults and disturbances and taking these into account in the objective function of the model predictive controller (MPC). Active FTC, on the other hand, attempts to reduce the fault effects by using active FTC elements, which are, for instance, the fault detection and diagnosis (FDD) components for the detection, isolation and identification of faults, and the FTC methods carrying out active fault accommodation or controller reconfiguration actions to reduce the effects of faults.

Traditionally, most FDD methods used in the active FTC strategies have been based on mechanistic models. In the modern process industries, however, there is an increase in the demand for data-based methods that rely on models acquired experimentally with statistical mathematical algorithms. The increased interest in the data-based methods is due to the complexity of chemical processes and the limited availability of mechanistic models. The need for the automated FDD and FTC is further emphasised by Venkatasubramanian et al. (2003a), who found that roughly 70% of industrial accidents are caused by human error. It is also stated that more than USD 20 billion are lost annually in the North American oil refining industry alone due to the improper handling of abnormal situations. As a result, financial issues are the major driving force behind the continuous development of the data-based FDD and the active FTC strategies.

In addition to the FDD component, the controllers and the control algorithms are an important part of the FTC strategy. During the last few decades, the development of process control methods has been focused on MPC, which has become one of the most commonly used advanced control methods in the oil refining industry. The popularity of MPC has also been verified in the comprehensive MPC review by Qin and Badgwell (2003); in the milestone report concerning industrial applications by McAvoy et al. (2004); and in the general review of the current status and future needs of advanced control strategies by Bars et al. (2006). The advanced control methods, such as MPC, have made it possible to run the processes close to the quality and safety limits thereby increasing profitability, ensuring the better quality of the end products, and enhancing safety in the plants.

Reviews on the traditional MPC have been presented in numerous papers; for instance, Morari and Lee (1999) have looked at the past, present and future of MPC; Rawlings (2000) have presented a general overview of MPC, while Qin and Badgwell (2003) have examined MPC by describing the development of the industrial MPCs from simple optimisation algorithms to modern software packages. The current status of the nonlinear MPC has been reviewed by Cannon (2004); the survey of traditional robust MPC algorithms covering the period 1999-2006 has been published by Jalali and Nadimi (2006); and the latest advances in the field of nonlinear min–max-based robust MPC has been presented by Raimondo et al. (2009). What is evident from all of these reviews is that the number and popularity of improved MPC applications, such as nonlinear or robust MPCs, has increased over the years. However, some challenges related especially to nonlinear formulations of MPC and the reliability and stability issues caused by process faults and disturbances have still remained largely unresolved, even though a number of nonlinear and fault-tolerant MPC approaches have been presented in the past.

MPC's success and the remaining reliability issues have activated interest in the study of active, data-based, fault-tolerant control methods. The active fault-tolerant control methods have usually been categorised into fault accommodation-based and controller reconfiguration-based methods depending on how the effects of the faults on the target process are handled. The fault accommodation-based approaches usually modify the control strategy without changing the control structure itself, while the controller reconfiguration-based approaches attempt to enhance the plant operation by modifying both the control parameters and structure of the control strategy. The fault accommodation uses the adaptation of the controller to counter the effects of the faults by, for instance, accommodating the faulty measurements with the estimations of the measurements. The reconfiguration approach, on the other hand, attempts to use only the healthy part of the system for control by turning off the faulty parts, such as measurements or actuators. A number of review papers have been published in the active fault-tolerant MPC (FTMPC) area showing the research interest in the field. These papers include a general overview of fault-tolerant control by Blanke et al. (1997); a paper concentrating on the problem of supervision and FTC by Staroswiecki and Gehin (2001); and recently, a comprehensive review of active reconfigurable FTC by Zhang and Jiang (2008).

The development of FTC has been focused on only using the individual FTMPC components. The applications of the active fault-tolerant MPCs have been designed either for fault accommodation or controller reconfiguration, but not for both approaches. In the fault accommodation-based FTC strategies, the focus is in the prevention of sensor faults while in the controller reconfiguration-based strategies, the availability of a perfect FDD is assumed when the structure of the controller is reconfigured in case of actuator faults. In these cases, the FTC is thus able to detect and prevent only one type of fault instead of taking into account the full range of different faults appearing in industrial-scale processes. The combination of the fault accommodation and controller reconfiguration strategies in one application would possibly offer an opportunity to even further improve industrial FTMPCs, and thus also to significantly increase the profitability of the plants.

1.2 Research problem and hypothesis

The major research problem and the motivation for this thesis is to improve the control performance of an MPC controlling an industrial dearomatization process, the solvent dearomatization process unit, LARPO, an abbreviation from the Finnish term 'Liuottimien aromaattien poisto'. The dearomatization process is located in the Naantali refinery, Finland, and owned by Neste Oil Oyj. The performance improvement can be gained by diminishing the effect of sensor and actuator faults by utilising the active data-based FTC methods taking into account faults in the analyser, flow, temperature and pressure measurements, and in the actuators. The higher control performance increases the reliability and stability of the controller, decreases the off-spec production, and improves the target process profitability.

In order to develop the active FTMPC, a set of tasks needs to be accomplished. The main tasks in this doctoral thesis are to study, develop, implement, test and analyse the fault-tolerant control for the industrial dearomatization process. The effectiveness of the active data-based FTMPC is to be tested by studying the effects of different types of faults on the control performance of the FTMPC. The fault types to be tested are drift- and bias-shaped faults for analysers and sensors and a stuck valve fault for the control valves.

The hypotheses of the thesis are:

(1) The integration of the data-based FDD methods and the fault accommodation and the controller reconfiguration FTC methods provide the control system of a dearomatization process with the tools needed to overcome the typical process and measurement disturbances and faults in the dearomatization process environment.

(2) The availability and profitability of the dearomatization process are enhanced by the compensation of the critical faults using the fault accommodation and the controller reconfiguration FTC methods.

In order to prove the hypotheses, five tasks must be carried out:

1. Determine the target process requirements for the active data-based FTC strategy.

2. Determine the candidates for the active data-based FDD and FTC components, the design scheme and the structure for the FTMPC.

3. Compare data-based FDD components within a preliminary testing environment and select the best suitable FDD component for the FTMPC

4. Validate the performance of the integrated FTMPC in the simulated dearomatization process.

5. Analyse the results and evaluate the economic benefits of implementing the integrated FTMPC to the actual industrial dearomatization process.

The first task is carried out by analysing the target process behaviour and applying expert knowledge acquired from target process users and experts in order to gather the requirements for the active data-based FTC strategy.

Task 2 is carried out by performing a literature survey on recent developments in the passive and active FTC fields, and by taking into account the requirements set in Task 1. Based on preliminary knowledge, the requirements and the literature survey, the suitable active data-based FDD and FTC components and the FTC design schemes are selected.

In Task 3, three data-based FDD components are tested within a preliminary process environment, which is selected based on the similarity to the dearomatization process and the popularity in literature. The results are discussed and the performance of the FDD methods is compared to select the best FDD method for the final integrated FTMPC.

Task 4 consists of validating the performance of the integrated FTMPC in the target simulated dearomatization process with faults in analysers, sensors and actuators.

Task 5 comprises assessing the performance and the financial benefits of implementing the proposed active data-based FTMPC in the actual industrial dearomatization process.

1.3 Content of the thesis work

The aim of this thesis is to develop an active data-based FTMPC to take into account faults in the process analysers, sensors and actuators of an industrial dearomatization process, LARPO, located in the Naantali refinery owned by Neste Oil Oyj, Finland.

The state-of-the-art of passive and active FTC in industrial processes is given in Chapter 2. In Chapter 3, the design schemes for the integrated FTMPC for a complex industrial process are described.

The comparison of three data-based FDD methods is described in Chapter 4. In this chapter, the active data-based FTC strategy proposed in Chapter 3 for the analyser and sensor faults is tested with three data-based FDD methods in a simulated industrial benchmark process. Based on the preliminary performance testing, the FDD component with best performance is selected as the FDD component of the integrated FTMPC for the simulated dearomatization process.

Chapter 5 presents the target dearomatization process and the existing control strategy, while Chapter 6 proposes the integrated FTMPC for the simulated dearomatization process.

Chapter 7 presents the testing platform and the industrial process simulator, ProsDS, which is used for the simulation of the complex industrial dearomatization process located in the Naantali refinery. Further, the linearity of the target process and the control performance of the nominal MPC are tested and the control performance of the integrated FTMPC is evaluated when the target process is affected by faults. Finally, the results are discussed and the economic benefits of the integrated FTMPC are assessed.

Chapter 8 analyses and discusses the performance of the integrated FTMPC and the conclusions based on the results are drawn.

The first hypothesis is asserted in Section 7.3 and the second hypothesis in Section 7.4.

1.4 Main contributions

The main contribution and novelty of the thesis is the integrated FTMPC containing the three parallel-running active data-based FTC strategies developed by the author.

The first strategy consists of a recursive partial least squares (PLS) and a fault accommodation-based FTC methods developed by the author for the analyser and sensor faults in the controlled variables (CV) and in the disturbance variables (DV). The second FTC strategy uses the recursive PLS and the combination of fault accommodation- and the controller reconfiguration-based FTC methods that has been developed by the author for the sensor faults in the manipulated variables (MV). The third FTC strategy utilises an FDD method monitoring the difference between the measurement and setpoint that has been developed by the author and a controller reconfiguration-based FTC method for the MV actuator faults.

In order to support the thesis work, the author has developed a software platform for the FTMPC development. The process simulator (ProsDS) and the FTMPC testing platform are described in more detail in Section 7.1.1.

The contribution of the author has been presented in the following publications:

- The fault accommodation-based FTC strategy for the analyser and sensor faults in a simulated crude distillation column has been presented in Kettunen and Jämsä-Jounela (2006a), Kettunen and Jämsä-Jounela (2006b) and Kettunen et al. (2008).

- The author has been assisting in the design and demonstration of an FTC strategy for an industrial dearomatization process with faults in the analyser measurements. This work has been presented in Koivisto et al. (2008).

- The integrated FTMPC and the FTC strategies for the DV and MV sensor faults and for the MV actuator faults have not yet been published, but an article Kettunen and Jämsä-Jounela (2010) has been submitted to the Journal of Industrial and Engineering Chemistry Research containing these results.

2 Fault-tolerant model predictive control: state-of-the-art

MPC has firmly established its position in the oil refining industry as one of the most popular advanced control methods. In a number of both passive and active FTC applications, an MPC is used as a control component of the FTC, optimising the process variables over time and providing inherent passive robustness. According to Camacho & Bordons (2004), the other MPC benefits are: the ease of use and tuning; the suitability for a wide range of processes; the built-in compensation for the dead times due to the process model; and the intrinsic handling of multivariable control and measured disturbances.

One passive way to increase tolerance for faults is to increase the robustness of the controller itself. A robust controller, such as a robust MPC, should reach given objectives without a change in the control law even in the presence of faults. In effect, robustness is reached if the control moves are computed by taking into account the uncertainty derived from the disturbances and faults by including these effects in MPC objective function.

Active FTC strategies (AFTCS) attempt to enhance the availability of a plant affected by faults by using active FDD and FTC components for adjusting the control law in order to reach the given control objectives. The AFTCS are commonly categorised in fault accommodation- and controller reconfiguration-based FTCs. In the fault accommodation, the controller is adapted to counter the effects of the faults by, for instance, accommodating the faulty measurements with the estimations provided by the FDD methods. Generally, the fault estimation can be carried out by using the mechanistic models or the data-based FDD methods, such as principal component analysis (PCA) or partial least squares (PLS). According to Blanke et al. (2003, pp. 266-268), the controller reconfiguration uses different input-output relations and, in general, utilises a switching logic to change the input and output (I/O) relations. If the controller reconfiguration refers to a change in both the controller parameters as well as the structure of the control system, these methods are referred to as restructuralisation methods (Zhang & Jiang, 2008). Generally, in the controller reconfiguration-based FTC, the faulty part of the controller is turned off and only the healthy part is used for the control.

2.1 Passive FTMPC

The robust MPCs address the model mismatch problems and are able to maintain the stability of the control system in the open loop case. There are several robust MPC methods available, e.g. methods based on a model set, weights, constraints and horizons. Nonlinear robust MPC has recently been studied intensively, allowing stable control of the nonlinear processes with faults by using an MPC-based control strategy. The downside of the acquired robustness is its huge computational load, which makes this method unfeasible for processes that require a fast response time.

The concept of robust MPC was first introduced by Campo and Morari (1987), based on the standard robust control theory. They proposed that instead of assuming that one linear time invariant (LTI) model could describe the process explicitly, the process behaviour in the robust MPC could be described by one LTI model selected from a set of models by using the min–max approach. In the passive min–max approach, originally presented by Witsenhausen (1968), the goal is to maximise the performance of the predictive controller by minimising the worst-case tracking error (the largest difference between the prediction and the actual measurement) of the predictive controller. This is accomplished by adding the estimation of the uncertainties (faults, disturbances) as an input to the predictive controller and taking it into account in MPC objective function. Although the robust MPC presented by Campo and Morari (1987) behaved in a more robust way than the previous approaches, according to Zheng and Morari (1993), the method could not guarantee robust stability since the algorithm did not take into account the general principle of MPC - the point of using only the first optimal input move from the calculated input series, i.e. the receding horizon principle. In essence, this flaw in design of the algorithm caused the open loop optimal solution to differ from the actual feedback optimal solution. One popular method for increasing the robustness of an MPC is to apply the min–max approach.

Ralhan and Badgwell (2000) developed two robust MPCs for simulated linear integrating plants: a one-stage and a two-stage integrating, robust linear quadratic regulator (RLQR). The one-stage version considered only the steady state, while the two-stage robust MPC optimised the state over the entire prediction horizon. The robustness of the controller was achieved by adding constraints to the cost function in order to restrict the future behaviour of the cost function itself. According to the results, the robust MPC worked efficiently compared to other approaches on the robust MPC field. However, as it is evident from the results, the performance of the robust MPC is better than a nominal MPC, but the differences to the standard min–max robust approach are minimal and the improvement in the stability of the control strategy is relatively small compared to the traditional robust MPC methods. Nevertheless, the RLQR response time was still faster than the traditional min–max algorithm, which is a small improvement to the previous robust MPC approaches.

Wu (2001) extended the linear matrix inequality (LMI)-based robust MPC, originally presented by Kothare et al. (1996), for a class of uncertain linear systems with structured time-varying uncertainties. The developed robust MPC algorithm was presented in their study and it was implemented and tested with a constrained control problem by using an industrial continuous stirred tank reactor (CSTR). According to the results, the presented robust MPC performs better than the traditional MPC. However, a comparison with the other robust MPC approaches is lacking and it is thus difficult to determine whether the proposed method is actually more effective than the previous robust MPC approaches. Nonetheless, the paper describes well the applicability and effectiveness of the method in an industrial-scale environment.

Wang and Romagnoli (2003) proposed a robust model predictive control (RMPC) design that utilised a generalised objective function for dealing with model-plant mismatch problems. Controller robustness is achieved by a selecting a proper objective function for each different situation from a set of pre-determined functions. The developed method was tested using a simulated linear CSTR as a case study. Again, the performance of the developed robust MPC was compared to a nominal MPC and a traditional min–max-based robust MPC. Based on the results, the difference to the min–max approach is small with the traditional method being even more effective in some cases than the proposed method. However, compared to the traditional MPC results, the proposed method shows better performance and stability. In general, the method seems to offer very small performance improvement compared to the previous approaches, and the main benefit of the algorithm is the reduced computational load.

Bemporad et al. (2003) developed an optimal feedback controller based on min–max control for the discrete-time uncertain linear systems with constraints on the inputs and states. The effectiveness of the control strategy was verified by comparing the computation times of the nominal and optimised receding horizon controller (RHC). The main advantage of the algorithm developed by Bemporad et al. (2003) is the optimal robust piecewise affine control law allowing implementation of the min–max-based robust MPC even for applications limited by computational capacity. The developed technique therefore significantly reduces computational load compared to the traditionally used algorithms, offering an important improvement to future robust MPC approaches based on the min–max approach.

Richards (2005) have proposed a robust MPC for linear time-varying systems that guarantees the feasibility of the optimisations and satisfies the given set of constraints in all cases. Robust feasibility was achieved primarily by tightening the constraints in the online optimisation. The developed algorithm was tested with linear and nonlinear examples with 100 simulations with random disturbances carried out. According to the results, the developed algorithm is feasible also for nonlinear cases, as long as the nonlinear systems are linearized around the operating point. In general, the proposed approach has promising results, although the paper and presented examples were for the most part theoretical.

Mhaskar and Kennedy (2008) considered the problem of the stabilisation of nonlinear process systems with a set of constraints on the change rate and the magnitude of the control inputs in the presence of uncertainty. The proposed robust MPC was based on the formulation of stability constraints that are feasible from an explicitly characterised set of initial conditions and minimisation of the rate constraint violation. This approach guarantees the system stabilisation and the handling of the rate constraints within the soft constraints. The effectiveness of the developed MPC was verified with theoretical proofs and a few simulation cases. The applicability to an actual nonlinear industrial case was not considered in the paper, although there is much future potential in the presented method.

Lazar et al. (2008) studied discrete nonlinear systems affected by parametric uncertainties and other disturbances. In their paper, Lazar et al. (2008) proposed an approach that was applicable to the classical setup of a min–max MPC problem; the proposed approach can be used to design nonlinear min–max MPC schemes with guaranteed input-to-state stability (ISS). Based on the results, the developed methodology allows the design of an asymptotically stable min–max MPC without assuming beforehand that the additive disturbance inputs reach zero as the closed-loop system state converges towards the origin. Although the proposed methodology was successfully demonstrated with a nonlinear example case and the proposed min–max MPC, the method is not directly applicable to an actual industrial application; however, it might provide a good basis for future innovations in the research area.

Huang et al. (2009) presented a design methodology for a robust nonlinear model predictive controller (NMPC) with dynamic first principles models. The proposed strategy is based on multi-scenario nonlinear programming (NLP) formulation, which is extended to an advanced step NMPC. The benefits of this strategy were demonstrated by using a large-scale, air-separation process unit. As an improvement to the existing NMPC formulations, the proposed strategy reduces the computation times without losing control performance. However, since only a brief case was presented in the paper to demonstrate the effectiveness of the method, the actual applicability of the method is unclear, even though the preliminary simulation results were promising.

2.2 Active FTMPC

Active FTMPC has been under study in an increasing number of FTC projects during the last decade. The most important active fault accommodation-based and controller reconfiguration-based FTC applications over the years are presented and discussed below.

2.2.1 Active fault accommodation-based fault-tolerant control

Pranatyasto and Qin (2001) studied the data-based fault-tolerant control of a simulated fluid catalytic cracking (FCC) unit under MPC control. The simulation model of the FCC was created by McFarlane et al. (1993) which, according to Pranatyasto and Qin (2001), is sufficiently complex to capture the major dynamic effects taking place in the actual FCC unit. PCA was first used as a fault detection procedure to classify the data; the *Q* method, also referred to as the squared prediction error (SPE) index by Jackson and Mudholkar (1979), was then used to detect faults and evaluate the difference between the measurement and the model output. The Hotelling T^2 index, based on the work by Hotelling (1947), was used for cross-reference purposes; however, this was found to be too unreliable for the detection itself. The Hotelling T^2 index measures how close the variances of two samples are to each other. The quadratic dynamic matrix control (QDMC) MPC-algorithm was used for control of the target process. The dynamic behaviour was introduced into the test process with the controller feedback. The faults tested in the paper included a large ramp in a coke formation factor, small changes in a coke formation factor, and changes in the ambient temperature. The results of this well-constructed paper are impressive as the faults in the simulated measurements were promptly detected and accommodated, which demonstrates that such FTC application could also provide good results in an actual industrial environment.

Prakash et al. (2002) studied a model-based supervisory combination of an FDD with an MPC. The FTC strategy consists of a supervisory component using the FDD information to modify the MPC inputs or outputs. The generalised likelihood ratio (GLR) by Willsky and Jones (1976) was used in the study for FDD purposes; the fault detection part used a fault detection test created by Narasimhan and Mah (1988). For the control of the case study process, a standard dynamic matrix control (DMC)-controller and a set of standard PID-controllers were used. The performance of the FTC was tested using a non-isothermal CSTR example presented by Marlin (1995). In the test setting, the developed fault-tolerant control strategy (FTCS) performed significantly better than conventional control settings, and was able to detect sequential faults introduced in the CSTR measurements. However, due to a degree of plant-model mismatch, there clearly was a degree of disturbance caused in the non-faulty variables. This disturbance effectively reduced control performance, although the performance was better than in the case without FTC.

Theilliol et al. (2002) developed a model-based FTC strategy that takes into account both sensor and actuator faults in a three-tank process controlled by a feedback controller. A linearized model of the target process was used for FDD purposes and analytical redundancy methods for the FTC. An unknown input observer scheme was implemented and a bank of unknown input observers generated for the FDD. The FTC strategy was able to estimate sensor values and effectively keep the process under control even when a sensor was completely destroyed. However, in order to verify the effectiveness of the method in an actual industrial-scale process, the method should be tested with more complex examples. In a more complex case, however, there would probably be difficulties in attaining a suitable analytical model for the method.

Patwardhan et al. (2006) improved and compared two model-based fault-tolerant control strategies: an FTCS based on the research work done by Prakash et al. (2002), and a reformulated MPC based on an identified state space model originally presented by Muske and Rawlings (1993). The FDD of the FTCS is based on a Kalman filter-based GLR, which estimates the fault magnitudes only for the identified faults; this provides a more efficient and less-computationally demanding method of detecting faults than mere parameter estimation-based methods. The FTC strategy was tested with a laboratory-scale continuous stirred tank heater (CSTH) process and a simulated benchmark process of a crude oil distillation column - the Shell control problem (Prett & Morari, 1987), SCP. The results of the both approaches were compared with the conventional MPC and both the state-space MPC (SSMPC) and FTCS provided superior performance compared to the conventional MPC. As comparisons to other types of FTC systems are lacking, it is difficult to determine the real effectiveness of the method. However, methods like this promote the effectiveness of the data-based FTC methods on actual industrial applications.

Mendonca et al. (2008) proposed an application of a model-based FTC with weighted fuzzy predictive control that was tested on an experimental three-tank process with faults. Fault detection was handled by means of a model-based approach and fuzzy modelling, and fault isolation with fuzzy decision-making application. Fault accommodation was carried out by using fuzzy models for different fault situations and the decision-making component was used for selecting the correct model for the fuzzy MPC in the case of a process fault in the target process. With the FTC strategy, the MPC model compensated for the process faults and was able to operate significantly better when the FTC strategy was active. However, the selection of correct weights for the fuzzy MPC might be a difficult and time-consuming task when implementing the system to a more complex process environment. Further, as only two fault cases were considered in a 2x2 process, reliable determination of the actual benefits in an actual process application is not possible based on these results.

Manuja et al. (2008) improved the model-based FTCS developed by Patwardhan et al. (2006) and Prakash et al. (2002) that was based on GLR for fault detection and isolation (FDI), and fault accommodation for the FTC. The existing FTC strategy was improved by reducing the dimensions of the models used for the FDI and control purposes. The improved FTC strategy was tested using a nonlinear version of an ideal 20-tray, single feed binary distillation column example by Luyben (1990). According to the test results, the modifications allow the implementation of the FTCs in large dimensional processes and improve the diagnostic performance of the FTC strategy. The main innovation of the paper comes from the model reduction for models used by both FDI and a predictive controller. However, the differences and the real benefit between the reduced model-FTC and the regular FTCs were small in general, even though a large number of simulations were run.

Deshpande et al. (2009) continued the research work on the model-based FTCs by Patwardhan et al. (2006) and Prakash et al. (2002) by using a nonlinear model for the FDI and the MPC. The performance of the modified FTCS is better, which was verified by testing the methods using a three tank benchmark process and a strongly nonlinear, fed batch bioreactor example case. A general nonlinear system was used for testing the control performance of the developed strategy. In all test cases the FTC performed well; however, as it was recorded in the paper, the system was tested in a single operation point of the process. Therefore, the FTCS does not take into account large changes in the dynamics of the processes, which may pose problems in actual plant applications. Also, as the system was adapting the models to the changes in the process, there is a possibility that the effects of undetected faults can spread to the models, causing false alarms and lowering the control performance.

2.2.2 Active controller reconfiguration-based fault-tolerant control

Griffin and Maybeck (1997) used a model-based moving-bank multiple model adaptive estimation and control (MMAE/MMAC) scheme to solve single controller robustness problems. Kanev and Verhaegen (2000) extended this concept generated by Griffin and Maybeck (1997), and used a generalised predictive control (GPC) algorithm as a controller and an interacting multiple model (IMM) estimator as a switching logic between the different predetermined GPCs. In this case, a piecewise linear (PWL) system was used for approximating the actual nonlinear process. Although the presented scheme is effective in some cases, the performance is severely reduced in case of unexpected process faults since the strategy is relying on the a priori knowledge of the faults.

Zhou and Ren (2001) developed a combination of model-based FTC and robust FTC strategy - a generalised internal model control (GIMC). The new control structure attempted to overcome the conflict between the robustness and performance of a normal feedback controller. The most important feature of the GIMC is that it is able to show, in a structured way, how the controller can be designed separately for performance and robustness purposes. Based on the results of the study, the developed control structure would be a beneficial alternative to the traditional robust MPC algorithms even though the control performance of the proposed strategy was not clearly reported in the paper.

Gani et al. (2007) studied model-based FTC of a simulated nonlinear polyethylene reactor. Gani et al. (2007) studied the effects of actuator faults and presented a way to prevent the effects of these faults by designing a fault-detection filter for actuator faults, a set of stabilising feedback controllers, and a stabilising switching law that orchestrates the re-configuration of the controller. The FTC strategy was implemented in the closed-loop simulations based on the target process model and the performance of the FTC strategy was verified. The study was application-oriented, thus promoting the use of FTC in industrial applications. However, the simulations were run without noise in the measurements, which is not realistic in actual industrial applications. This issue was only briefly assessed at the end of the paper with a non-filtered measurement.

Rodrigues et al. (2007) developed an active, model-based FTC strategy to prevent the effects of actuator failures on polytopic linear parameter varying (LPV) systems. The FTC strategy is said to be able to preserve the system performance by redesigning the controller in case of an actuator fault. The developed FTC strategy can redesign multiple controllers, which are able to maintain closed-loop stability even for combinations of multiple actuator failures. The effectiveness of the developed strategy was tested with an example case with actuator failures. The proposed approach was able to stabilise the example system with multiple actuator failures; however, as the example used in the paper was linear and somewhat theoretical, the real applicability of the presented strategy in an industrial environment cannot be estimated based on the results presented in the paper.

Mhaskar et al. (2007) studied the stability of a controller reconfiguration-based FTC strategy for sensor faults. The FTC strategy consists of a built-in determination mechanism to determine current operating regions and a switching logic for switching into a suitable control configuration in case of a fault in the measurements. The performance of the proposed FTC strategy was demonstrated using a nonlinear model of a polyethene reactor. The approach in the paper focused only in the reconfiguration of the faulty measurements, and did not take the FDD into account and therefore, the interaction between the FDD and FTC was not measured or determined and the availability of a perfect FDD was assumed.

Koivisto et al. (2008) used an active data-based FTC strategy for fault-tolerant control of a full-scale industrial dearomatization process with on-line analyser faults. The FTC strategy includes a process model to predict the process outputs and a supervisory system for FTC actions and for changing control objectives if needed. Based on the tests on the target process, the FTC strategy was able to successfully prevent off-spec production and unnecessary abrupt actions in the target process. The approach used in the paper was based on different levels of reconfiguration actions, which depend on the type of fault affecting the system. The value of the paper rests in the actual industrial application, as most of the FTC strategies have been tested with laboratory-scale processes, at most.

2.3 Conclusions of the state-of-the-art in FTC

As presented in the literature review on the FTC field, a number of good quality scientific papers on the FTC have been published over the last decade with a large number covering passive MPC strategies. These strategies have usually focused on improving and optimising the robustness of MPC from the theoretical point of view. The most notable reviewed robust MPC strategies include the original robust MPC by Campo and Morari (1987); the optimal min–max-based controller by Bemporad et al. (2003); the min–max-based controller for the discrete nonlinear systems by Lazar et al. (2008); and the recent nonlinear robust approach by Huang et al. (2009).

The reviewed active FTC strategies, on the other hand, are often more straightforward and driven by the increase of fault tolerance in a target process or processes. These methods have often been based on the fault accommodation or the controller reconfiguration FTC methods. Further categorisation has been made on the basis of the related FDD components, which have been based either on mechanistic process models or process data. The most effective active FTC strategies are the data- and fault accommodation-based FTC strategy for the simulated FCC unit by Pranatyasto and Qin (2001); the supervisory model- and fault accommodation-based approach by Prakash et al. (2002); the nonlinear controller reconfiguration-based strategy by Mhaskar et al. (2007); the application-oriented data-based reconfigurable FTC by Koivisto et al. (2008); and the nonlinear model- and fault accommodation-based strategy by Deshpande et al. (2009).

Generally, the passive FTC strategies and methods are more focused on theoretical improvements; a good example of this is the paper by Bemporad et al. (2003), where the computation load of the existing min–max method has been reduced by optimising the existing control algorithm. The active FTC methods, on the other hand, are more application-oriented and focus on specific applications such as the controller reconfiguration-based strategy by Koivisto et al. (2008) or the fault accommodation-based strategy by Deshpande et al. (2009). From the perspective of developing an industrial fault-tolerant application, the active data-based FTC strategies are more appealing candidates due to the more straightforward implementation and better focus on the application itself, even though a passive approach might be equally effective.

The active data-based FTC methods presented in the state-of-the-art literature review offer an excellent opportunity to solve fault- and disturbance-related problems commonly encountered in industrial plants. As it is evident from the number of reviewed papers, various methods have successfully been developed and implemented in a number of cases; however, the combination of the fault accommodation and controller reconfiguration FTC methods within the same FTC strategy have not been successfully demonstrated with an industrial case. The combination of the active FTC methods and utilisation of the active data-based FDD methods should thus provide the FTMPC with the necessary tools to significantly reduce the effects of the faults and disturbances, and improve the profitability of the industrial plants.

3 Design of the active FTMPC

Under normal operating conditions, most of the modern advanced control strategies, such as MPC, are able to ensure closed-loop stability and an optimal control performance. A properly tuned MPC can also survive a degree of model inaccuracy and process disturbances on a multivariable constrained system. While the early MPC formulations based on the linear quadratic gaussian (LQG) already had powerful stabilising properties due to the infinite prediction horizon, they were not able to handle constraints, process nonlinearities or uncertainty on multivariable systems as stated by Qin and Badgwell (2003). When the constraints and the finite horizon principle were implemented in order to use MPC for actual process applications, MPC faced severe stability problems. Attempts to achieve stability included various prediction and control horizon approaches and the introduction of a terminal cost to MPC objective function. These methods were criticised by Bitmead et al. (1990) since there were no clear conditions to guarantee stability. The stability of MPC was thus studied actively during the late 1980s and early 1990s by Keerthi and Gilbert (1988) and Mayne and Michalska (1990), for example, who were among the first to explore the stability issues with the constrained MPC. Most modern commercial MPCs have since been forced to use soft output constraints in order to avoid the stability issues (Qin and Badgwell 2003).

As the number of potentially faulty components in the control systems is greater than before due to the increased use of complex control strategies, the component faults have, however, become more common. At the same time, if a disturbance or a deviation from the target trajectory is caused by a fault, the corrective actions made by the MPC decrease the control performance instead of optimising the plant operation. In such a case, it is evident that the standard MPC alone is not able to operate at the optimal operating point or guarantee reliable control when affected by faults.

Design schemes can be used as a preliminary tool for the design of an active fault-tolerant MPC. These schemes describe the active FTC strategies that add extra functionality around the nominal controllers. Some of these strategies affect the controller directly, while others leave the controller intact and concentrate on mitigating the effects of the faults before they are relayed to the controller itself.

In this chapter, first the faults in dynamic systems and their locations in the industrial processes are specified. Second, the target process in the schemes is given as a linear model. Third, the MPC used for controlling the process in the schemes is described. Fourth, the FDD component of the FTC strategies is discussed. Finally, the chapter is concluded with the descriptions of the fault accommodation, controller reconfiguration and integrated FTC design schemes that are used in the development of the FTMPC for the industrial dearomatization process.

3.1 Faults in dynamic systems

According to Isermann and Ballé (1997) and Mahmoud et al. (2003), a fault is defined as an unpermitted deviation of at least one characteristic property or parameter of the system from the acceptable behaviour. In essence, a fault is defined as a state that may lead to a malfunction or a failure. Failure, on the other hand, is defined as a permanent interruption of the system's ability to perform a required function under the specified operating conditions. Generally, it is difficult to determine the difference between faults and disturbances, since in most cases there is no physical distinction. This is due to the fact that both are unknown (or known in case of measured disturbances) extra inputs acting on the plant. As such, Gertler (1998) has defined the faults as those extra inputs whose presence is wished to be detected and prevented with FDD and FTC methods, while generally the effects of the disturbances are prevented with other input variables.

According to Mahmoud et al. (2003), faults may take place in any system component (actuators, sensors, plant components, or any combination). Faults are generally categorised by the time characteristics or physical locations of faults in the system and the effect of faults on the system performance. Faults in physical locations can be divided into three locations: the sensor faults, the actuator faults and the process component (or parametric) faults. In complex industrial processes, such as in the oil refining process units, faults in sensors, actuators and process components are common, although highly undesired phenomena that have a significant effect on the quality of the final products and the production efficiency of the unit. Due to the small component size and low costs, traditional, yet expensive, way to increase the sensor reliability is by using the parallel hardware redundancy (multiple measurements) followed by a majority voting scheme. Figure 1 presents the general diagnostic framework and the potential locations of faults.

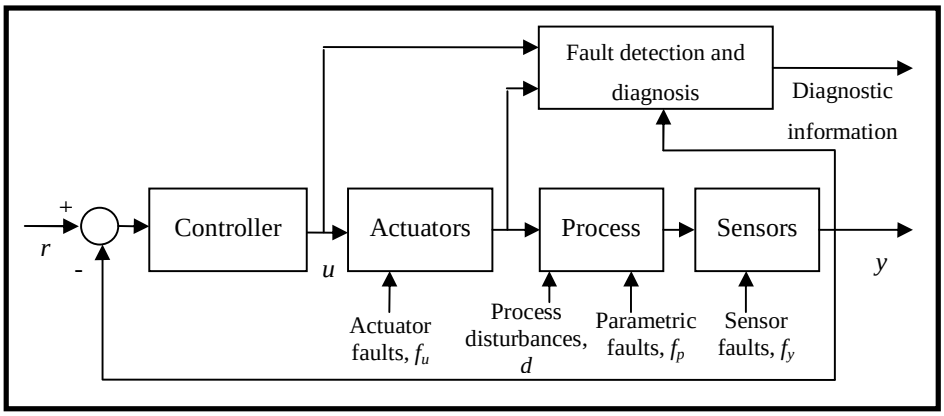

Figure 1. The general diagnostic framework and the locations of potential faults in a control system.

According to Bao et al. (2003), some examples of the typical faults for feedback controllers are a burned-out thermocouple, a broken transducer or a stuck valve. Unless the system is robust enough, the failures in the control components cause instability, severely degrade the controller performance and decrease the safety of the entire system.

For sensors, such as a temperature or a flow measurement, the most typical fault types according to Dunia et al. (1996) are a bias fault, a complete failure, a drifting fault and a precision degradation fault (see Figure 2), which also apply to faults in process analysers.

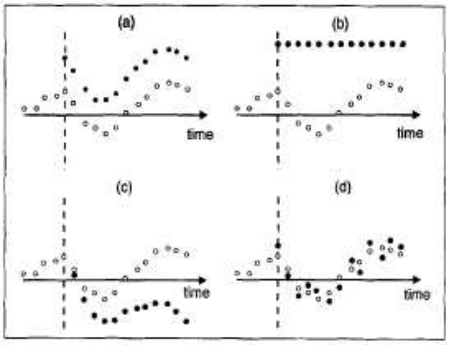

Figure 2. The types of faults found in process data. The dashed line shows when the fault occurs. ○: data free of fault, ●: corrupted data for the following cases: (a) bias; (b) complete failure; (c) drifting; and (d) precision degradation (Dunia et al., 1996).

According to Mahmoud et al. (2003), the actuator faults include the loss of partial control effectiveness (stuck valve) and a complete loss of control (broken valve). The actuator faults usually have a severe effect on the performance of the system and it is generally very difficult to add the extra hardware redundancy (multiple actuators) to increase the reliability since the actuators usually are both expensive and large.

The parametric faults have effect on the dynamic relationship among the system variables. Generally, these faults are caused by the physical parameter changes in the system and appear as coefficients in the dynamic model of the controlled process.

3.2 Linear model of an industrial process

The target process can be presented with a linear model, which can be composed of a standard state-space representation. In this model a state vector *x(t)*, where *A*, *B*, *C* and *D* are matrices of appropriate dimensions can be defined:

$$\begin{cases} \dot{x}(t) = Ax(t) + Bu(t), \;\; x(0) = x_0 \\ y(t) = Cx(t) + Du(t) \end{cases} \tag{1}$$

If *D* is assumed to be a zero matrix, and if disturbance *d* with the input matrix *E* are added to the model, then the following system can be achieved:

$$\begin{cases} \dot{x}(t) = Ax(t) + Bu(t) + Ed(t), \;\; x(0) = x_0 \\ y(t) = Cx(t) \end{cases} \tag{2}$$

The state-space formulation, including additive input or state faults f_u and output faults f_y, can be presented in the following way:

$$\begin{cases} \dot{x}_f(t) = Ax(t) + Bu(t) + Ed(t) + F_u f_u(t) \\ y_f(t) = Cx(t) + F_y f_y(t) \end{cases} \tag{3}$$

The multiplicative parametric faults, ΔA, ΔB and ΔC, commonly presented as f_p, modify the model in the following way:

$$\begin{cases} \dot{x}_f(t) = (A + \Delta A)x(t) + (B + \Delta B)u(t) + Ed(t) + F_u f_u(t) \\ y_f(t) = (C + \Delta C)x(t) + F_y f_y(t) \end{cases} \tag{4}$$

Finally, a linearized dynamic process model of a single-input and single output (SISO) or a multi-input and multi-output (MIMO) system with faults and disturbance *d* can then be described as shown in Figure 3:

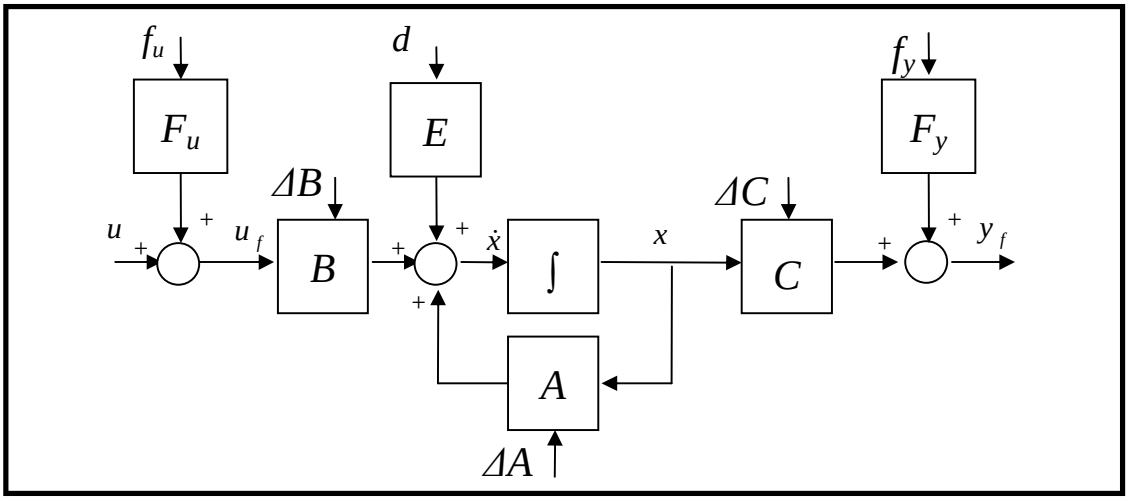

Figure 3. Linearized dynamic SISO/MIMO process model with disturbances d, additive input or state faults f_u , output faults f_y, and parametric faults ΔA, ΔB and ΔC.

In order to visualise the complete presentation of the process, including the controller, a linear output feedback controller is used as an example:

$$u(t) = -Ky_f(t) + Vy_r(t) \tag{5}$$

where y_f is the faulty measurement and y_r is the reference input for the controller. By using this controller together with the plant input u, plant output y and the setpoint signal y_r, the full controlled nominal plant can then be presented by the following system:

$$\begin{cases} \dot{x}(t) = (A - BKC)x(t) + BVy_r(t) + Ed(t), \;\; x(0) = x_0 \\ y(t) = Cx(t) \end{cases} \tag{6}$$

3.3 Linear MPC for industrial processes

The linear MPC is a suitable choice as the basic control component of the active FTC strategies due to its inherent stabilising properties and widespread use in the process industry. The main task of MPC is to stabilise the target process through optimisation. For the calculations required by MPC optimisation, the linear continuous time system can be given in the following discrete state-space form:

$$\begin{aligned} x_{k+1} &= Ax_k + Bu_k, x_0 = x_{start} \\ y_k &= Cx_k \end{aligned} \tag{7}$$

where x_k represents the state, u_k the control input and y_k the system output at time instant k, x_{start} is the value of x during the time step k=0. A basic MPC optimisation problem may then be formulated in the following way:

$$\min_u \left[x_p^T P_0 x_p + \sum_{i=k}^{k+p-1} x_i^T Q x_i + \sum_{i=k}^{k+m-1} u_i^T R u_i \right] \tag{8}$$

where P_0 and Q describe the weights set for the predicted state and R is the weighting matrix for the controlled input. Also, p represents the length of the prediction horizon and m the length of the control horizon with $p \geq m$.

As described by Lee and Cooley (1997), Morari and Lee (1999) and Bemporad et al. (2007), the objective function is solved using the process data and the model of the target process. The objective function may be considered as a tool with which to reach the set goal of the system that is often to drive the MPC output to a path following an optimal setpoint or a target trajectory. The way of implementing this depends of the algorithm in use and the needs of the user. As a result, the objective function is modified appropriately for each different case to fulfil the different user or process requirements. In addition to the objective function, a set of constraints is usually defined in order to constrain the MPC operation near or at the controller limits. These constraints can be set hard (the constraint should never be crossed) or soft (the constraint can be crossed for some amount of time) and this softness of the constraint affects MPC optimisation.

3.4 Fault detection and diagnosis component for the active FTC strategies

The FDD is one of the most important components in the active FTC strategies. Frank et al. (2000) state that without proper fault detection, isolation and accommodation, the process is vulnerable to faults, which may easily render the process unprofitable, unstable and even unusable. Therefore, fault diagnosis plays a crucial role in active FTC - with proper fault detection and isolation, the FTC strategy can utilise the correct FTC actions; and with proper fault identification, the effects of the fault can be reduced by using the estimation of the fault magnitude and direction with the fault accommodation methods.

Generally, FDD methods are divided into model-based and data-based methods as stated in a comprehensive FDD review by Venkatasubramanian et al. (2003a) and review of FTC methods by Zhang and Jiang (2008). As was evident in the state-of-the-art FTC literature study in Chapter 2, the most suitable FDD candidates for the integrated fault-tolerant MPC are the data-based FDD methods. Based on the literature study, the model-based approaches have generally been proven to be effective as well; however, as the complexity of the process increases, so does the difficulty in obtaining suitable models for the FDD. Also, in general, it is possible to combine both model- and data-based methods, but an approach like this would unnecessarily increase the complexity of the application, which in turn would decrease the usability of the FDD or FTC on actual industrial applications.

Venkatasubramanian et al. (2003b) state that PCA by Jackson and Mudholkar (1979) and PLS by Gerlach et al. (1979), in addition to statistical pattern classifiers, are the most commonly used statistical feature extraction methods and are thus the prime candidates as the FDD methods for the active data-based fault-tolerant MPC. Furthermore, a doctoral thesis by Vermasvuori (2008, pp. 50-57), which has been made in the same project in which the author has worked in, proposes to use PCA, PLS, independent component analysis (ICA), subspace model identification (SMI) or a monitoring method based on dissimilarity (DISSIM) for linear, or near-linear processes.

As the comprehensive analysis of data-based fault diagnosis has already been published in the same project by Vermasvuori (2008) and by Kettunen et al. (2008), the fault diagnosis is not analysed in detail in this thesis; rather, the focus is on the overall design of the active FTMPC.

Based on earlier studies, the PCA, PLS and SMI have been found to be the most promising data-based FDD candidates for the final active data-based FTC strategy. In the following sections, these data-based FDD methods are described in more detail.

3.4.1 Description of the principal component analysis-algorithm

One approach to FDD is PCA, which has been presented in FDD use by Jackson and Mudholkar (1979), originally introduced by Pearson (1901) and later independently developed by Hotelling (1933). Generally, PCA attempts to reduce the variable dimension by transforming a number of possibly correlated variables into a smaller number of uncorrelated variables. With this transformation, it is possible to create a statistical model of the target process, which can then be used to predict the variable values and to detect possible faults in these variables by using a suitable fault detection index, such as SPE or Hotelling T^2. In this section, the PCA model determination, the SPE and Hotelling T^2 limit calculation procedures and the fault detection procedure are presented.

3.4.1.1 PCA model determination from the training data set

1) The original training data X is zero-meaned and the variance is set to unit variance

2) The covariance matrix C is calculated:

$$C = \frac{1}{n-1} X^T X \tag{9}$$

where n is the number of observations

3) The eigenvalues $\lambda_{1\ldots m}$ of the covariance matrix are calculated, where m is the number of variables (measurements):

$$\det(C - \lambda_{1\ldots m} I) = 0 \tag{10}$$

While the eigenvectors $e_{1\ldots m}$ are solved from the following equation:

$$(C - \lambda_{1\ldots m} I) e_{1\ldots m} = 0 \tag{11}$$

The eigenvalues are reorganized in the matrix Λ in decreasing order:

$$\Lambda = \begin{bmatrix} \lambda_1 & 0 & \ldots & 0 \\ 0 & \lambda_2 & \ldots & 0 \\ \ldots & \ldots & \ldots & \ldots \\ 0 & 0 & \ldots & \lambda_m \end{bmatrix} \tag{12}$$

The eigenvectors, also called as the principal components (PC) of the *X*, are kept in the same order as the eigenvalues $\lambda_{1...m}$:

$$V = [e_1 \ e_2 \ ... \ e_m] \tag{13}$$

4) Based on the selected captured variance (selection based on, for instance, a certain variance limit), the number of principal components, *k*, is determined:

$$Captured\,Variance(PC_k) = \frac{\sum_{i=1}^{k} \lambda_i}{\sum_{j=1}^{m} \lambda_j} \cdot 100\% \tag{14}$$

5) The eigenvalue matrix Λ_K and transformation matrix V_k are formed using the *k* first principal components, where *k* << *m*:

$$\Lambda_k = \begin{bmatrix} \lambda_1 & 0 & \dots & 0 \\ 0 & \lambda_2 & \dots & 0 \\ \vdots & \vdots & \ddots & \vdots \\ 0 & 0 & \dots & \lambda_k \end{bmatrix} \tag{15}$$

$$V_k = [e_1 \ e_2 \ ... \ e_k] \tag{16}$$

The principal components can be used to estimate the values of from the zero-meaned and normalised (in regards to the standard deviation) values of $\hat{x}$:

$$\hat{x}^T = x_{scaled}^T \cdot V_k \tag{17}$$

6) The SPE limit is calculated with the equations by Jackson (1979):

The SPE-limit Q_α is acquired by using the following equation and by making the approximation that the probability distribution of *Q* is normally distributed:

$$Q_\alpha = \theta_1 \left[\frac{c_\alpha \sqrt{2\theta_2 h_0^2}}{\theta_1} + \frac{\theta_2 h_0 (h_0 - 1)}{\theta_1^2} + 1 \right]^{\frac{1}{h_0}} \tag{18}$$

where c_α is the normal density distribution corresponding to the upper $(1-\alpha)$ percentile of the normal deviate and θ is defined in equation 19 and h_0 in equation 20:

$$\theta_i = \sum_{j=k+1}^{m} \lambda_j^i, i = 1,2,3 \tag{19}$$

where *k* is the number of selected PCs and *m* is the total number of PCs .

$$h_0 = 1 - \frac{(2\theta_1\theta_3)}{3\theta_2^2} \tag{20}$$

7) The Hotelling T^2 limit was calculated using the following equation:

$$T^2{}_{\lim} = \frac{k(m-1)}{m-k} F(k, m-k, \alpha) \tag{21}$$

where k is the number of principal components, m is the number of measurements, $F(k, m-k, \alpha)$ corresponds to the probability point on the F-distribution with $(k, m-k)$ degrees of freedom and the α represents the user-defined confidence level.

3.4.1.2 Fault detection with the new measurement data set

1) Set the variance to unit variance by using the training data means and variance
2) Transform new, autoscaled data using the transformation matrix V_k

$$\hat{x}^T = x_{scaled}^T \cdot V_k \tag{22}$$

3) Calculate the value of T^2 for the new data, using the following equation:

$$T^2 = x_{scaled}^T \cdot V_k \cdot \Lambda_k{}^{-1} \cdot V_k{}^T \cdot x_{scaled} \tag{23}$$

4) Calculate the SPE-value for the new data, using the equation by Pranatyasto and Qin (2001):

$$Q = (x - \hat{x})^T (x - \hat{x}) = x^T \left(I - PP^T\right)x \tag{24}$$

5) Compare the SPE value to the SPE limit; if the value is over the limit, the fault is detected.
6) Calculate the individual variable contributions to the SPE-value:

$$contribution_i(\%) = 100\% \times (x_i - \hat{x}) / \sum_{i=1}^{m} \left| x_i - \hat{x} \right| \tag{25}$$

where m is the number of variables (measurements) and $\hat{x}$ is the predicted measurement.

3.4.2 Description of the nonlinear iterative partial least squares-algorithm

According to Abdi (2010), from the theoretical point of view the PLS is a more optimal approach than the PCA, since the PLS regression minimises the correlation between input (X) and output variables (Y) by finding the X which are most relevant to Y. This minimisation is carried out by searching for a set of components, which decompose X and Y in such a way that that these latent vectors explain as much as possible the covariance between them. As Abdi (2010) states, the main originality of PLS is derived from the preservation of the asymmetry of the relationship between predictor components and dependent variables, while other similar techniques such as canonical correlation and multiple factor analysis treat these symmetrically. In practice, however, when examining actual process data affected by noise and other variations, the difference between PCA and PLS is small or nonexistent. Since the PLS is by nature the more optimal method, the use of PLS over simple PCA is generally encouraged also in practical applications.

The recursive NIPALS algorithm by Wold et al. (1983) is presented next to obtain the matrices needed for PLS regression. The original version of the method was presented by Wold (1973). For two data blocks, X (N by K matrix) and Y (N by M matrix), the NIPALS is carried out iteratively as follows:

1. Select a K-weight vector w, for instance a normalised, non-zero row of X.
2. Calculate the score vector $t=X \cdot w$.
3. Calculate the Y-loading vector $q=Y^{\mathrm{T}} \cdot t$.
4. Calculate the Y-score vector $u=Y \cdot q$.
5. Calculate a new weight vector $w_1=X^{\mathrm{T}} \cdot u$. Scale w_1 to length 1.
6. If $|w-w_1|$ < convergence limit (user-defined), the convergence is obtained, otherwise $w=w_1$ and start at stage 2.

Here N is the number of samples, K is number of input variables and M is number of output variables. Now two score vectors, t (for X) and u (for Y) have been acquired.

To acquire the next pair of *t* and *u*, several methods are available; however in this context, in the following stages 7-11 by Wold et al. (1983), *X* is adjusted for the score vector and the regression of *Y* to *t* is calculated and finally *Y* is adjusted to the new results.

7. *X* loading vector *p* is now calculated with $p = X^T \cdot t/(t^T \cdot t)$
8. Adjust *X*: $X_{new}=X-t \cdot p^T$
9. Calculate regression of *Y* to *t*: $b = (Y^T \cdot t)/(t^T \cdot t)$
10. Adjust *Y*: $Y_{new} = Y-t \cdot b^T$
11. If more *(t,u)* pairs are needed, go back to stage 1 by using $X=X_{new}$ and $Y = Y_{new}$
12. If all the needed pairs of *(t,u)* have been acquired, the estimated Y_{pred} can be calculated from $Y_{pred} = T \cdot Q^T = X \cdot W \cdot Q^T = X \cdot R_{PLS}$, where R_{PLS} (*K* by *N* matrix*)* is the regression matrix, *T* is the scores matrix, *W* is the weights matrix and *Q* is the loadings matrix.

Faults can be detected and isolated by calculating the root mean square error of prediction (RMSEP) index for each variable and by setting the variable with highest value faulty:

$$RMSEP = \sqrt{\frac{\sum_{i=1}^{n} (\hat{v}_i - v_i)^2}{n}} \tag{26}$$

where *n* is the number of samples in the test data set, *v* is the output *y*, the disturbance *d* or the manipulated variable measurement *u* and $\hat{v}$ is the estimated value of *v*.

The latent variables (LV) of PLS are the terms of *T* containing the relevant information of high dimension data *X* that is compressed to the low-dimensional variable space of *T*. *T* is of dimension *N* by *A*, where *N* is the number of samples and *A* is the dimension of the LV space, determined by the NIPALS iteration. The latent variables are therefore the columns (t_1, t_2,…,t_A) of *T*. The relation to *X* and *Y* to *T* can be expressed through:

$$\begin{aligned} X &= T \cdot P^T + E \\ Y &= T \cdot Q^T + F \end{aligned} \tag{27}$$

where *E* and *F* are error terms, *T* has the latent variable scores for *X* and *P* and *Q* are the loading matrices for *X* and *Y*, respectively.

3.4.3 Description of the subspace model identification-algorithm

The SMI by Hyötynemi (2001) attempts to capture the behaviour of the target process by identifying the state-space matrices *A*, *B*, *C* and *D*, which can then be used as a fault-detection model for predicting the target process behaviour for FTC purposes. In this section, this SMI procedure is presented.

The identified discrete-time state space model is presented in the following form:

$$\begin{cases} X(k+1) = AX(k) + BU(k) + \varepsilon(k) \\ Y(k) = CX(k) + DU(k) + e(k) \end{cases} \tag{28}$$

where ε and e are white noise sequences and the input matrix U is composed of j input vectors u^T and the output matrix Y of j output vectors y^{T}:

$$u(k) = \begin{pmatrix} u_1(k) \\ \vdots \\ u_m(k) \end{pmatrix} \text{ and } y(k) = \begin{pmatrix} y_1(k) \\ \vdots \\ y_n(k) \end{pmatrix} \tag{29}$$

where m is the number of inputs and n is the number of outputs. Now, the system is observed in a time window with the width β at the time step k-β. The past and future input and output values can now be presented by using the following equations:

$$\begin{aligned} U_{past} &= \begin{pmatrix} u(\beta) & \cdots & u(k-\beta) \\ \vdots & \ddots & \vdots \\ u(1) & \cdots & u(k-2\beta+1) \end{pmatrix} \\ Y_{past} &= \begin{pmatrix} y(\beta) & \cdots & y(k-\beta) \\ \vdots & \ddots & \vdots \\ y(1) & \cdots & y(k-2\beta+1) \end{pmatrix} \end{aligned} \tag{30}$$

$$\begin{aligned} U_{fut} &= \begin{pmatrix} u(2\beta) & \cdots & u(k) \\ \vdots & \ddots & \vdots \\ u(\beta+1) & \cdots & u(k-\beta+1) \end{pmatrix} \\ Y_{fut} &= \begin{pmatrix} y(2\beta) & \cdots & y(k) \\ \vdots & \ddots & \vdots \\ y(\beta+1) & \cdots & y(k-\beta+1) \end{pmatrix} \end{aligned} \tag{31}$$

Next, χ is defined to be a matrix composed of all past input and output values and future input values and Z is defined to be composed of the future values of outputs:

$$\chi = \left(Y_{past} \middle| U_{past} \middle| U_{fut}\right) \tag{32}$$

$$Z = Y_{fut} \tag{33}$$

The mapping $F:\chi$ ->Z is acquired by using the least squares method: $F = (\chi\chi)^{-1}\,\chi^{T}Z$. Because the future input values are not known, the system is divided into two parts for the estimation purposes:

$$\begin{aligned} Z_{est} &= Z_{past} + Z_{future} = \left(Y_{past,est} \middle| U_{past,est} \middle| U_{fut,est}\right)F \\ &= \left(Y_{past,est} \middle| U_{past,est} \middle| 0\right)F + \left(0 \middle| 0 \middle| U_{fut,est}\right)F \end{aligned} \tag{34}$$

Now the variables in Z_{past} can be estimated to contain all the information from the system past and a refined data matrix without the future input contribution can be defined:

$$X = Z_{past} = \left(Y_{past,est} \middle| U_{past,est} \middle| 0\right)F \tag{35}$$

The matrix X can now be considered to contain the preliminary system states. The originally dynamic problem has now been reduced to a static one and the static dimension reduction methods, such as PCA or PLS, can reduce the dimension of the preliminary system states. Next, for the purposes of identification, the following input and output matrices are defined:

$$U = \begin{pmatrix} u^T(\beta) \\ \vdots \\ u^T(k-\beta-1) \end{pmatrix} \text{ and } Y = \begin{pmatrix} y^T(\beta) \\ \vdots \\ y^T(k-\beta-1) \end{pmatrix} \tag{36}$$

Also the submatrices X^{+} and X^{-} are defined, where X^{+} is a matrix X without the first row (oldest state) and X^{-} is the matrix X without the last row (newest state). The state representation now has the following form:

$$\left(\hat{X}^{+} \middle| \hat{Y}\right) = \left(\hat{X}^{-} \middle| U\right)\begin{pmatrix} A^T & C^T \\ B^T & D^T \end{pmatrix} \tag{37}$$

Finally, the parameter matrices A, B, C and D can be solved by using the least squares:

$$\begin{pmatrix} A & B \\ C & D \end{pmatrix} = \left(\hat{X}^{+} \middle| \hat{Y}\right)^{T}\left(\hat{X}^{-} \middle| U\right)\left[\left(\hat{X}^{-} \middle| U\right)^{T}\left(\hat{X}^{-} \middle| U\right)\right]^{-1} \tag{38}$$

The FDD with the SMI can be carried out by calculating the residual between the predictions of the SMI model and the actual process measurements. If the absolute residual between the measurement and the predicted output is higher than the limit, then a fault can be declared in that variable. The magnitude and sign of the fault can be estimated as the difference between the outputs of the model and the measurement.

3.5 Design schemes for the active FTMPC

In this section the focus is on the most important design schemes and control structures for the design of the active fault-tolerant MPC. The components of the active FTC strategies are included in the general schematic diagram of the active fault-tolerant MPC and presented in Figure 4.

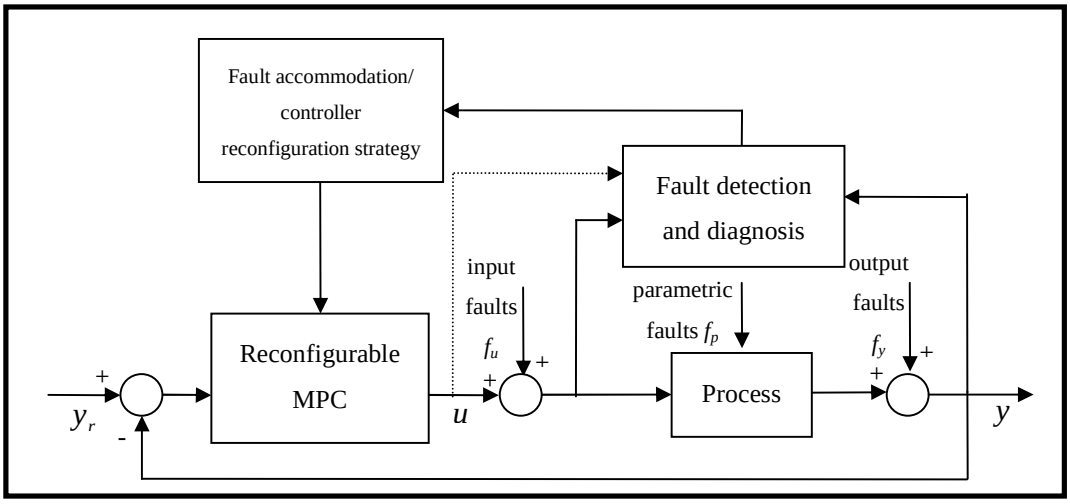

Figure 4. The schematic diagram for the active fault-tolerant MPC.

The main task of an active, data-based fault-tolerant MPC is to extract information from faulty or non-faulty process data through FDD, and to ensure optimal operation through the use of FTC strategies and a reconfigurable MPC. The information from the target process can be captured by applying statistical mathematical methods, such as PLS, to process history data and then using this information to detect, isolate and identify faults. In different fault-tolerant MPC schemes, this extracted information can be used to ensure optimal operation by carrying out FTC strategies, such as the fault accommodation or the controller reconfiguration. The active FTC design schemes for developing the active FTC strategies are presented in the following sections with schemes for fault accommodation, controller reconfiguration and finally, for the integrated FTC strategy.

3.5.1 FTC scheme based on fault accommodation

A commonly used active FTC scheme is based on fault accommodation. The active FTC strategy designed by this scheme is able to analyse and accommodate MPC inputs, outputs and process parameters based on the fault information and measurement predictions provided by the data-based FDD. The estimations are based on the measurements, controller input signals, actual cascade controller measurements and disturbances relayed to the FDD. This kind of strategy effectively masks both the process and the controller from faults through fault residuals r_u and r_y, while still taking advantage of both the faulty and the correctly functioning parts of the process. A general description of an active fault accommodation-based FTC scheme is given in Figure 5 with an MPC, the process around operating point U_0, Y_0 and input, output and parametric faults f_u, f_y and f_p.

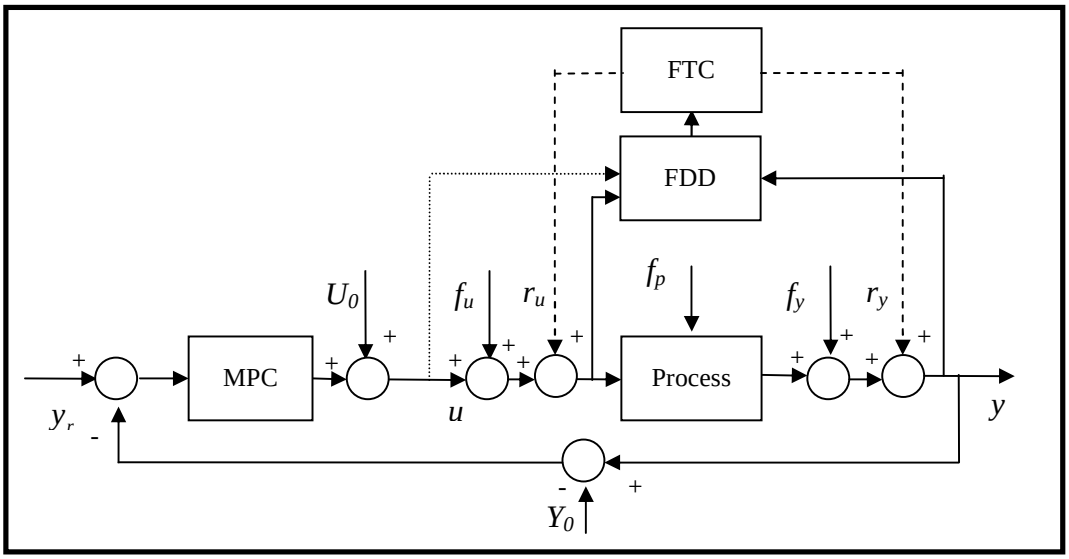

Figure 5. The fault accommodation-based FTC scheme.

In the data-based fault accommodation-based design scheme, a fault accommodation block is used for accommodating the faulty input and output measurements. This fault accommodation block is set between the nominal controller and the plant. In this block, the faulty input or output measurement is accommodated using the fault estimations from the data-based FDD methods.

In this design scheme, a data-based FDD can be used to predict the non-faulty measurement values of the faulty CV, DV or MV measurements. A fault accommodation block is set between the plant and the nominal controller. This fault accommodation block uses historical process data to predict the measurement values from the input values *u*, the output values of *y* or the disturbance values of *d*, and the past process output values y_{past}, input values u_{past} or disturbance values d_{past}. If necessary, the faulty CV, DV or MV measurement can be accommodated in order to prevent the effects of the faults on the target process. The fault accommodation block for CVs is presented in Figure 6, for DVs in Figure 7 and for MVs in Figure 8.

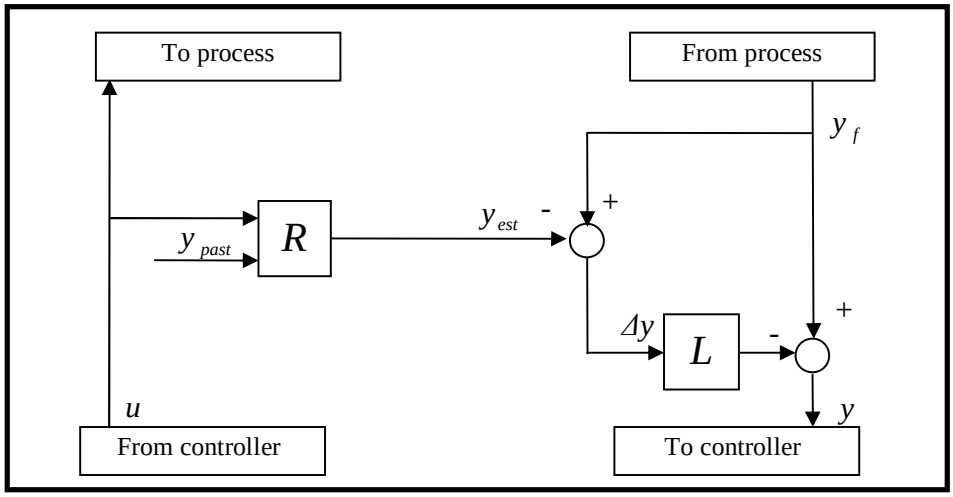

Figure 6. The data-based fault accommodation block with a faulty input vector y_f and an accommodated CV measurement y.

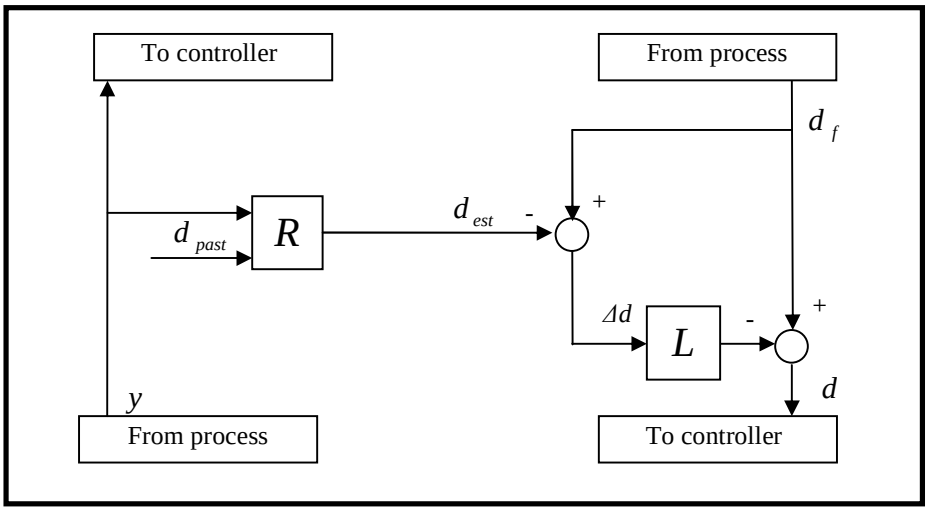

Figure 7. The data-based fault accommodation block with a faulty disturbance vector d_f and an accommodated DV measurement d.

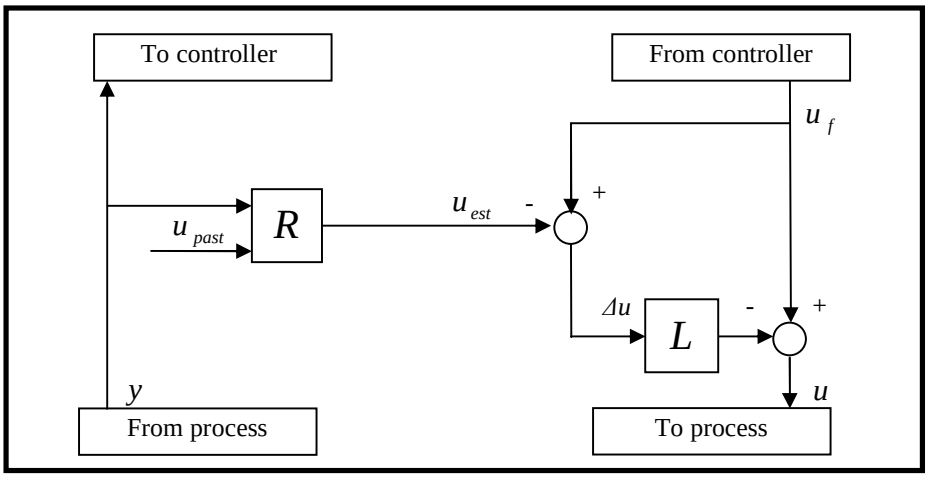

Figure 8. The data-based fault accommodation block with a faulty input vector u_f and an accommodated MV measurement u.

In the following, the value estimated by the data-based FDD for y_{est}, d_{est} and u_{est} are represented with variable v_{est} for each case. In the figures, *R* is the estimation matrix containing the non-faulty model of the target process and *L* is the parameter matrix affecting the degree of fault accommodation based on the probability of the fault. If no fault is detected, the probability of the fault is zero and the *L* matrix is a zero matrix. When a fault is detected, the probability of the fault is increased during each time step and the *L* matrix is adjusted accordingly to increase the degree of the accommodation.

L is the dependant of the period of time the fault has been detected: the longer the time, the higher the L matrix diagonal value that corresponds to the faulty variable, finally ending up to value of 1 in the diagonal entry of the faulty variable allowing full accommodation of the faulty measurement. If a fault is detected, the procedure increases the fault probability counter by one; if the delay counter is over the min limit, the FTC actions are initiated. The values of the ith diagonal entry of the parameter matrix L is calculated by using the following equation:

$$L_i = \frac{c_{i,t} - c_{i,\min}}{c_{i,\max} - c_{i,\min}}, c_{i,t} \geq c_{i,\min}, c_{i,t} \leq c_{i,\max} \tag{39}$$

where $c_{i,t}$ is the value of the fault probability counter of the ith diagonal entry at the time step t, $c_{i,max}$ is the maximum value of the ith fault probability counter and the $c_{i,min}$ is the minimum limit for the fault detection of the ith sensor. Accordingly, during each time step when no fault is detected, the counter $c_{i,t}$ is decreased by one and if the counter falls below the min limit $c_{i,min}$, the accommodation of the ith measurement is stopped.

The fault estimation is carried out by using the data-based FDD methods on process data. The input matrix X in each case is the inputs u, the current measurements y or the disturbances d and the past values of y_{past}, u_{past} or d_{past}.

With PCA, equation (22) can be modified and used to estimate new variable values in the following form:

$$v_{est}^T = X^T \cdot V_k \tag{40}$$

where V_k is the PCA transformation matrix and X is the input data matrix with the past values of y, d or u and the current measurements of y, d and u.

With PLS, this can be expressed with the following equation:

$$v_{est} = X \cdot R_{PLS} \tag{41}$$

where R_{PLS} is the PLS regression matrix:

$$R_{PLS} = W \cdot Q^{\mathrm{T}} \tag{42}$$

where W is the weight matrix of the input matrix X, and Q the loadings of y, u or d, which are estimated from the set of process data with the nonlinear iterative partial least squares (NIPALS) regression algorithm by Wold et al. (1983), presented in 3.4.1. Alternatively, the parameters can be estimated with the simple partial least squares regression (SIMPLS) algorithm by de Jong (1993), but this approach is not used in the thesis.

With SMI, the value of the v_{est} can be estimated by using the state-space matrix in equation (27) with the identified matrices A, B, C and D.

The difference between v_{est} and v_f, Δv, is then measured:

$$\Delta v = v_f - v_{est} \tag{43}$$

With PCA, the SPE index presented in equation (24) can be used, with PLS the RMSEP index between the estimated and the measured value, presented in Section 3.4.2, can be used and with the SMI, the absolute residual between the measured and the estimated value can be utilised.

If the RMSEP value is greater than the empirically determined threshold value, then the probability of the fault and the individual cell value of matrix L corresponding to the faulty variable is increased. The accommodated measurement can then be acquired through:

$$v = v_f - L\Delta v \tag{44}$$

where Δv is the residual between the faulty value and the estimated value, and v is either y, d or u depending on which variable is monitored.

As a result, the following equation describes the total accommodation of the faulty measurement $v_{f,i}$ during the time instant of i to a healthy measurement v_i by using process data and the data-based FDD methods:

$$v_i = v_{f,i} - L\left(v_{f,i} - v_{est,i}\right) \tag{45}$$

where the $v_{est,\,i}$ contains the estimation of either y, d or u at time instant of i and recursive inputs y_{past}, d_{past} or u_{past} and L is the parameter matrix controlling the degree of accommodation.

The main advantages of an active fault accommodation-based design are the flexibility and its adaptability to a range of different controllers, and the advantage of being able to take full benefit from the process information stored in the nominal controller parameters, models and constraints. As the FDD and FTC are separate components, no direct modifications to the existing controller are required. The downside of the fault accommodation scheme is the limitation in reaction times due to the delay caused by the fault verification of the FDD component, and a separate component structure. Further, the accuracy of the process model affects the performance since without sufficient accuracy, successful fault accommodation actions cannot be carried out.

3.5.2 FTC scheme based on controller reconfiguration

An active controller reconfiguration-based FTC scheme relies on directly adjusting the controller itself by changing the controller structure, models or parameters through parameter vector r_p. The pure reconfiguration-based (restructurisation) strategy uses only the correctly functioning part of the system for control purposes. The advantage of the active controller reconfiguration-based FTC scheme is the ease of implementation and lower accuracy requirements of the process models. Furthermore, it is easy to adapt the active controller reconfiguration-based scheme to a wide range of controllers and situations. The shortcoming of the method is the loss of information and controllability of the target process since only the correctly functioning part of the system is used for control. As a result, part of the information stored in the controller parameters, constraints and models is lost due to the reconfiguration actions. The controller reconfiguration-based FTC scheme is presented in Figure 9 with an MPC, the process around the operating point U_0, Y_0 and input, output and parametric faults f_u, f_y and f_p.

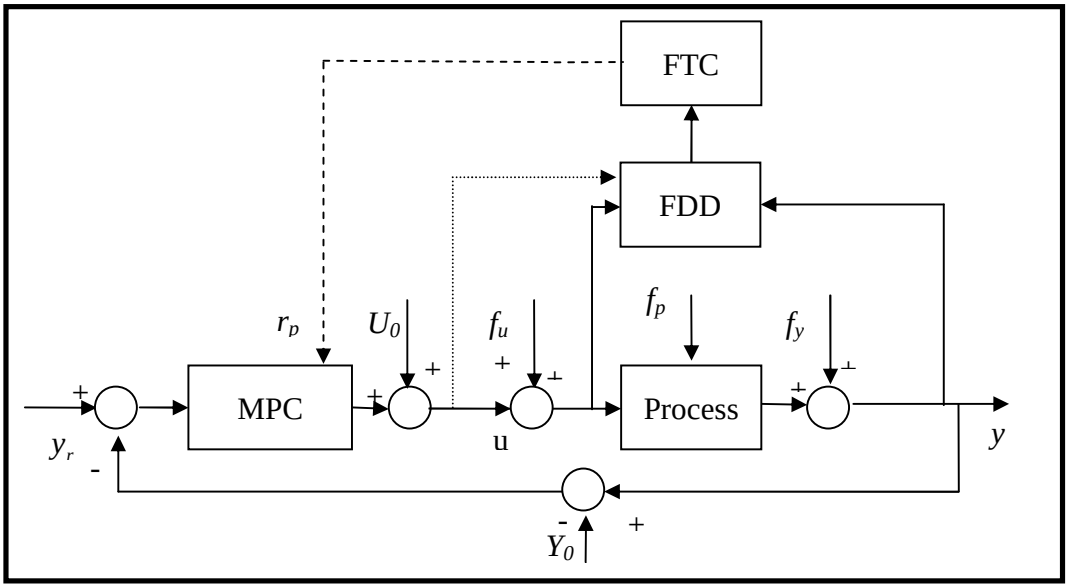

Figure 9. The controller reconfiguration-based FTC scheme.

Control allocation (CA) is one approach to handling MV actuator faults in the FTC strategy designed with the controller reconfiguration-based scheme. A special case of CA is the ‘daisy-chaining principle’ (DCP), which Buffington and Enns (1996) and Maciejowski (1998) have discussed. The idea of the daisy-chaining principle, adopted from the principle by Buffington and Enns (1996), is used for the controller reconfiguration FTC strategy. In the principle, two sets of variables are formed: the primary set containing manipulated variables to be monitored and the secondary set containing disturbance variables that can be used instead of the primary variables should some of the primary variables become faulty. In case of a fault in a primary variable, the faulty primary variable is disabled and the first disturbance variable in the secondary set is enabled as a manipulated variable. If more MVs turn faulty, the next available DV is again set as an MV from the secondary set. Maciejowski (2002) also states that the CA-based FTC can be further improved with an active FDD component which will provide the controller with, in this case the MPC, fault information as soon as it is detected in order to change the control configuration before the fault can affect the performance of the controller.

The main requirement for being able to apply controller reconfiguration for MV actuators to a process controlled by an MPC is that there should be sufficient redundancy in the target process in order to allow compensation of the faulty control variables. This can be accomplished by, for example, replacing the faulty manipulated variable with a measured disturbance variable in MPC formulation. Without the extra redundancy, the reconfiguration is still possible; however, if no extra variables are available for control, the controller reconfiguration will decrease the control performance (although the performance will be better than without the reconfiguration action).

The failure of an actuator can be detected by calculating the root mean square error (RMSE) index from actual measurements and the reference trajectory set by the MPC, and by comparing the index value to a detection threshold. This index is presented in the following equation:

$$RMSE = \sqrt{\frac{\sum_{i=1}^{n} \left(u_{ref,i} - u_i\right)^2}{n}} \tag{46}$$

where n is the number of measurements, u_{ref} the input reference given by the MPC, and u is the measured MV value. The scheme of a setting for a fault-tolerant MPC is presented in Figure 10.

Figure 10 includes the diagonal matrices of the controlled variable matrix *CV*, the manipulated variable matrix *MV* and the measured disturbance matrix *DV* and the selected controlled variable measurements y_{CV}, references for the controlled variables y_r, the selected measured disturbance values y_{DV} and the selected control inputs u_{MV}.

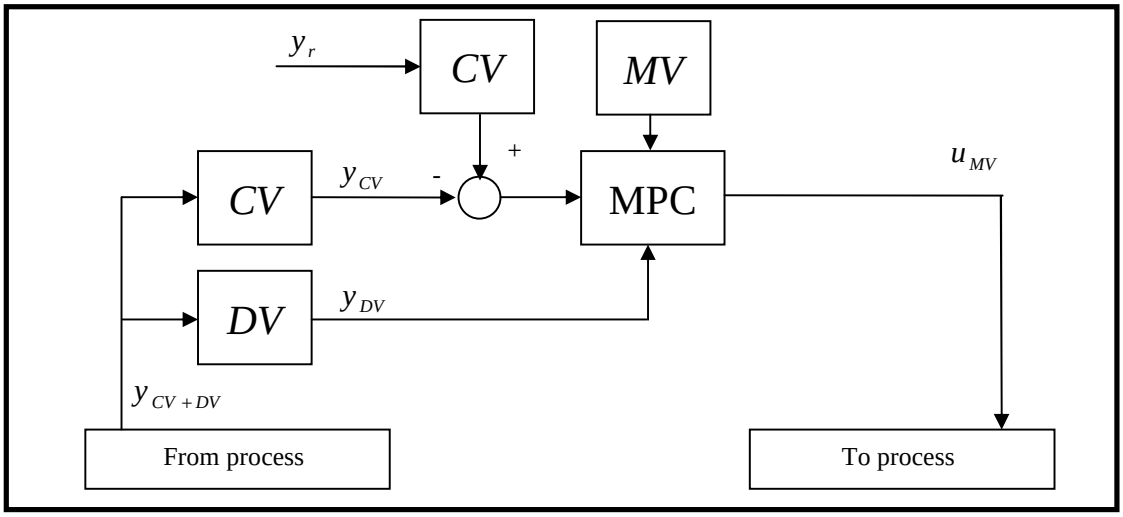

Figure 10. The structure of an MPC with the variable determination matrices CV, MV and DV and an MPC component for optimising the future output.

If the RMSE (for manipulated variable actuator faults) value of u_i has been over the detection threshold for a sufficiently long period, the controller reconfiguration action is carried out: the control configuration of the nominal controller is changed by adjusting the matrix *MV* and the matrix *DV*, which determine how MPC handles MV and DV variables. In essence, in case of a fault in the *i*th manipulated variable, the diagonal entry *i* of the matrix *MV* is set to value of 0 and the *i*th diagonal entry of the matrix *DV* is set to a value of 1. This sets the faulty manipulated variable as a measured disturbance.

In order to compensate for the loss of an *MV*, the measured disturbance d_j can be set as a manipulated variable by setting the diagonal entry $K+j$ of the matrix *MV* to the value of 1 and the diagonal entry $K+j$ of the matrix *DV* to the value of 0. The K in this case corresponds to the number of the manipulated variables.

The controller reconfiguration approach is explained with an example described in Figure 11. In this example, there are 2 manipulated variables and 2 disturbance variables, and therefore the size of the matrices *MV* and *DV* is 4x4 each. If the 2nd manipulated variable is set faulty, the 2nd diagonal entry of the MV matrix is set to value of 0 and the 2nd diagonal of the matrix *DV* is set to value of 1 corresponding to the change of a manipulated variable to a disturbance variable. Accordingly, the 1st disturbance variable (located in the 3rd diagonal entry) is set to value of 0 in the matrix *DV* and value of 1 in the matrix *MV* (in the 3rd diagonal entry) corresponding to a change of a disturbance variable to a manipulated variable.

$$MV: \begin{bmatrix} 1 & 0 & 0 & 0 \\ 0 & 1 & 0 & 0 \\ 0 & 0 & 0 & 0 \\ 0 & 0 & 0 & 0 \end{bmatrix} \rightarrow \begin{bmatrix} 1 & 0 & 0 & 0 \\ 0 & 0 & 0 & 0 \\ 0 & 0 & 1 & 0 \\ 0 & 0 & 0 & 0 \end{bmatrix}, \quad DV: \begin{bmatrix} 0 & 0 & 0 & 0 \\ 0 & 0 & 0 & 0 \\ 0 & 0 & 1 & 0 \\ 0 & 0 & 0 & 1 \end{bmatrix} \rightarrow \begin{bmatrix} 0 & 0 & 0 & 0 \\ 0 & 1 & 0 & 0 \\ 0 & 0 & 0 & 0 \\ 0 & 0 & 0 & 1 \end{bmatrix}$$

Figure 11. Example case of the controller reconfiguration strategy with 2 manipulated variables and 2 disturbance variables: a fault in the 2nd manipulated variable causes the 2nd MV to change to a disturbance variable and the 1st disturbance variable to a manipulated variable.

3.5.3 Integrated FTC scheme

The optimal active FTC strategy is based on an integrated FTC scheme, in which the controller has built-in options for the fault accommodation and controller reconfiguration methods. This kind of approach allows more flexibility and a greater degree of freedom to handle possible faults than the other FTC design schemes presented earlier since the integrated FTC scheme contains tools for both fault accommodation and controller reconfiguration-based FTC methods for sensor and actuator faults. Therefore, this kind of scheme will be used to develop the final FTMPC. The integrated FTC scheme is presented in Figure 12 with the process around the operating point U_0, Y_0 including the plant model and input, output and parametric faults f_u, f_y and f_p.

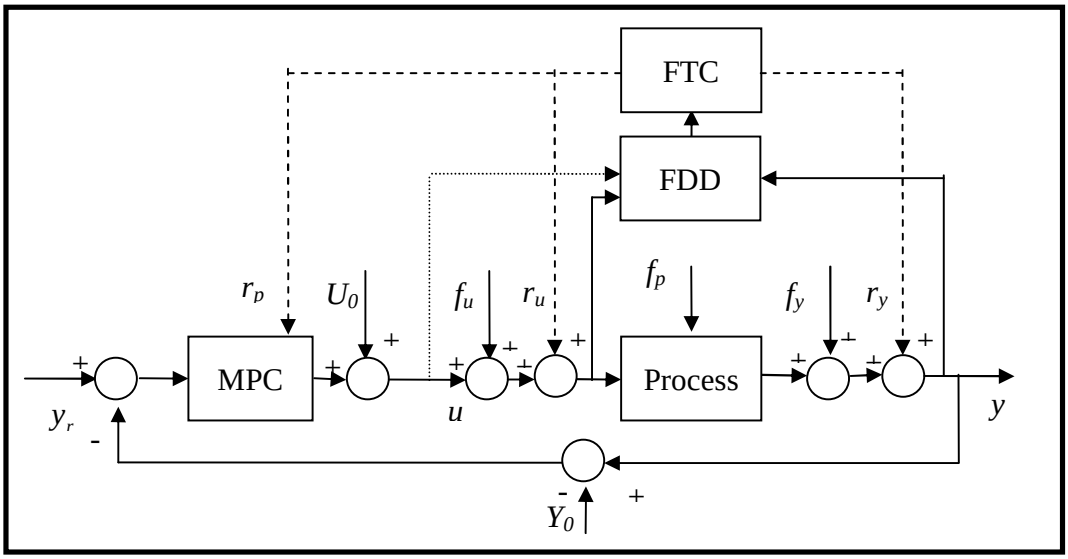

Figure 12. The integrated FTC scheme.

Based on this design scheme, an integrated FTMPC can be designed, including three parallel-running active FTC strategies that reduce the effects of different fault types. The fault types to be countered in this kind of setting are the sensor or, for example, process analyser faults (drift- or bias-shaped faults) for the CVs, DVs and MVs and MV actuator faults.

The first FTC strategy is based on the fault accommodation and on the data-based FDD for the sensor and, for example, process analyser faults in the CVs or DVs. The second FTC strategy uses the data-based FDD and the combination of the fault accommodation and controller reconfiguration FTC methods for the sensor faults in the MVs. The third FTC strategy utilises the controller reconfiguration FTC method for the MV actuator faults. The more detailed description of the integrated fault-tolerant MPC is presented in Figure 13. In this figure, $y_{CV+DV+MV}$ contains measurements for the CVs, DVs and MVs; f_1, f_2 and f_3 contain the fault diagnosis information for each of the FTC strategies; $L\Delta y_{CV+DV}$ contains the corrections for the CV and DV measurements; $L\Delta u_{MV+DV}$ contains the correction values for the MV outputs of the MPC; *MV+DV* contains the matrices for the MPC to determine, of which the MVs and DVs are used as MVs if the controller reconfiguration action occurs.

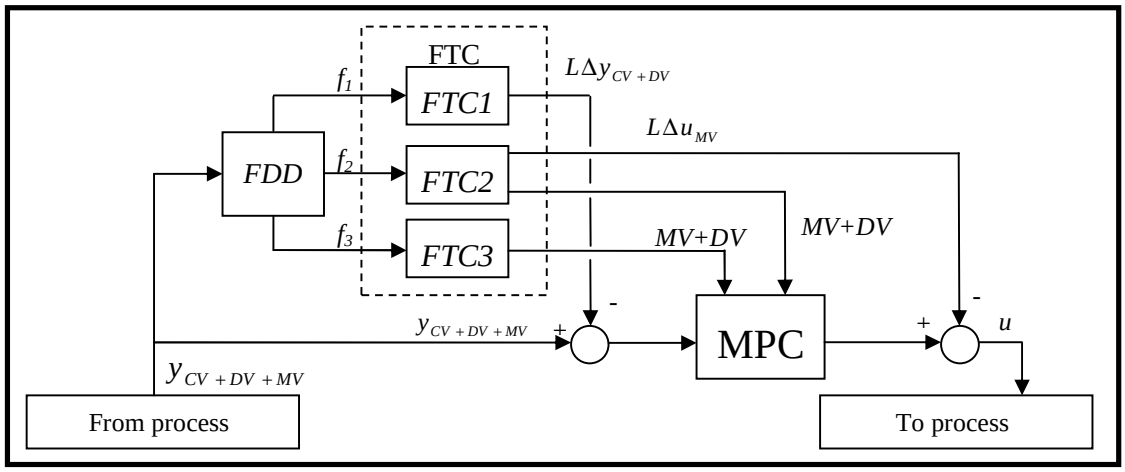

Figure 13. The integrated FTMPC with three FTC strategies.

4 Testing the data-based FDD methods with the fault accommodation-based FTC strategy for the analyser and sensor faults in the oil refining benchmark process

The aim of this chapter is to compare the performance of data-based FDDs and a fault accommodation-based FTC strategy in controlling a well-known benchmark process with faults in the CV analysers and sensors. The fault accommodation-based FTC strategy is based on the fault accommodation design scheme from Section 3.5.1 and the benchmark process is presented in the Shell control problem by Prett and Morari (1987). Based on the performance testing, the most suitable data-based FDD method is selected for the final integrated FTMPC.

In this chapter, the target benchmark process, its dynamic model and the MPC strategy are presented and the performance of the MPC strategy is tested first. Second, the structure of the FTC is briefly described. Third, the FDD and FTC parts of the strategy are tested and finally, the summary of the results is given and the performance of the tested FDD methods is compared.

4.1 Description of the target benchmark process, its dynamic model and MPC strategy

4.1.1 Description of the target benchmark process and its dynamic model

The target process for the preliminary analysis is an oil refining benchmark process that has been presented in the Shell control problem by Prett and Morari (1987), which contains a crude oil distillation column model with a set of control objectives and constraints.

The Shell control problem includes a distillation column, four heat exchangers (three side reflux units and one condenser at the top), one side stripper, a reflux drum, one feedstock stream and three product draws. Hot, mixed-phase oil is fed to the unit and then cooled down using the three reflux flows located at the side of the distillation column, which remove the heat so that the separation procedure in the distillation column can be carried out. The bottom reflux is controlled with an enthalpy controller that removes heat from the bottom part of the column by controlling the amount of steam produced by the reflux. Product separation in the column is based on the condensation and boiling properties of the crude oil fractions, the heaviest fractions being drawn off from the bottom and the lightest fractions as a distillate from the top. The quality requirements for the top draw product distillation end point and for the side draw product distillation end point set the limits for control of the column. There is also a temperature limitation for the bottom part of the column. The target process used in the preliminary study is described in Figure 14.

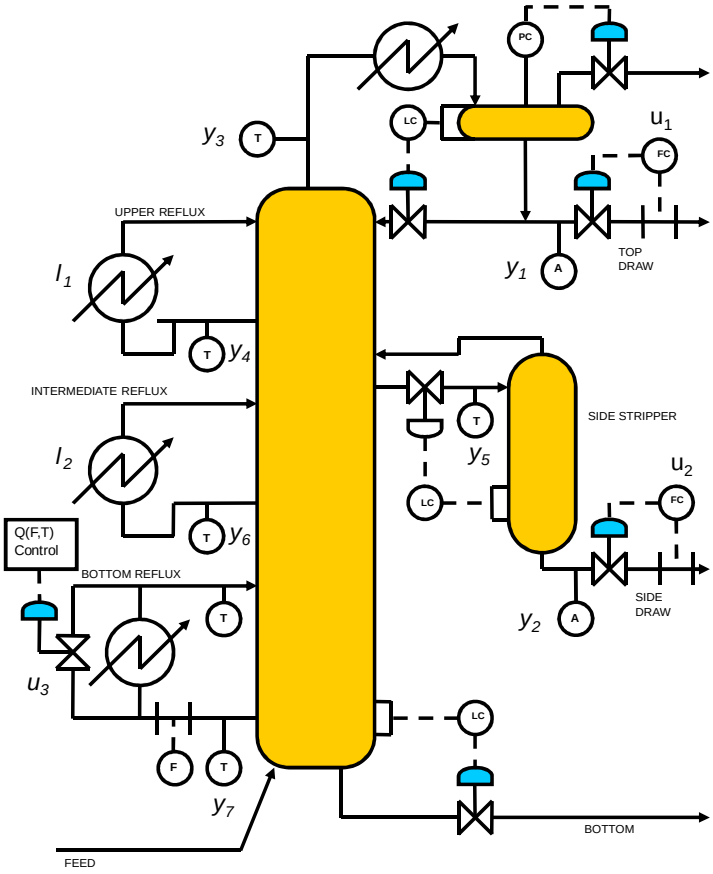

Figure 14. The Shell control problem according to Prett and Morari (1987).

The process model by Prett and Morari (1987) shown in Table 1 has been reported to be able to satisfactorily describe the dynamical behaviour of the crude oil distillation column. The normal way to acquire such a process model composed of first order plus time delay transfer functions is to measure the open-loop steady-state step responses. The model produces normalised responses, so everything including the constraints and measurement values are in relative units in the benchmark. Overall, the distillation column benchmark process and the dynamic model have been selected to act as a testing environment for comparing the performance of the data-based FDD methods for the industrial dearomatization process.

Table 1. The model of the Shell control problem according to Prett and Morari (1987).

	TOP DRAW FLOW RATE u_1	SIDE DRAW FLOW RATE u_2	BOTTOM REFLUX HEAT TRANSFER RATE u_3	INTERMEDIATE REFLUX HEAT TRANSFER RATE l_2	UPPER REFLUX HEAT TRANSFER RATE l_1
TOP END POINT y_1	$\frac{4.05e^{-27s}}{50s+1}$	$\frac{1.77e^{-28s}}{60s+1}$	$\frac{5.88e^{-27s}}{50s+1}$	$\frac{1.20e^{-27s}}{45s+1}$	$\frac{1.44e^{-27s}}{40s+1}$
SIDE END POINT y_2	$\frac{5.39e^{-18s}}{50s+1}$	$\frac{5.72e^{-14s}}{60s+1}$	$\frac{6.90e^{-15s}}{40s+1}$	$\frac{1.52e^{-15s}}{25s+1}$	$\frac{1.83e^{-15s}}{20s+1}$
TOP TEMPERATURE y_3	$\frac{3.66e^{-2s}}{9s+1}$	$\frac{1.65e^{-20s}}{30s+1}$	$\frac{5.53e^{-2s}}{40s+1}$	$\frac{1.16e^{-0s}}{11s+1}$	$\frac{1.27e^{-0s}}{6s+1}$
UPPER REFLUX TEMPERATURE y_4	$\frac{5.92e^{-11s}}{12s+1}$	$\frac{2.54e^{-12s}}{27s+1}$	$\frac{8.10e^{-2s}}{20s+1}$	$\frac{1.73e^{-0s}}{5s+1}$	$\frac{1.79e^{-0s}}{19s+1}$
SIDE DRAW TEMPERATURE y_5	$\frac{4.13e^{-5s}}{8s+1}$	$\frac{2.38e^{-7s}}{19s+1}$	$\frac{6.23e^{-2s}}{10s+1}$	$\frac{1.31e^{-0s}}{2s+1}$	$\frac{1.26e^{-0s}}{22s+1}$
INTERMEDIATE REFLUX TEMPERATURE y_6	$\frac{4.06e^{-8s}}{13s+1}$	$\frac{4.18e^{-4s}}{33s+1}$	$\frac{6.53e^{-1s}}{9s+1}$	$\frac{1.19e^{-0s}}{19s+1}$	$\frac{1.17e^{-0s}}{24s+1}$
BOTTOM REFLUX TEMPERATURE y_7	$\frac{4.38e^{-20s}}{33s+1}$	$\frac{4.42e^{-22s}}{44s+1}$	$\frac{7.20e^{-0s}}{19s+1}$	$\frac{1.14e^{-0s}}{27s+1}$	$\frac{1.26e^{-0s}}{32s+1}$

4.1.2 MPC strategy of the benchmark process

The control objectives of the crude oil distillation unit by Prett and Morari (1987) are to keep the top draw distillation end point measurement y_1, the side draw distillation end point measurement y_2 and the bottom reflux temperature measurement y_7 at their setpoint values by manipulating the top draw flow rate u_1, the side draw flow rate u_2 and the heat transfer rate u_3 of the bottom reflux. The heat transfer rate u_3 is further adjusted using a control loop with the hot steam flow rate as a control variable. There are also two measured disturbances in the process: the heat transfer rate of the upper reflux l_1 and of the intermediate reflux l_2. These flows remove the heat from the process and are re-boiled in other sections of the plant. The control constraints for the inputs, outputs and variable change rates are set according to the specifications by Prett and Morari (1987) in relative units, and are presented in Table 2.

Table 2. The control constraints of the Shell control problem process.

Variable	Lower limit	Upper limit
y_1	-0.5	0.5
y_2	-	-
y_7	-0.5	-
u_1, u_2, u_3	-0.5	0.5
Δu_1, Δu_2, Δu_3	-0.05	0.05

The MPC-based control strategy is developed next by using the Matlab MPC toolbox by Bemporad et al. (2007). A series of test runs was performed in order to determine the proper MPC parameters; the MPC was then tuned on the basis of results. The MPC parameters were adjusted according to the dynamics of the simulated process. The prediction horizon *p* was set long enough to be able to react to most situations occurring in the simulated process. Since the dead times in the process varied between 0-28 minutes and the time constants between 6-60 minutes, the prediction horizon was set to 120 minutes. The control horizon *m* was set to 40 minutes on the basis of the balance between the calculation resources and accurate control actions. The sample time with the process and with the MPC was adjusted to 1 minute. The weights for the controlled variables y_1, y_2 and y_7 were set to 45, indicating equal control priorities for all three controlled variables. All three MV weights were set to 0.01, indicating that all MVs are used equally. The weights for the MV rates were set as high as 1,000 for Δu_1, Δu_2 and Δu_3 in order to dampen the effect of the noise and sudden changes in the output values. These weight value settings provided more stable and reliable control actions than with lower values. The MPC parameter values are summarised in Table 3.

Table 3. The MPC parameters for controlling the Shell crude oil distillation column.

Parameter	Values
Prediction horizon p	120
Control horizon m	40
Weights, CV [y_1, y_2, y_7]	[45 45 45]
Weights, MV [u_1, u_2, u_3]	[0.01 0.01 0.01]
Weights, MV rates [u_1, u_2, u_3]	[1000 1000 1000]

Finally, the control performance of the MPC-based control strategy was tested by first introducing a step change to the setpoint of the CVs. The results of the step response testing with the MPC, when a setpoint change of 0.4 was introduced at the time step t = 100 minutes to the setpoint of the top draw product end point y_1, are presented in Figure 15. The setpoint 0.4 for the top draw product end point was reached at the time step t = 264 minutes. There was also a small effect on the other variables, which were quickly corrected and can be seen in Figure 15.

Next, the disturbance rejection capacity of the MPC was tested by introducing a step change of 0.5 to the DV l_1, the upper reflux heat transfer rate, in the time step t = 100 minutes and a step change of -0.5 to the DV l_2, the intermediate reflux heat transfer rate, during the time step t = 300 minutes. The results of the disturbance testing are presented in Figure 16. Disturbance l_1 was completely rejected within 100 minutes and the disturbance l_2 in 200 minutes as can be seen in Figure 16.

Based on the testing of the MPC, the target process was stabilised both under setpoint changes and the step changes in the disturbances. Overall, the performance of the MPC was good as can be seen from Figure 15 and Figure 16. Further, based on the testing in Kettunen et al. (2008), the response of the PI-based control strategy was much slower than with MPC-based control strategy. This caused the CVs to differ from the given setpoints for a longer time, which is one of the reasons why MPC is more suitable for the control of the target process. More details of the testing can be found in Kettunen et al. (2008).

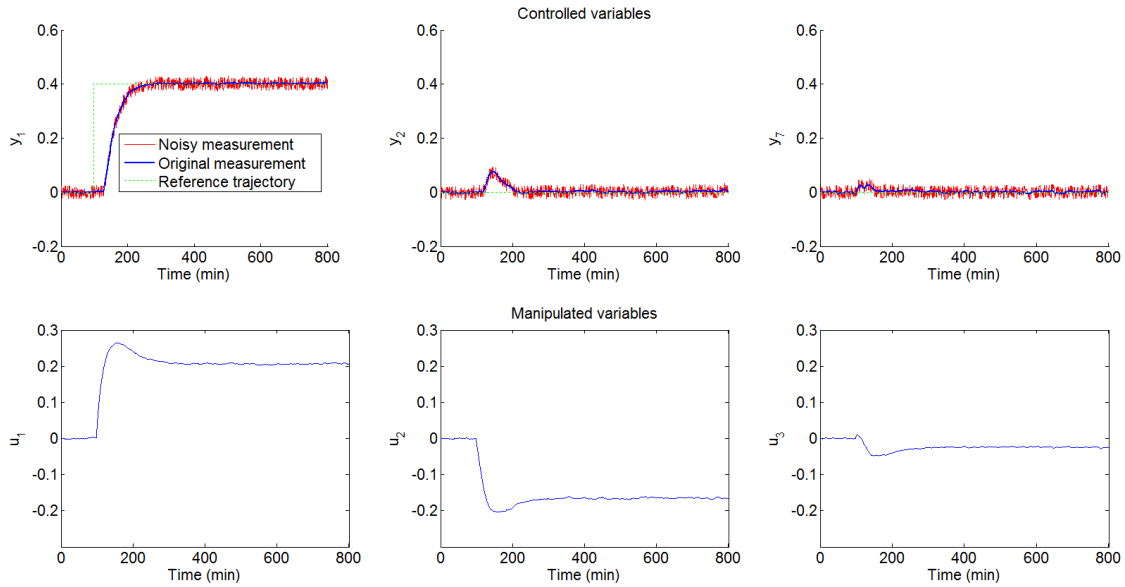

Figure 15. The CVs and MVs with a positive step change of 0.4 introduced to the setpoint of y_1 at t = 100 minutes.

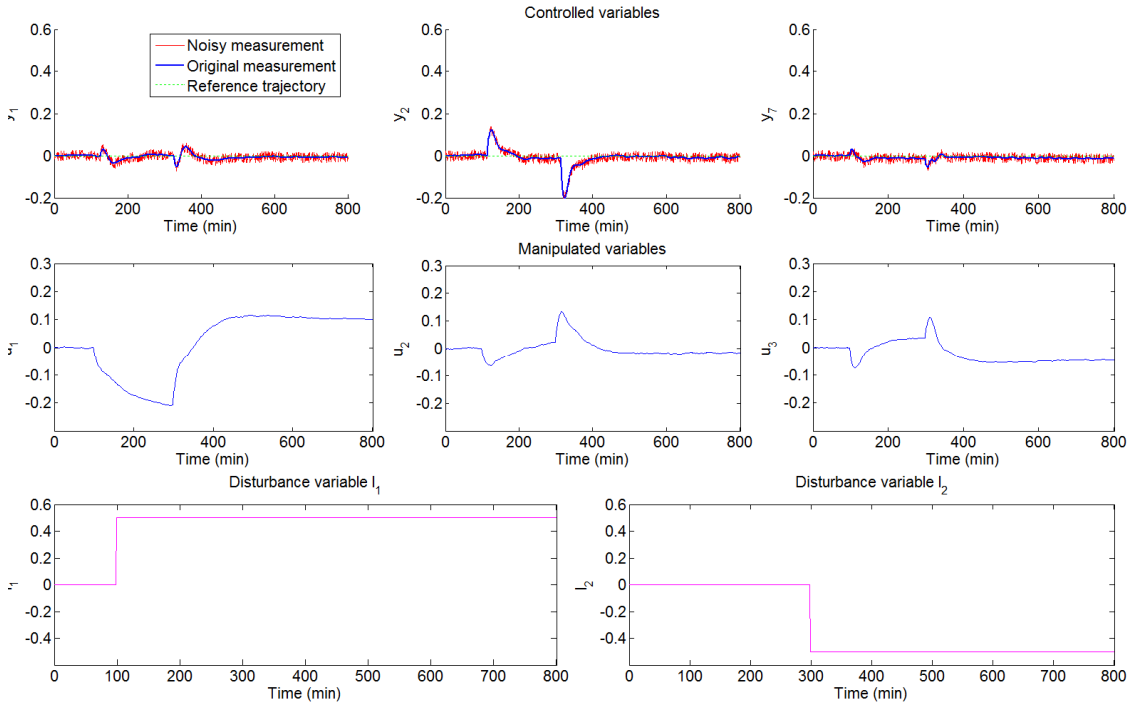

Figure 16. The CVs, MVs and DVs with a step change of 0.5 to the DV l_1 at t = 100 minutes and a step change of -0.5 to the DV l_2 at t = 300 minutes.

4.2 Components of the active fault accommodation-based FTC strategy for the benchmark process

Based on the active fault accommodation FTC design scheme presented in Section 3.5.1, the proposed active, fault accommodation FTC strategy consists of three parts: the FDD component for detecting the fault, the fault accommodation-based FTC part for carrying out the necessary FTC actions required to minimise the effects of the fault and the nominal control part for controlling the process.

Since the benchmark process and the industrial dearomatization process are assumed to be linear and complex, and since fast fault detection is preferred, linear data-based methods, such as PCA, PLS or SMI, are tested as the FDD components as suggested in Section 3.4. SPE index is used for detecting faults with PCA-based FDD, RMSEP index with the PLS-based FDD and the residual between the predicted and measured values with the SMI-based FDD. The faulty signal is accommodated using the fault estimate derived from the FDD methods, which is based on the difference between the model estimate and the actual measurement. The PCA-, PLS- and SMI-based FDD methods have earlier been presented in detail in sections 3.4.1, 3.4.2 and 3.4.3, respectively.

As an addition to the FDD and FTC, a cumulative sum mechanism is implemented in order to avoid false alarms. The cumulative sum requires that the fault is detected at least three time steps before the fault is declared. After these three steps, fault compensation is started with a gradually increasing compensation value to reach the final compensation value after three more time steps. In the following three sections, a general description of each of the methods is given.

The usage of MPC is taken into account in fault detection, since the FDD methods are trained in closed loop, which makes sure that the MPC behaviour is included in the FDD model. However, MPC may cause nonlinear behaviour when operating near constraints (constraint-induced nonlinearity) and this nonlinearity is higher, the harder the constraint is. This nonlinearity is caused, because the MCP attempts to avoid crossing the constraint at any cost.

4.3 Results of testing the data-based FDD methods

In this chapter, the results of the PCA-, PLS- and SMI-based FDD testing and the results of the combining the FDD component with the active data-based FTC strategy are presented. In the following, all of the test cases with different active data-based FTC strategies are presented on the timeframe of 1…800 minutes. All of the faults were set to occur at the time step t = 100 minutes; however, only one fault was introduced during each simulation as in this way the effects of different faults and FDD methods can be compared.

4.3.1 Description of the analyser and measurement faults and the faulty data set

Two different kinds of fault are common in the oil refining process analysers and sensors: abrupt bias faults and slowly increasing or decreasing drift faults. The bias faults are usually caused by contamination of the analyser sample, while the drift faults can be caused by the slow accumulation of substances in the sensors, analysers or sample lines.

The data set used for testing consisted of 800 minutes of the simulated process data that included measurement faults. The bias and drift faults were introduced into the simulated process measurements. In the test setting, a positive bias fault with a magnitude of 0.5 was introduced into the top draw product quality variable y_1 at the time step t = 100 minutes, and the fault ended at the time step t = 300 minutes. Another fault, in this case a positive drift fault, was introduced into the top draw product quality variable y_1 at the time step t = 100 minutes, and the fault ended at the time step t = 300 minutes, at which time the fault magnitude is 0.5, which was the maximum hard constraint allowed for the top draw product end point y_1. In order to be able to use the FDD components as a part of the active data-based FTC strategy, a separate set of fault-free training data was used for the training the FDD methods. This training data set was used to train the PCA-, PLS- and SMI-based FDD methods to detect faults in the analysers and process measurements.

4.3.2 Testing the FDD methods

In this section, the results of testing the PCA-, PLS- and SMI-based FDD methods are presented and discussed. First, the training of the methods is discussed; second, the results of the testing are presented; and finally, the summary of the results is given.

4.3.2.1 Training the FDD methods

PCA-based FDD was implemented with three separate PCA models, each containing delay-compensated input variables and a controlled variable. The structure of the models is: $PCA_1 = [y_1\ u_1\ u_2\ u_3\ l_1\ l_2]^T$, $PCA_2 = [y_2\ u_1\ u_2\ u_3\ l_1\ l_2]^T$ and $PCA_7 = [y_7\ u_1\ u_2\ u_3\ l_1\ l_2]^T$, where the variables are the upper reflux heat duty l_1; the intermediate reflux heat duty l_2; the top draw product end point y_1; the side draw product end point y_2; the temperature measurement y_7; the top draw flow rate u_1; the side draw flow rate u_2; and the bottom reflux heat transfer rate u_3. The PCA models were able to take the process disturbances into account while detecting faults in the process. For each PCA model, three principal components were used with 84.1%, 96.5% and 83.8% variance. For FDD purposes, SPE and Hotelling T^2 limits were calculated using 95% confidence.

Three PLS models were used for the FDD: the models contain delay-compensated measured disturbances l_1 and l_2, and three control inputs u_1, u_2 and u_3 as the input variables. The output variables of the models PLS_1, PLS_2 and PLS_7 are y_1, y_2 and y_7, respectively. In the final models, there were three latent variables which capture 79.7%, 94.6% and 80.3% of the output variance, and 35.8%, 83.1% and 31.3% of the input variance, respectively.

The identified subspace model was trained using the same training data as with the PLS. The inputs for the subspace identified system are the two measured disturbances l_1 and l_2, and three control inputs u_1, u_2 and u_3. The outputs are the seven outputs, y_1, y_2, y_3, y_4, y_5, y_6 and y_7. While creating the state-space models, the order of the model was reduced from a 35^{th} order to a 10^{th} order model by limiting the state-space model order during the model identification in order to reduce the calculation load with the method.

4.3.2.2 Testing the FDD component based on PCA

In the first FDD testing, the PCA-based FDD was able to detect both bias- and drift-shaped faults. For the bias fault, both the SPE and the Hotelling T^2 detected the fault at time step t = 103 minutes, i.e. 3 minutes later than the fault starts to affect the process. The drift fault was detected by the SPE at the time step t = 130 minutes. With the Hotelling T^2 the fault was not detected until at the time step t = 232 minutes. Based on the results, the SPE had a significantly faster detection rate than with the Hotelling T^2 when using the same confidence levels for both methods. Due to the better sensitivity to the faults, only the SPE index was used for the fault detection with PCA. The SPE index and the Hotelling T^2 indices for the bias-and drift-shaped faults are presented in Figure 17.

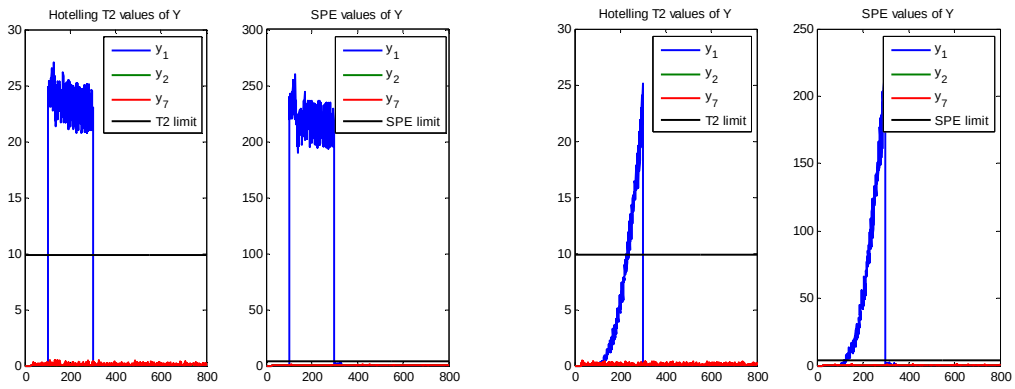

Figure 17. The Hotelling T^2 and the SPE indices for the bias-and drift shaped faults in the measurement y_1.

The fault isolation was based on the largest SPE value higher than the detection limit. If more than one SPE value was higher than the detection limit, then the one with the highest SPE value was selected as the faulty one. The fault magnitude and sign were estimated as the difference between the model output and the measurement.

4.3.2.3 Testing the FDD component based on PLS

The PLS-based FDD utilised the RMSEP as a fault detection index. This index measures the residual between the model outputs and the measurements. The limit for detecting the faults was set to 2.5, which was clearly above the noise level of the process. The faulty variable was isolated from the RMSEP plots, the highest value being selected as the faulty one. Fault magnitude and sign were determined by comparing the PLS model predictions to the corresponding measurement value. A bias-shaped fault was affecting the top draw distillation end point measurement at the time step t = 100. The fault was detected and isolated at the time step t = 103 minutes, after a delay caused by the cumulative sum algorithm. Next, the drift fault affecting measurement y_1 starting from the time step t = 100 was detected at the time step t = 120 minutes. The values of the RMSEP for bias and drift faults is presented Figure 18.

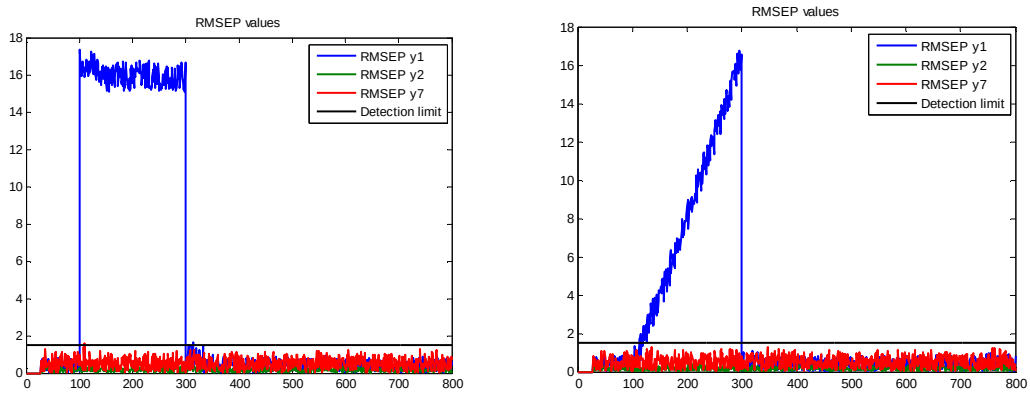

Figure 18. The RMSEP in the case of bias and drift faults in an output y_1.

4.3.2.4 Testing the FDD component based on SMI

In the case of the SMI-based FDD, the faults were detected by comparing the SMI model outputs with the measurement outputs. If the residual between the measurements and the SMI model outputs value was higher than a fault threshold, then a fault was detected and isolated to that specific measurement. The fault threshold was set to 0.07 in order to be high enough to exceed the noise level of the process, yet low enough to detect the faults as soon as possible. The fault delay mechanism designed for to prevent the effect of outliers and random noise caused a small disturbance at the beginning and the end of the fault. Otherwise, the FDD component was able to detect the faults in the measurements successfully; the bias fault was detected at the time step t = 103 minutes. The drift fault was detected after a delay of 33 minutes at the time step t = 133minutes. The results for bias and drift faults are presented in Figure 19.

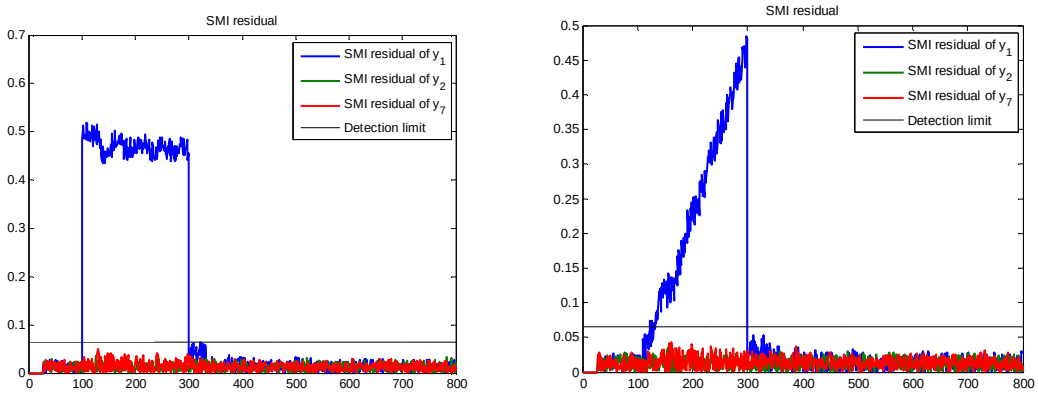

Figure 19. The SMI residuals for y_1 in the case of bias and drift faults in an output y_1.

4.3.2.5 Summary of testing the FDD components

In this section the results of testing the PCA-, PLS- and SMI-based FDD components are presented with bias and drift faults in the measurement y_1. The differences in terms of detection times were generally small between the methods as presented in Table 4, where the fault detection times are briefly summarised.

However, as can be seen from the results, the PLS had the shortest detection time in drift faults, therefore suggesting that it is the fastest FDD method. In the following sections the performance of the FTC is presented with these FDD methods and the results of using the different FTC combinations is described.

Table 4. Detection times for the PCA-, PLS- and SMI-based FDD methods.

FDD component	**Bias fault: detection time**	**Drift fault: detection time**
PCA	3 min	30 min
PLS	3 min	27 min
SMI	3 min	33 min

4.3.3 Testing the FDD methods with the fault accommodation-based FTC strategy

The PCA-, PLS- and SMI-based FDD methods were then tested with the fault accommodation-based FTC strategy with a fault in the top draw product end point y_1. The goal of the testing is to demonstrate the difference in the performance of different FDD with the FTC.

First, a positive bias fault with a magnitude of 0.5 was introduced into the top draw product quality variable y_1 at the time step t = 100 minutes, and the fault ends at time step t = 300 minutes. Second, a positive drift fault was introduced into the top draw product quality variable y_1 at the time step t = 100 minutes, and the fault ends at the time step t = 300 minutes, at which time the fault magnitude is 0.5.

All three FTC combinations were able to handle both fault types. The simulation results for the FTC strategy with the PLS-based FDD is presented and compared against the nominal control strategy results in Figure 20 with bias fault in the measurement y_1. Other cases are presented similarly in Appendix B. As can be seen from the figure, the effect of the fault on the process was significant; without the FTC the variable y_1 was driven towards the lower constraint limit with the manipulated variables also being severely disturbed. Due to the fault, off-spec product would have been generated in actual process unit and the process would have been disturbed for at least 300 minutes.

When the active data-based fault accommodation FTC strategy and PLS-based FDD was active, the fault was rapidly detected and compensated at the time step t = 103 minutes and, due to the fast fault detection, the fault had almost no effect on the measurements. The small spike in y_1 at the beginning of the fault was caused by the delay in fault detection, which was implemented in order to eliminate the effect of random spikes and noise in the measurements. In addition, when the fault ended, there was also another spike caused by the delay mechanism. Overall, the effect of the delay mechanism was small, which can also be seen from Figure 20.

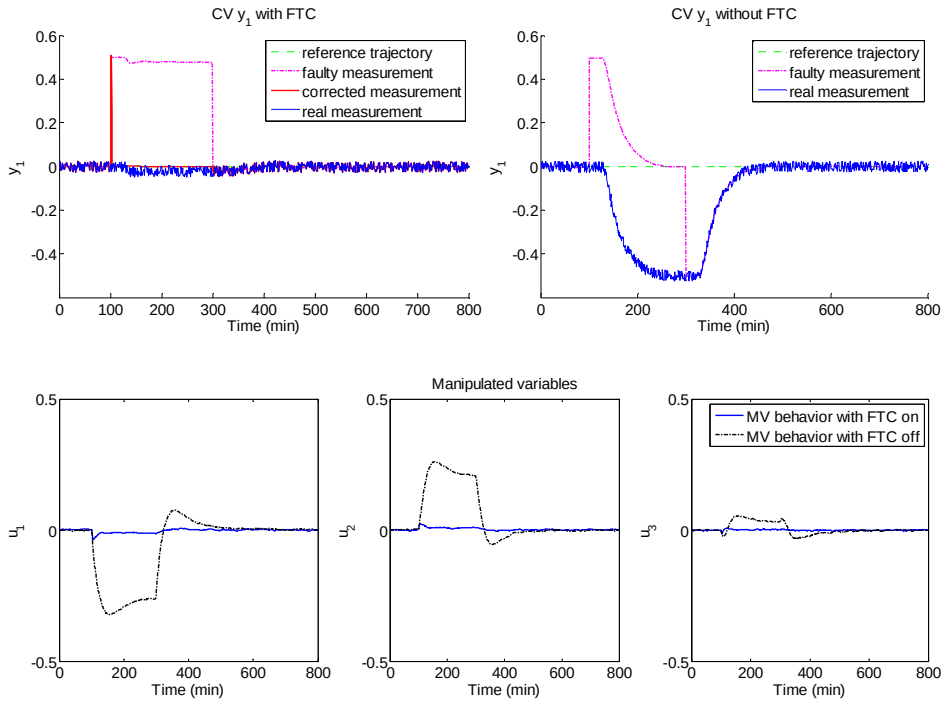

Figure 20. The performance of the fault accommodation-based FTC strategy with the PLS-based FDD in the case of a bias fault in y_1.

In order to reflect the accuracy of the FDD method prediction while testing the FTC, the integral of squared error (ISE) index is calculated and it is presented in Table 5 for each of the FTC combinations. In essence, the ISE-index presents numerically the deviation of the variable from the setpoint value. The higher the score is, the less accurate the FDD and less effective FTC combination are.

Table 5. The ISE index values for different FDD components when a bias or drift fault is affecting the distillation analyser endpoint measurement y_1.

FDD component	**Bias Fault: ISE**	**Drift Fault: ISE**
PCA	0.6281	0.613
PLS	0.6201	0.5299
SMI	0.6879	0.6883

Finally, the performance of the fault accommodation FTC strategy with the different FDD methods is compared by measuring the computation times for the whole duration of the simulation (800 minutes in simulation time). The simulation was first run without any FTC active and then with each of the FDD methods and the fault accommodation FTC strategy for the 10 times for each method. The average of the computation times for each combination was then calculated and is presented in Table 6.

Table 6. The average computation times (in real time) of the simulation lasting 800 minutes (in simulation time) for different FDD methods, when a drift fault is affecting the distillation analyser endpoint measurement y_1.

FDD method:	**Drift fault: average computation times (10 simulations)**
No FTC	48.31 s
PCA	50.61 s
PLS	49.74 s
SMI	50.28 s

The processor for running the simulations was Intel Core 2 Extreme running at 3.2 GHz and the computer was equipped with 4 GB of RAM. When none of the FDD methods were active, the simulation took in average 48.31 seconds to run, with PCA 50.61 seconds, with PLS 49.74 seconds and with SMI 50.28 seconds on average. Based on these computation times, the PLS is the fastest method requiring only 1.5 seconds more average computation time than the simulation without any of the FDD methods or the FTC active. It should be noted that as the average computation times of all of the methods were within 1 second of each other, the differences in the average computation times were small.

Based on all of the testing and the results, the active fault accommodation FTC strategy with the PLS as an FDD method had overall the best FDD performance and it is therefore the most promising FDD component for the fault accommodation-based FTC strategy.

4.4 Summary of testing the data-based FDD methods with the fault accommodation-based FTC strategy for the analyser and sensor faults

In this chapter, the developed active fault accommodation-based FTC strategy was tested with PCA-, PLS- or SMI-based FDD methods for controlling a simulated crude oil distillation column model from the Shell control problem by Prett & Morari (1987). The active fault accommodation-based FTC strategy composed of three different FDD components and a fault accommodation-based FTC part was successfully implemented for the detection, isolation, identification and accommodation of the faults in the simulated analyser outputs and process measurements. Based on the results of the preliminary testing, the presented methods have proven to be effective and the active fault accommodation-based FTC strategy was able to counter bias and drift faults in the measurements of the simulated oil refining process unit. With the PCA-based FDD method, the PCA model was calculated for each output variable and the SPE index was used for the fault detection with the Hotelling T^2 index only being used for comparison purposes. The RMSEP index calculation based on latent variables of the PLS, was used for the fault detection in the PLS-based FDD. The SMI-based FDD utilised the residual between the identified model output and the measurement value to determine whether a fault is present in the measurement. A cumulative sum algorithm was implemented with the FTC in order to avoid false alarms and to dampen the effect of the FTC on the measurement signal when the fault no longer affects the process.

In general, the performance of the tested FDD methods and the active fault accommodation-based FTC strategy was good; the maximum deviation between the faulty and the compensated measurement values is small - less than 12% of the maximum fault magnitude in all cases. The tested the PCA, PLS or SMI as the FDD methods and the active fault accommodation-based FTC strategy effectively detected, isolated and accommodated the faults that were introduced into the process measurements. The bias faults were detected only after the delay caused by the cumulative sum algorithm. For drift-shaped faults, the fault detection rate varied between 27 - 33 minutes (14 - 17% of the time the fault is affecting the target process), where the PLS-based FDD was the fastest and the SMI-based FDD the slowest. Generally, in all cases the fault was detected early enough so that the effect of the fault on the measurements was small, less than 12% of the magnitude of the fault. The best performance in terms of the smallest effect on the measurements was achieved using PLS for both fault types. The computation times for different methods were also calculated and the PLS was the fastest method with 49.74 seconds average computation time, even though the differences between the computation times were small in general.

All of these results indicate that the presented methods have the potential to be used for the fault-tolerant control of more complex industrial processes. The fault accommodation part of the FTC strategy also worked efficiently in combination with the FDD methods. In general, however, the PLS had the best performance and the PLS is therefore the best candidate as an FDD component in the final FTC strategy.

Overall, the results of the experiments suggest that the tested active fault accommodation-based FTC strategy is effective, fast and able to counter different kinds of faults. As the crude oil distillation columns are in a crucial position in complex refineries, a fault-free operation of the unit is essential in order to ensure a reliable supply of raw materials to the other parts of the plant. The effects of the tested faults in a process without the active fault accommodation-based FTC strategy are given in Appendix B. In general, the impact of the faults was large, the magnitude of the disturbances being at the maximum value or near to the maximum value of the hard constraint limit of the variables. Such faults would definitely cause problems in actual process unit and lead to additional disturbances, and possibly even result in serious financial losses and equipment damage if they remain undetected.

The more detailed test results of the fault accommodation-based FTC strategy are presented in Kettunen et al. (2008), where the author has tested the FTC strategy together with the PI-based control strategy and compared the differences and the effectiveness between the PI-based FTC and MPC-based FTC.

5 Description of the target dearomatization process and its control strategy

After the theoretical background for developing an FTC strategy has been developed, it is possible to describe the target testing process along with the control objectives. Generally, a suitable testing environment for a fault-tolerant MPC is a complex industrial process, such as LARPO dearomatization process at the Naantali refinery, with faults in the measurements, actuators and, for example, the process analysers. In this chapter, the description of the target industrial dearomatization process and its control strategy are given.

5.1 Description of the dearomatization process

The target process for the FTMPC is a complex industrial dearomatization process, LARPO, located in the Naantali refinery owned by Neste Oil Oyj. The purpose of the LARPO dearomatization process is to remove aromatic compounds from the solvent feedstock through catalytic hydrogenation in a continuous process. Exothermic saturation reactions take place in the reactors, which remove the aromatic compounds from the feed. The product quality parameters, such as the initial boiling point (IBP) or flashpoint (FP), are adjusted in the distillation part of the unit. LARPO is in a crucial position in the Naantali refinery because most of the solvent products of the refinery are non-aromatic, and a failure in the product quality analysers may cause large quantities of off-spec products and thus significant financial losses. Potentially, a low quality end product may have an effect on the customers and create problems in selling the final products.

The LARPO dearomatization process is composed of two trickle-bed reactors with packed catalyst beds to remove the aromatic compounds; a distillation column used to control the specifications of the end products; several heat exchangers, which import and export energy in the process; separation drums; a filling plate stripper as well as other process equipment, which carry out supplementary tasks in the unit. The flow diagram of the LARPO process is presented in Figure 21 according to Vermasvuori et al. (2005).

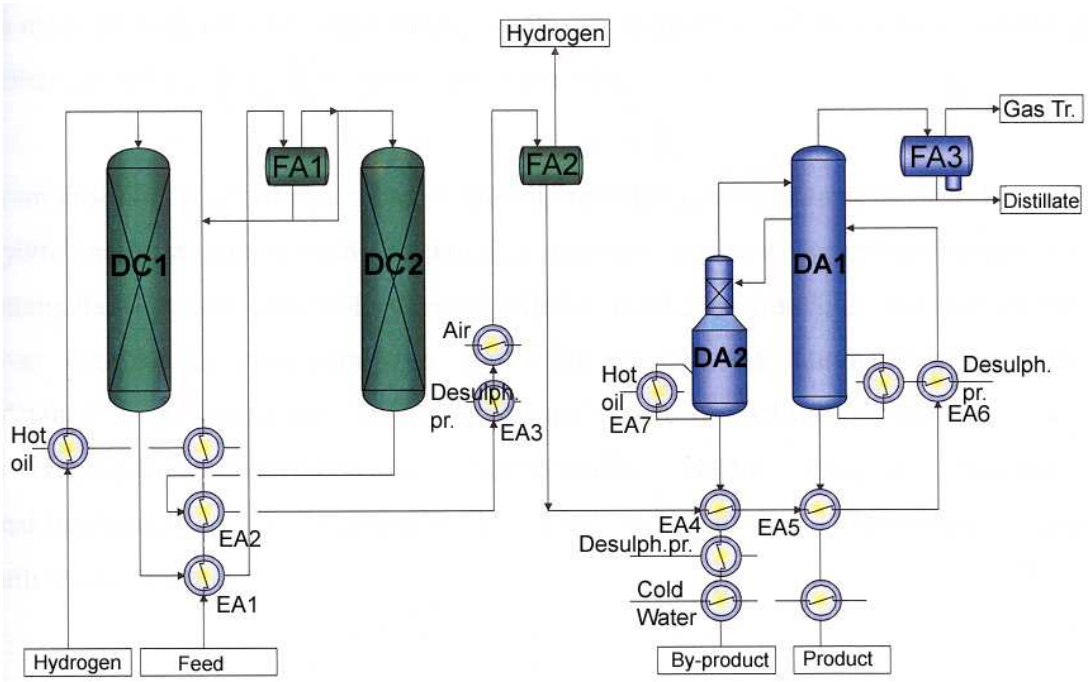

Figure 21. The industrial dearomatization process, LARPO, according to Vermasvuori et al. (2005).

The feedstock fed into the unit is heated up to reaction temperature using the heat circulated from the reactors through heat exchangers EA1 and EA2, as well as a hot oil heat exchanger. This heated stream is then fed to reactor DC1, together with the recycled liquid feed and heated hydrogen feed composed of fresh and recycled hydrogen. If the catalyst of the first reactor is at the beginning of the catalyst's life-cycle, most of the aromatic compounds are removed in the first reactor; however, at the end of the catalyst's life-cycle, more and more reactions also take place in the second reactor DC2.

After passing from the first reactor DC1, the product feed is cooled down in heat exchanger EA1 and then fed to gas separation drum FA1, where gaseous and liquid products are separated. A low-aromatic feed is cut off and fed back to reactor DC1 in order to ensure a higher feed rate and lower end product aromatics content. Separated gas, the rest of the liquid products and quench hydrogen are fed to reactor DC2. In reactor DC2, the level of aromatics in the products is further decreased until it meets the final quality requirements of the end products.

The product of the dearomatization process in the second reactor DC2 is cooled down in heat exchangers EA2 and EA3, and by using an air cooler. This stream is then fed to the second gas separation drum, FA2, where gaseous and liquid products are again separated. The gaseous product mainly contains unreacted excess hydrogen, and this hydrogen flow is mixed with fresh hydrogen feed and fed back to the first reactor, thereby increasing the total hydrogen pressure in the unit and improving the hydrogenation process. The liquid low-aromatic product stream is heated in heat exchangers EA4 and EA5 using heat from the product and by-product streams. Before reaching the distillation column, the feed is further heated at heat exchanger EA6 using desulphurised product feed from another process unit.

In distillation column DA1 (contains 42 trays), heat exchanger EA6 provides distillation column DA1 with energy with which to boil column DA1 feed. A side stream is conducted to by-product stripper unit DA2 (contains 4 trays), which is heated by heat exchanger EA7 using hot oil. The by-product stream is drawn off from the bottom of the stripper unit DA2, and heats the feed of column DA1 at heat exchanger EA4. The stream from column DA1 overhead is cooled and this stream is then fed to the overhead drum FA3. In overhead drum FA3, the liquid is divided into distillate and reflux flows; the gaseous part is then separated and removed from the unit. Column DA1 distillate contains lighter compounds, such as gasoline, and is forwarded to other units for further processing. The non-aromatic main product is drawn off as a bottom product of column DA1. The DA1 bottom product is then cooled down in heat exchanger EA5, which also heats up the feed to column DA1. The quality of the final product is measured with flashpoint and distillation curve analysers. The quality of the by-product from stripper unit DA2 is also monitored by means of a flashpoint analyser. The laboratory analyses of the main product and the by-product feeds are carried out three times a day in order to ensure the quality of the end products.

The feedstock type of the dearomatization unit is changed once every four days on average. The properties of the feedstock vary and there are as many as six different types of petroleum and light gas oil cuts used as feed for the unit. The heavier part of the distillation curve, the distillation end point property of the product, is mainly adjusted in the previous process units; however, the lighter end of the distillation curve, the initial boiling point and flashpoint properties are adjusted in the LARPO distillation column DA1 based on the product specifications.

The Naantali refinery is a special products plant, which has a wide product palette containing over 140 different oil refining products. The capacity of the refinery is relatively small - some three million tons of crude oil is processed each year - compared to most oil refineries in Europe, which ranks the refinery in the fourth quarter of European refineries based on the amount of processed crude oil. The major part of the production and income in the refinery is composed of the production of low-sulphur fuel and diesel products. Some 25% of all products are exported, the rest being supplied to domestic markets. One of the most profitable products in the Naantali refinery is the special solvents produced out of naphtha, kerosene and middle distillates.

In a small refinery such as Naantali, the quality of the end products is of high importance. There are several factors affecting the quality requirements of specialty products such as their potentially high price and the increasing quality and safety demands. It is therefore important to ensure the continuous, stable production of in-spec quality products. For this reason, the correct and accurate operation of the analysers, process measurements and controllers is an especially critical factor for the successful operation of the solvent units and the production of special solvent products.

5.2 Control strategy of the dearomatization process

In this section, the control strategy for the LARPO dearomatization process is presented by introducing the basic control strategy, the MPC objectives and the MPC control variables of the target process.

5.2.1 Basic control strategy of the dearomatization process

As the dearomatization process is a complex industrial unit, a large number of measurements and sub-level controllers are utilised to stabilise and control the reactions and flows within the unit. In the following, the basic controls of the LARPO unit are presented.

The liquid feedstock volume flow rate to the unit is usually determined by the amount of desulphurised feed coming directly from the previous process unit. The feed flow controller can be set in a cascade mode in order to adjust the feed rate on the basis of production volumes of the previous unit. The LARPO unit can also take feed from a feed tank, in which case the flow rate is set manually by the operating personnel. The fresh hydrogen flow rate to the first reactor, DC1, is adjusted with a flow controller. The goal of the fresh hydrogen feed controller is to provide hydrogen to successfully carry out hydrogenation and to protect the catalyst from coking.

The temperature of the liquid feed entering the first reactor is controlled by adjusting the bypass of feed heat exchangers EA1 and EA2, and by controlling the hot oil flow to the hot oil heat exchanger before the first reactor DC1. The hot oil temperature controller also adjusts the hydrogen temperature, because the same amount of hot oil flows through the hydrogen feed flow. As the hydrogenation reaction is highly exothermic, the temperatures within reactors DC1 and DC2 are monitored carefully with four temperature sensors located in each reactor bed, and in the inlet and outlet of reactors DC1 and DC2.

After the first reactor, DC1, part of the liquid product and hydrogen is relayed back to the unit feed by means of flow controllers. This liquid recycle feed keeps the hydrogenation process under control and further prevents catalyst coking. The recycled hydrogen further improves the removal of aromatic compounds, adjusts the pressure of the first reactor DC1 and maximises the hydrogen-to-oil-ratio, depicting the relative amount of hydrogen against the feed flow rate, and also protects the catalyst from coking.

After reactor DC2, the mixed flow is cooled down in heat exchangers EA2 and EA3 and the air cooler by using a temperature controller that adjusts the air cooler air flow rate and the effectiveness of the cooler.

The cooled down liquid flow is separated from hydrogen in the second separation drum, FA2, and, based on the unit pressure, the excess hydrogen is then forwarded through a pressure controller to other hydrogen consuming units in the refinery. The level controller of the second separation drum, DA2, adjusts the liquid flow rate onward.

The liquid non-stabilised feed of the column DA1 is heated up again in heat exchangers EA4 and EA5, and finally by means of a temperature controller cascaded with two flow controllers; part of the feed is relayed through heat exchanger EA6, while part of the feed flows directly to column DA1. The temperature of column DA1 is controlled both by the feed temperature and also by the reboiler of column DA1 recycling hot flow in the bottom part of column DA1. When the temperature of column DA1 is increased, the bypass of the reboiler is closed, and when the temperature is lowered the bypass valve of the reboiler is again opened.

The separation accuracy and the temperature of the top part of column DA1 are adjusted with the reflux flow that feeds part of the distillate back to column DA1. The liquid distillate flow is adjusted on the basis of the level measurement of overhead drum FA3. The pressure of column DA1 is adjusted with the purge gas flow from the overhead drum.

The feed rate of stripper unit DA2 is adjusted by a flow controller and its temperature is adjusted by a hot oil reboiler.

The primary product flow from the bottom of column DA1 is controlled with the DA1 level controller. A similar arrangement is set to stripper unit DA2, where by-product flow from the bottom of stripper unit DA2 is controlled by the DA2 level controller. The final product and by-product are finally cooled down by using the heat energy to first heat up the column feed, and then by using a temperature controller adjust the water flow to the product heat exchangers.

The basic controllers of the LARPO process are also presented in Figure 22 (HO = 'Hot Oil' and CW = 'Cooling Water').

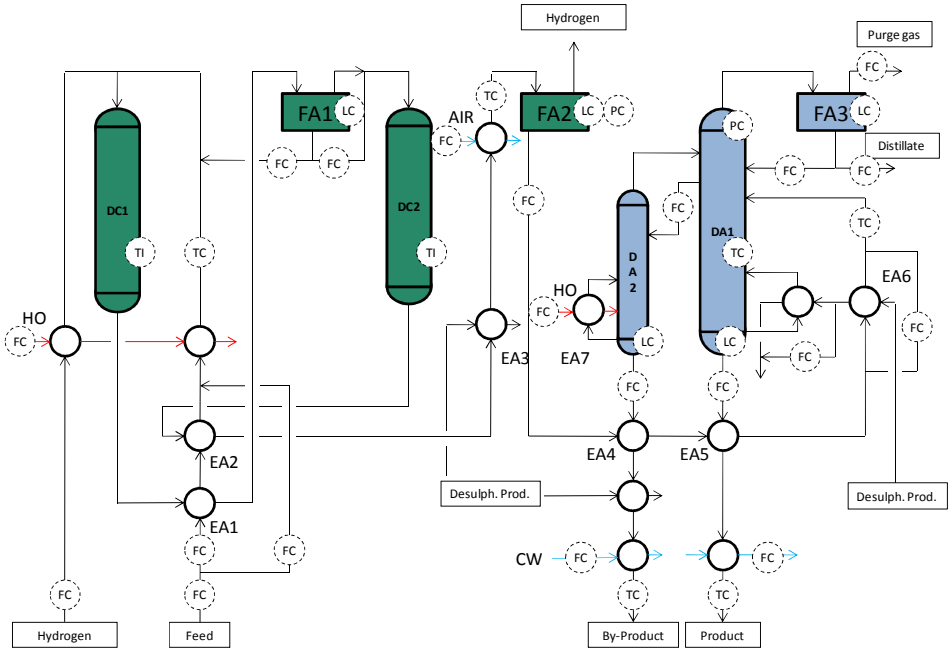

Figure 22. The controllers of the industrial dearomatization process, LARPO, located at the Naantali refinery.

5.2.2 Control objectives of the MPC for the dearomatization process

The primary control objective for the MPC of the LARPO dearomatization process is to keep the distillation column DA1 bottom product above the product quality limit. A secondary objective is to minimise the additional production costs by aiming to keep the product quality as close as possible to the specifications while maximising the feed rate. In practice, the goals are to maintain the DA1 bottom product within the specifications (initial boiling point, flashpoint or DA1 temperature), and to minimise the DA2 bottom product flashpoint within the by-product specification limits.

In the measurements of both the DA1 and DA2 bottom product, the product quality should never fall below the minimum specification limits. If the quality specifications are not met, off-spec production occurs and an over-quality product needs to be mixed with the off-spec product in order to meet the specifications. However, if the value of the variables is higher than the minimum limit, energy and financial losses increase because a larger amount of valuable product goes for reprocessing with the overhead distillate flow.

5.2.3 Control variables of the MPC for the dearomatization process

Five controlled variables are defined for the MPC of the LARPO dearomatization process: column DA1 bottom product initial boiling point (DA1_BP_IBP); DA1 bottom product flashpoint (DA1_BP_FP); DA1 liquid distillate flow rate (DA1_DIST_FC); DA1 pressure-compensated temperature (DA1_TC); and column DA2 bottom product flashpoint (DA2_BP_FP). The LARPO controlled variables are presented in Table 7 along with the control objectives in parenthesis.

Of these controlled variables, DA1_BP_IBP, DA1_BP_FP and DA1_TC are alternative variables and thus only one of these can be used at a time for control. Only DA1_BP_FP is relevant to the specific heavy feedstock that is studied in this thesis.

Overhead flow rate DA1_DIST_FC is minimised by controlling by-product flashpoint DA2_BP_FP, and thus maximising flow to by-product stripper unit DA2 and therefore minimising overhead flow rate DA1_DIST_FC.

Four disturbance variables are used in the MPC: the DA1 feed flow rate (DA1_FEED_FC); the DA1 feed temperature (DA1_FEED_TC); the DA1 heating medium temperature (DA1_HEAT_TC); and the DA1 pressure (DA1_PC). The LARPO disturbance variables are presented in Table 8.

Four manipulated variables are used for the control of the process: the DA1 reflux flow rate (DA1_REFLUX_FC); the EA6 hot stream feed rate (DA1_EA6_FEED_FC); the DA2 feed flow rate (DA2_FEED_FC); and the EA7 hot stream feed rate (DA2_EA7_FEED_FC). The LARPO manipulated variables are presented in Table 9 along with the control objectives in parenthesis.

Table 7. The LARPO controlled variables.

Variable name	**Variable description**	**Unit**
DA1_BP_IBP	DA1 bottom product initial boiling point *(target)*	*°C*
DA1_BP_FP	DA1 bottom product flashpoint *(target)*	*°C*
DA1_DIST_FC	DA1 liquid distillate flow *(minimise indirectly)*	*kg/h*
DA1_TC	DA1 pressure-compensated temperature *(target)*	*°C*
DA2_BP_FP	DA2 bottom product flashpoint *(target, minimise)*	*°C*

Table 8. The LARPO disturbance variables.

Variable name	**Variable description**	**Unit**
DA1_FEED_FC	DA1 feed flow rate	*t/h*
DA1_FEED_TC	DA1 feed temperature	*°C*
DA1_HEAT_TC	DA1 heating medium temp.	*°C*
DA1_PC	DA1 Pressure	*kPa*

Table 9. The LARPO manipulated variables.

Variable name	**Variable description**	**Unit**
DA1_REFLUX_FC	DA1 reflux flow rate (*maximise*)	*t/h*
DA1_EA6_FEED_FC	EA6 hot stream feed rate (*minimise*)	*t/h*
DA2_FEED_FC	DA2 feed flow rate (*maximise*)	*t/h*
DA2_EA7_FEED_FC	EA7 hot stream feed rate (*keep steady*)	*t/h*

6 Integrated FTMPC for the industrial dearomatization process

As continuous plant operation is essential especially in a plant producing highly profitable products, the careful design of an FTMPC is critical for the plant's fault-free operation. This usually requires, in addition to theoretical research, extensive interviews with the plant personnel and the study of logbooks, incidence reports and maintenance department records. Based on this gathered information the specification of the design schemes can be made and an active integrated FTMPC for control of the target process delivered.

In this chapter, the requirements for the active FTMPC for the target dearomatization process are presented first. Second, the faults in the target process are discussed and finally the integrated FTMPC with its three parallel-running FTC strategies are described.

6.1 The requirements of the FTMPC for the industrial dearomatization process

In order to successfully apply the FTC design schemes while creating an FTMPC for the dearomatization process, the user requirements of the FTMPC are determined. The requirements for an FDI strategy to be implemented in the Naantali refinery have earlier been determined by Vatanski et al. (2005) in the same project in which the author has been working in. These user requirements have been determined through interviews carried out in the Naantali refinery during autumn 2004. The interviews were based on four topics. First, the user interface, interface to other parts of the control strategy and the installation, upkeep and updating of the active FTC strategy were discussed. Second, typical faults in the process analysers were determined. Third, the information and tools for detecting faults by the plant personnel were recorded. Fourth, the FTC actions after the detection of the fault were decided upon and the needs for the automated actions were charted. Based on the responses, a set of requirements was determined for an FDI strategy, but the results of the interviews apply to the development of the FTMPC as well.

The resulting user requirements were focused on five topics. First, the fault types to be detected should contain at least a drifting fault. Second, the fault detection should happen as early as possible. Third, the FDI method should provide enough background information about the fault detection and diagnosis. Fourth, the external factors and specially the operating point changes should be taken into account; and finally, the measurement device calibrations should be taken into account and not categorised as faults. These requirements are presented in following Table 10.

Table 10. The requirements for the FDI strategy in the Naantali refinery according to Vatanski et al. (2005).

Requirement topic	**Requirement**
Detected types of fault	The FDI strategy shall detect incipient faults that do not cause variables to violate their alarm limits.
	The FDI strategy should detect faults especially drifting of the measuring devices.
Time instant of fault detection	The strategy should be able to inform the operator about faulty conditions as early as possible. When the faults are detected in time their effects are easier to mitigate and have smaller impact on the overall process.
Background information about the FDI methods	The strategy shall provide background information about the fault detection and isolation methods used, as well as the assumptions used in diagnosis.
FDI taking into account external factors	The FDI strategy shall identify and be aware of the current operating point in order to be able to detect smaller deviations from nominal operation conditions
	The change in the operation point shall also be detected and must not be categorised as a fault.
Being aware of the calibration of measurement devices	The effects of calibrating measurement devices shall be stored and taken into account in fault diagnosis because calibration produces sudden changes in measurement values, and these might be detected as faults.
	The date of calibration shall be used as one reliability measure of the measurement.

6.2 Faults in the target dearomatization process

In a study carried out by Liikala (2005), the process diary and process history of the Naantali refinery were examined in order to gather information of the faults in the dearomatization process. During the time period covered in that study, nearly 70% of all faults in the LARPO unit were related to analysers as shown in Figure 23.

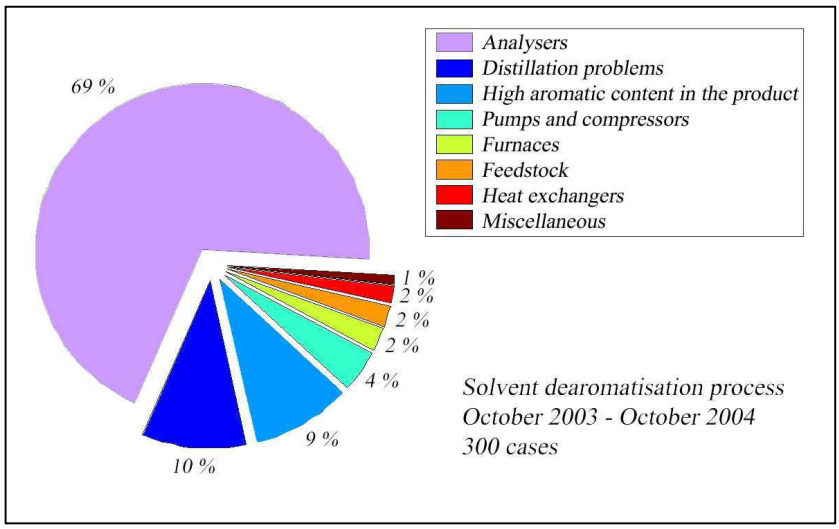

Figure 23. The most common faults in the dearomatization process during one year of operation (Liikala, 2005).

In order to gather more information on the faults and their effects on the process, data from the Naantali refinery maintenance department were studied during 09/2008-09/2009 by the author. During this period, faults such as temperature, flow and pressure measurements, control valves and process analysers were taken into account. All faults requiring maintenance work were included in the study. The fault data was divided into three categories: analyser faults, measurement device faults and control valve faults. Based on the results, 42% of the faults were located in the analysers; 42% in the measurement devices; and 16% in the control valves. The results are given in Figure 24.

In addition to data from the maintenance department, the flashpoint analyser output on a heavy grade feed run was compared to the laboratory measurements during the period 09/2008 - 09/2009. The flashpoint analysis utilises EN ISO 2719-2002 M method and the method has a repeatability of 2.8°C on the given data set. The aim of the comparison was to determine the number of measurements in which the analyser measurement differed from the laboratory measurement by more than 2.8°C, which in practice means that the analyser measurement was faulty. In addition, the downward faults causing off-spec and upward faults resulting in over-quality products were categorised.

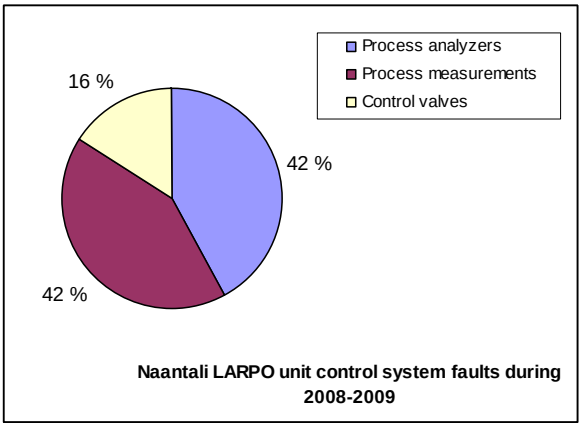

Figure 24. The LARPO sensor, measurement and actuator faults during 09/2008 - 09/2009.

Based on the data, it was estimated that off-spec was produced due to the analyser faults in 3% of the cases and too high quality product was produced in 3% of the cases. In total, 6% of the analyses during the heavy grade run differed by more than 2.8°C from the analyser readings, causing either off-spec production or too high quality production.

Based on these studies, it can be concluded that most of the faults in the LARPO unit were located in process analysers, although also some faults have been present in other measurements and control valves of the unit. The fault types to be tested with the final active FTC strategy are thus narrowed down to bias- and drift-shaped faults for the analysers and sensors of controlled variables, a bias-shaped fault for the sensors of disturbance and manipulated variables and a stuck valve fault for the actuators.

6.3 Description of the three parallel-running FTC strategies of the integrated FTMPC for the industrial dearomatization process

Three parallel-running FTC strategies of the integrated FTMPC for the target dearomatization process are next proposed based on the integrated FTC design scheme presented in Section 3.5.3.

The first FTC strategy includes a fault accommodation-based strategy for the CV and DV sensor faults based on the fault accommodation FTC design scheme presented in Section 3.5.1 and the recursive PLS as an FDD. The second strategy is composed of the fault accommodation- and controller reconfiguration-based FTC strategies presented in sections 3.5.1 and 3.5.2 for the MV sensor faults, where the controller reconfiguration part is adopted from DCP principle by Buffington and Enns (1996). The last strategy is composed of the controller reconfiguration-based FTC strategy for the MV actuator faults based on the DCP principle, the controller reconfiguration FTC design scheme presented in Section 3.5.2 and an FDD method based on the difference between MV setpoint and measurement. In the following, these three parallel-running FTC strategies are described.

6.3.1 Active fault accommodation-based FTC strategy for the sensor faults of the controlled and disturbance variables

The first FTC strategy is used to reduce the effect of the faults in the CV or DV sensors or, for example, in process analysers. The fault accommodation-based FTC is used for accommodating the faults with the fault estimation gained from the FDD. A recursive PLS is used for estimating the values of the faulty measurements.

The active FTC strategy for both the CV and DV sensor faults is based on the fault accommodation FTC design scheme presented in Section 3.5.1 and in Figure 5. In this FTC strategy, the faults in the CV or DV sensors are first detected by the FDD. After successful fault detection, the magnitude of the fault is estimated and this estimation is then used to accommodate the faulty measurement. As soon as the fault is removed from the process, the correction value is removed. Detection of the fault is based on the PLS RMSEP index, and the suitable threshold for each variable is determined on the basis of the RMSEP values during the nominal unit operation.

6.3.1.1 FDD for the fault accommodation-based FTC strategy for CV or DV faults

The FDD for the CV or DV sensor faults is based on the PLS and the commonly known NIPALS algorithm by Wold et al. (1983), which has been described earlier in Section 3.4.2. The PLS method has also been presented in a paper by Vermasvuori et al. (2005); however, the PLS method used in the thesis utilises a PLS algorithm, enhanced by the author to use recursive inputs, which essentially adds a dynamic element to the PLS formulation. In the recursive PLS, two models are implemented for each variable in order to prevent the accumulation of faults through recursive inputs. One of the PLS models controls fault detection (preventing faulty information to be relayed to the fault estimations); the other carries out fault estimation. These modifications essentially make the algorithm used in the final application of the thesis different from that used by Vermasvuori et al (2005). The author also wishes to note that the focus of this thesis is not on FDI (as it is in the paper by Vermasvuori et al., 2005), but in the development of the integrated FTMPC.

The CV values are estimated by using all of the control system DVs and MVs an input to the PLS. The delay the CV estimation is the maximum delay between each of the input variables (DV or MV) and the CV. In addition, two past values of the outputs are used as inputs; one value from the time step $t\text{-}d_1$, and the other from the time step $t\text{-}d_2$, where $d_1<d_2$. The past values introduce a recursive element to the PLS, thus significantly increasing the estimation accuracy of the models. The first set of PLS models is used for fault detection and the second set for the fault estimation. The measurements used to estimate the CVs are: the DA1 feed flow rate (DA1_FEED_FC); the DA1 feed temperature (DA1_FEED_TC); the DA1 heating medium temperature (DA1_HEAT_TC); the DA1 pressure (DA1_PC); the DA1 reflux flow rate (DA1_REFLUX_FC); the EA6 hot stream feed rate (DA1_EA6_FEED_FC); the DA2 feed flow rate (DA2_FEED_FC); and the EA7 hot stream feed rate (DA2_EA7_FEED_FC).

Since the recursive element may also carry over faulty data before this fault is detected, another PLS model is required to estimate the measurement values with non-faulty data. This means that the active FTC strategy has enough time to detect the faults before the fault contaminates the PLS estimation models through the recursive input. This second set of models have exactly the same input values, except for the past output measurement values, which are derived further from the past from the time step $t\text{-}d_3$ and the time step $t\text{-}d_4$, where $d_1<d_2<d_3<d_4$. The second set of PLS models is used for fault estimation. The accuracy of the second model is not as good as the first because the delay between the past output values and the current output is larger, but the accuracy should be sufficient enough to provide a reliable fault estimation.

The DV values are estimated by using the current output values. In this case, the delay of the DV fault detection is the maximum delay between the DV to be predicted and the measurements used for estimating the DV values. Since the FTC for the CV sensor faults is partially based on DV values, a different set of measurements is used for the estimation of the DV values. The measurements used for the DV estimations are the DA1 overhead temperature measurement (DA1_TEMP_1); the temperature at tray 13 (DA1_TEMP_3); the temperature at tray 21 (DA1_TEMP_4) and the column DA1 overhead gas flow rate (DA1_OVHD_FLOW_FC).

The estimation of the DV values also utilises recursive PLS. The two past values of the output are used as inputs; one value from the time step $t\text{-}d_{max}\text{-}d_3$ and the other from the time step $t\text{-}d_{max}\text{-}d_4$, where d_{max} is the maximum delay between PLS inputs and outputs and d_3 and d_4 are the delays for the dynamic FDD. The first PLS model is used for detecting the faults and the second for estimating the fault magnitude.

6.3.1.2 FTC for the fault accommodation-based FTC strategy for CV or DV faults

The FTC part of the fault accommodation-based FTC strategy is based on the fault accommodation design scheme presented in Section 3.5.1. As described in the scheme, the degree of fault accommodation is handled with a fault detection delay counter, which increases the amount of accommodation during each time step the fault is detected. In essence, the delay counter is increased by one after each one minute control cycle has passed and a fault is detected. When the value of the counter exceeds the preset low limit *LL*, the FTC action is engaged. In this case the fault accommodation is carried out and the faulty CV or DV is accommodated with the fault estimation Δy provided by the PLS and multiplied with the degree of accommodation L presented in equation (38). On the other hand, if no fault is detected, the counter is decreased by one after one minute control cycle has passed and if no fault is detected. If the counter value goes below the limit *LL*, the fault accommodation is disabled and the correction value is removed.

The procedure and the flowchart for the CV or DV sensor faults are presented in Appendix A.1.

6.3.2 Active fault accommodation and controller reconfiguration-based FTC strategy for the sensor faults of the manipulated variables

The second FTC strategy is used to reduce the effect of the faults in the MV sensors. The fault accommodation- and controller reconfiguration-based FTC is used to accommodate the faults with the fault estimations gained from the FDD. A recursive PLS is used to detect the faults and estimating the values of the faulty measurements.

The active FTC strategy for MV sensor faults is based on the fault accommodation and controller reconfiguration FTC design schemes presented in Sections 3.5.1 and 3.5.2 and in Figure 5 and Figure 9. If a fault is detected in an MV measurement, it is adjusted by the magnitude of the fault estimation and, after this, the reconfiguration actions are engaged; the faulty MV is moved to the opposite direction by the amount of fault magnitude and the MV is set as a DV in the MPC and an auxiliary DV is used as an MV. When the fault is removed from the process, the original MPC and FTC structure is restored and the MV can again be used for control.

6.3.2.1 FDD for the fault accommodation- and controller reconfiguration-based FTC strategy for MV sensor faults

The MV values in the past are estimated by using the current measurement outputs as an input to the PLS. As with the DVs, the delay is the maximum delay between the MV and the measurements used for the estimation. The measurement set used for the estimation of the MV values is slightly different from that with the DV value estimation; in this case, each of the MV has a unique set of input variables to be used for the estimation. This kind of approach is required because without careful variable selection, the performance of the control system is greatly affected. For instance, if an input variable with a long delay to the MV is selected, this directly affects the delay in detecting the faults. Only one PLS model is used for the FDD in this FTC strategy.

Overall, the variables used for the estimations are the column DA1 overhead temperature (DA1_TEMP_1); the temperature at tray 5 (DA1_TEMP_2); the temperature at tray 13 (DA1_TEMP_3); the temperature at tray 21 (DA1_TEMP_4); the temperature at tray 41 (DA1_TEMP_5); the temperature of the bottom product (DA1_TEMP_6); the DA1 overhead gas flow rate (DA1_OVHD_FLOW_FC); the DA1 bottom product flow rate (DA1_BP_FC); the DA2 overhead gas flow rate (DA2_DIST_FC); the DA2 upper pressure measurement (DA2_PC1); the DA1 feed exchanger hot fluid flow rate (DA1_FEED_EA_FC); the DA2 bottom product temperature (DA2_BP_TC); and the DA2 bottom product flow rate (DA2_BP_FC).

6.3.2.2 FTC for the fault accommodation- and controller reconfiguration-based FTC strategy for MV sensor faults

The FTC part for the MV sensor faults consists of two parts: a fault accommodation part and a controller reconfiguration part. Again, the FTC actions are handled with a fault detection delay counter, which increases the amount of accommodation during each time step the fault is detected. The delay counter is increased by one after each one minute control cycle has passed and a fault is detected. When the value of the counter exceeds the preset low limit *LL*, the FTC action is engaged. In this case the faulty MV is moved to the opposite direction of the fault by the amount of fault estimation, the MV is accommodated with the fault estimation and the MV is set as a DV in the MPC. In addition, in order to cover for the loss of an MV, and auxiliary MV, DA1 feed temperature controller (DA1_FEED_TC) is used as an MV instead. On the other hand, if no fault is detected, the counter is decreased by one after one minute control cycle has passed and if no fault is detected. If the counter value goes below the limit *LL*, the previously faulty MV is set back as an MV in MPC, the fault accommodation is removed and the auxiliary MV DA1_FEED_TC is set back to DV.

The procedure and the flowchart for the MV sensor fault are presented in Appendix A.2.

6.3.3 Active controller reconfiguration-based FTC strategy for the actuator faults of the manipulated variables

The third FTC strategy is used for reducing the effect of the faults in the MV actuators. The DCP-based controller reconfiguration algorithm is used in the FTC strategy for the actuator faults. In this case, the FDD is based on the difference between the MV setpoint and the MV measurement value.

The active FTC strategy for MV actuator faults is based on the controller reconfiguration FTC design schemes presented in Section 3.5.2 and in Figure 9. If an actuator fault is detected, the FTC algorithm is triggered and the faulty variable is set as a DV and the auxiliary MV variable is set as an MV.

6.3.3.1 FDD for the controller reconfiguration-based FTC strategy for MV actuator faults

The FDD for the controller reconfiguration-based FTC for MV actuator faults is based on the difference between the setpoint and the measurement value of the MV. The detection of a stuck valve fault is based on the RMSE index, which is calculated from the difference between the MPC control output and the controller measurement. If the difference between the setpoint given by the MPC and the sub-level controller measurement is sufficiently large, and the cumulative sum has increased enough, the MV is declared faulty and the FTC actions are engaged.

The four MVs to be monitored are the DA1 reflux flow rate, the EA6 hot stream flow rate, the DA2 feed flow rate and the EA7 hot stream flow rate. These variables form the primary control set for column DA1, and the DA1 feed flow temperature is used as a secondary control set. Since all four MVs adjust the energy balance in the column, the column feed temperature controller can temporarily replace one or more of the MVs.

6.3.3.2 FTC for the controller reconfiguration-based FTC strategy for MV actuator faults

The FTC part for the MV actuator faults consists of controller reconfiguration. The FTC actions are handled with a fault detection delay counter, which increases the amount of accommodation during each time step the fault is detected. The delay counter is increased by one after each one minute control cycle has passed and a fault is detected. When the value of the counter exceeds the preset low limit *LL*, the FTC action is engaged. In this case the faulty MV is set as a DV in the MPC. In addition, in order to cover for the loss of an MV, and auxiliary MV, DA1 feed temperature controller (DA1_FEED_TC) is used as an MV instead. On the other hand, if no fault is detected, the counter is decreased by one after one minute control cycle has passed and if no fault is detected. This time the faulty MV cannot be automatically normalised, as the FDD is based on the difference between the setpoint and the measurement and thus this value is no longer updated when the MV is removed from the MPC. Therefore, the faulty MV needs to be manually returned by the operator when the fault has been corrected in the faulty actuator.

The procedure and the flowchart for the MV actuator fault are presented in Appendix A.3.

7 Performance validation and economic evaluation of the integrated FTMPC for the target dearomatization process

Before the implementation of the FTMPC to the actual process unit, it is highly beneficial to validate the control performance in an advanced process simulator with an accurate simulation model of the target process. In this way, any possible design flaws and benefits can be estimated in advance without disturbing the actual process. Therefore, in order to validate the performance of the active data-based integrated FTMPC defined in Chapter 6, the integrated FTMPC is utilised for controlling the simulated dearomatization process described in Chapter 5 in the presence of typical process faults given in Chapter 6. In order to economically justify the implementation of the developed FTMPC, the economical benefits of the proposed FTMPC are analysed based on the evaluation of the fault effects on the actual dearomatization process.

In this chapter, the simulation environment is first described by defining the testing platform and data pre-processing procedures along with the results of the process linearity testing and the definition of the nominal MPC based on the given control objectives, variables and constraints. Second, the results of testing a nominal MPC in the simulated dearomatization process are presented in order to be able to measure the economical benefits of the FTMPC. Third, the performance of the FTMPC is validated by showing the results of testing the sensor faults in the CVs, DVs and MVs, and the actuator faults in MVs and by summarising the results of the testing. Finally, the economic benefits of the FTMPC are assessed in order to justify the implementation of the FTMPC to the actual dearomatization process.

7.1 Description of the simulated process environment

In this section, the process simulator and data pre-processing, linearity testing of the target process and the definition and modelling of the MPC is presented.

7.1.1 Description of the testing platform

The simulation studies on the LARPO dearomatization process were carried out in the ProsDS (formerly known as PROSimulator) - a dynamic process simulator developed by Neste Jacobs Oy - which has simulation models representing the physical-chemical behaviour of the target process.

The simulation model for the LARPO unit contains a large number of measurements, analyser readings and low-level control loops in order to accurately present the behaviour of the target process. An accurate model thus enables the testing and development of different control strategies offline.

The measurements from the ProsDS were transferred in real time to the Matlab workspace, from where the measurements were further transferred to the Matlab-based software platform. The platform handled the orchestration and pre-treatment of data by using algorithms developed by the author. Pre-treatment includes noise and outlier removal by filtering and the data interpolation for missing data points.

The FDD component of the strategy uses the FDD based on the recursive PLS as described in Section 6.3. The FTC part of the platform processes data and, if necessary, accommodates or reconfigures the nominal controller based on the FDD estimations as presented in Section 6.3. Also, there was a delay mechanism in place for the FTC component, designed to prevent effect of random spikes and false alarms. This delay mechanism has been described in Section 3.5.1 and Section 6.3.

The nominal MPC component calculates the optimised control inputs based on the process measurements, which were then written to the Matlab workspace. From the Matlab workspace, the ProsDS read the optimised input values and adjusted the target sub-level controllers accordingly. Data were retrieved and recorded every five seconds and the FTC part and the nominal MPC operated once per minute. The structure of the software platform is depicted in Figure 25:

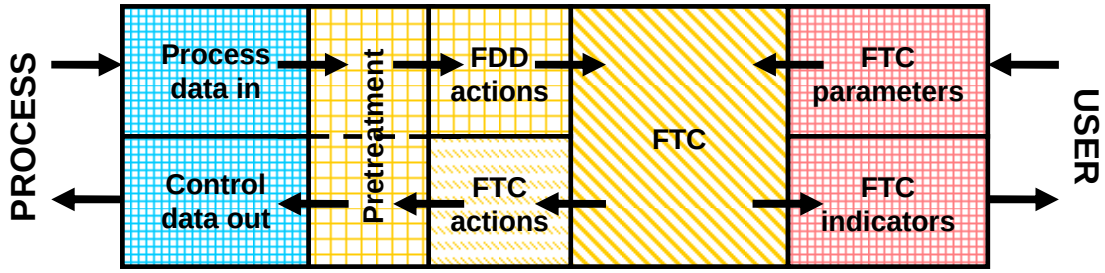

Figure 25. The structure and the data flow within the FTC software platform.

Industrial measurement data contains measurement noise and outliers, which usually have an effect on the control system performance. Also, according to Ray (1989, pp. 28-30), it is necessary to filter industrial data in order to reduce the effect of the noise and outliers on the measurements. In the simulation of the LARPO dearomatization process, all the measurements contain a degree of process noise; for this reason, pre-processing of the data was carried out to reliably control the target process.

A moving average filter was used in filtering the simulated LARPO process measurements. The moving average filter was utilised in the following formulation at each time step to remove noise from the measurements:

$$y_{f,t} = \frac{\sum_{i=t-w}^{t-1} y_i}{w} \tag{47}$$

where $y_{f,t}$ is the filtered measurement value at the current time step t; y_i the measurement value at the time step i; t the current time step; and w the window size.

The window size for the target measurements was set to 15 minutes for the DA1 distillation flow rate and three minutes for all the other measurements. The window length was set longer for the DA1 distillation flow rate due to the high noise variation and nonlinearity present in this measurement.

Occasionally, some measurement data were not recorded from the ProsDS to the Matlab due, for example, to a high computer load or a random error in the Matlab or ProsDS software or in the connection between ProsDS and Matlab. Therefore, it was necessary to determine the number of missing data points and to interpolate the missing values. Missing data was detected by using a timer variable in ProsDS, which was increased at every execution of ProsDS. The timer variable was monitored and the difference between the number of the current time steps and the previously recorded time step was measured. If the difference was larger than a single time step, then the values of the missing measurements were interpolated by using a linear interpolation method as presented in the following equation:

$$y_{t-i} = y_{t-m} + \frac{(m-i)(y_t - y_{t-m})}{m} \tag{48}$$

where t is the current time step, m is a number of the missing measurements, and i is an index for the missing measurements ($i = 0...m$).

Since the MPC control cycle was set to one minute, MPC control action data was interpolated between the one minute periods. In this case, the zero-order hold (ZOH) interpolation was used. In this procedure, the value of the variable is held constant until a new measurement is available. This means that the sub-level controllers receive constant set point values from the MPC.

For the MPC calculations, the CV or DV measurement values and the MV control values were normalised to operation point by using the following equation:

$$v_{norm} = v - V_0 \tag{49}$$

where V_0 is either Y_0, U_0 or D_0 at an operating point, v_{norm} is the averaged value y_{norm}, u_{norm} or d_{norm} and v is the measurement y, input u or the disturbance d, respectively.

For the PLS calculations, the inputs *u*, the outputs *y* and the disturbances *d* were normalised around the operating point Y_0, U_0 or D_0 by using the following equation:

$$v_{norm,pls} = \frac{v - V_0}{STD(v)} \tag{50}$$

where *STD(v)* is the standard deviation of *y*, *u* or *d*.

The DA1 bottom product IBP was updated only every 40 minutes due to the analyser cycle time. In order for the MPC to properly control the variable, an auxiliary variable was implemented to estimate the value of the variable in between the update periods. The value of the IBP was estimated using the MPC internal model, and the estimation was updated when a new analyser measurement was available. The update of the correction was done gradually over a period of 10 minutes, at which time the correction value reached 100% of the new measurement. A delay was introduced in the update because an abrupt correction of the estimations caused nonlinearity in the measurement and made it more difficult for the MPC to control the CV. The auxiliary variable allowed the MPC to receive a continuous measurement of the DA1 bottom product IBP, and thus the MPC was able to carry out the necessary control actions smoothly, when DA1 bottom product IBP was used for control purposes.

7.1.2 Testing the linearity of the target dearomatization process

In order to justify the use of the linear MPC and FDD methods, the linearity of the process was first investigated at the steady state operation point. The dearomatization process has, in general, slow dynamics and linear behaviour under normal operation. At the operation point, on the other hand, the constraints set for the LARPO process variables cause nonlinear behaviour in the open loop responses of certain variables. The linearity tests have been carried out by switching the MPC off during the testing but allowing the basic controllers to operate.

A linear process system has the following properties: invariance under scaling, additivity, and frequency fidelity. The superposition principle contains two of the three linear system properties: the invariance under scaling and additivity. Therefore, the invariance under scaling and multiple input additivity of the target process were tested in order to determine the linearity of the target process in terms of the superposition principle.

7.1.2.1 Testing of the invariance under scaling

In this part of the study, the invariance under scaling for the target process is tested in order to determine the linearity. The testing was carried out by comparing the responses of the output variables to the changes in the input variables. The response was then calculated as the difference between the output at the current time step *t* and the output at the beginning of the simulation (which is the steady state value of the variable), and this was divided by the change in the input variable. The unit step response Y_t between the input *u* and the output *y* during time *t* was calculated using the following equation:

$$Y_t = \frac{y_t - y_0}{u_1 - u_0} \tag{51}$$

To test the invariance under scaling and to measure the parameters for the step-response models, ±1%, ±5% and ±10% changes were carried out in the manipulated variables and disturbance variables, and the changes in the controlled variables was recorded. Each steady state gain was compared to a +1% change steady state gain in order to determine the difference between the responses. The differences in the responses of the controlled variable according to the variable input changes are presented in Tables 11 - 15. Nonlinearity is presented in the tables with different colours: red represents high nonlinearity (more than 30% difference); orange represents medium nonlinearity (less than 30% difference); yellow represents weak nonlinearity (less than 20% difference); and white almost no nonlinearity (less than 10% difference). The filtered step responses (normalised in relation to the standard deviation) with variable input magnitudes are presented in Appendix C.

Table 11. Differences in the DA1_BP_IBP responses when different-sized step changes of the input variables are induced in the LARPO process.

Change magnitude	DA1_FEED_FC:	DA1_FEED_TC:	DA1_HEAT_TC:	DA1_PC:	DA1_REFLUX_FC:	DA1_EA6_FEED_FC:	DA2_FEED_FC:	DA2_EA7_FEED_FC:
-10 %	8.7	16.2	29.2	1.1	6.5	5.1	32.1	87.0
-5 %	12.3	5.9	19.0	2.1	10.1	3.9	33.5	73.3
-1 %	19.9	5.2	7.8	13.8	19.2	14.7	48.4	5.9
1 %	0.0	0.0	0.0	0.0	0.0	0.0	0.0	0.0
5 %	8.2	28.2	31.7	10.6	13.5	2.9	29.9	84.8
10 %	11.4	63.6	43.4	16.2	17.9	4.2	33.6	87.9

Table 12. The differences in the CV DA1_BP_FP responses when different-sized step changes of the input variables are induced in the LARPO process.

Change magnitude	DA1_FEED_FC:	DA1_FEED_TC:	DA1_HEAT_TC:	DA1_PC:	DA1_REFLUX_FC:	DA1_EA6_FEED_FC:	DA2_FEED_FC:	DA2_EA7_FEED_FC:
-10 %	10.1	14.8	23.8	1.2	6.7	6.3	30.5	87.2
-5 %	12.7	5.2	15.0	3.0	9.9	4.8	32.1	74.0
-1 %	19.8	5.5	6.5	13.7	19.0	15.2	46.6	2.4
1 %	0.0	0.0	0.0	0.0	0.0	0.0	0.0	0.0
5 %	7.8	28.9	25.3	10.4	13.0	2.6	27.7	85.0
10 %	10.7	64.0	32.3	15.6	17.5	4.6	31.1	88.2

Table 13. The differences in the CV DA1_DIST_FC responses when different-sized step changes of the input variables are induced in the LARPO process.

Change magnitude	DA1_FEED_FC:	DA1_FEED_TC:	DA1_HEAT_TC:	DA1_PC:	DA1_REFLUX_FC:	DA1_EA6_FEED_FC:	DA2_FEED_FC:	DA2_EA7_FEED_FC:
-10 %	91.2	40.2	59.0	93.5	503.0	62.7	75.6	94.3
-5 %	93.8	31.4	38.0	79.7	511.3	66.1	80.1	95.7
-1 %	31.8	40.0	32.9	142.4	685.2	89.6	40.1	34.2
1 %	0.0	0.0	0.0	0.0	0.0	0.0	0.0	0.0
5 %	85.1	37.7	16.0	39.2	338.5	48.5	89.6	72.4
10 %	88.0	70.8	4.8	38.6	332.3	53.3	95.0	80.9

Table 14. The differences in the CV DA1_TC responses when different-sized step changes of the input variables are induced in the LARPO process.

Change magnitude	DA1_FEED_FC:	DA1_FEED_TC:	DA1_HEAT_TC:	DA1_PC:	DA1_REFLUX_FC:	DA1_EA6_FEED_FC:	DA2_FEED_FC:	DA2_EA7_FEED_FC:
-10 %	13.5	16.2	36.1	15.1	38.3	4.4	6.7	61.9
-5 %	13.3	10.7	23.7	12.1	31.9	9.3	27.6	463.6
-1 %	14.3	2.0	10.2	1.1	25.5	25.2	88.2	301.4
1 %	0.0	0.0	0.0	0.0	0.0	0.0	0.0	0.0
5 %	15.6	32.3	19.2	16.0	21.1	6.6	30.1	96.8
10 %	19.7	65.8	27.1	19.4	15.6	7.8	24.1	83.3

Table 15. The differences in the CV DA2_BP_FP responses when different-sized step changes of the input variables are induced in the LARPO process.

Change magnitude	DA1_FEED_FC:	DA1_FEED_TC:	DA1_HEAT_TC:	DA1_PC:	DA1_REFLUX_FC:	DA1_EA6_FEED_FC:	DA2_FEED_FC:	DA2_EA7_FEED_FC:
-10 %	27.5	73.6	8.5	18.8	22.3	31.7	30.1	86.7
-5 %	49.5	45.3	44.3	14.7	14.2	20.7	39.8	97.4
-1 %	70.8	19.2	8.9	16.8	16.4	30.1	62.5	159.9
1 %	0.0	0.0	0.0	0.0	0.0	0.0	0.0	0.0
5 %	19.2	36.6	5.5	1.8	7.3	0.6	43.5	51.5
10 %	11.5	67.8	21.0	5.7	19.2	2.3	45.8	63.1

As can be seen from Table 11 - 15 and Appendix C, the response of the system was nonlinear in a few cases. The response of DA2_EA7_FEED (the DA2 reboiler feed flow rate) was nonlinear in almost all cases, since the response to the changes was mostly smaller than the overall level of the measurement noise and it was therefore difficult to get a proper response. Nonlinearity was also clearly detected in DA1_DIST_FC (the DA1 distillate flow rate). The distillate flow rate was controlled indirectly through the overhead drum level controller, causing nonlinear responses. Nevertheless, accurate control of the distillate flow rate was not required, since the main goal was to minimise the distillate flow. As a result, this variable could be minimised indirectly by minimising the side product flashpoint, DA2_BP_FP.

Overall, nonlinearity manifested itself with large positive step changes (+10% or more), which indicated that in those cases, some of the process variables were driven towards the constraints, thereby causing nonlinear behaviour in the variables. Close proximity to the constraints causes asymmetry, also because large positive input changes behave differently compared to the negative input changes. When pushed to or near the variable constraints, the process variables began to behave nonlinearly, as suspected. Therefore, it is imperative, according to the step testing, to set strict constraint limits for the MPC.

7.1.2.2 Testing the multiple input additivity

The multiple input additivity of the system was tested next by changing two or more variables at the same time and then monitoring the combined effect of the inputs. If the system has additivity properties in terms of the superposition principle, then the combined effect of the input changes should match the sum of two individual responses. Since there were as many as eight input variables and five output variables, the total number of possible input combinations would have been very high. Therefore, only the most important combinations of two input variables were changed at a time in order to simplify the testing procedure. Each of the variables was stepped with +5% and -5% changes with different combinations. The following variable combinations were tested:

- DA1_FEED_TC + DA1_FEED_FC
- DA1_HEAT_TC + DA1_FEED_TC
- DA1_PC + DA1_HEAT_TC
- DA1_EA6_FEED_FC + DA1_PC
- DA1_REFLUX_FC + DA1_EA6_FEED_FC
- DA2_FEED_ FC + DA1_REFLUX_FC
- DA2_EA7_FEED_FC + DA2_FEED_ FC
- DA1_FEED_FC + DA2_EA7_FEED_FC

The combinations of two simultaneous variable changes versus the sum of the two individual variable responses are presented in Table 16 as a percentage of the difference between the values compared to the summed responses. The white cells in the table represent values with a difference of less than 10% compared to the summed values; the yellow cells a 10-20% difference; the orange cells a 20-30% difference; and the red cells a difference of more than 30%. The values in bold describe changes with a difference of over or near 100%.

As can be seen from Table 16, in most cases the combined responses were relatively close to the sum of the original individual responses. In some cases, the difference was more than 100%; however, in all of these cases the changes in the CVs were less than the process noise level, thereby producing variation and error in the combined and summed outputs. In a few cases, the output variables also reached the hard constraints and caused a difference in the combined and summed outputs. According to the results, DA1_DIST_FC behaved in the most nonlinear way. Furthermore, while some nonlinearity was present in DA1_TC, most of it could be explained by the high noise level compared to the changes in the variable, which caused deviation in the variable output. In most cases, the differences versus the nominal level of the variable were less than 1.5%, except for DA1_DIST_FC, where the changes were as large as 15%. Therefore, based on the multiple input additivity testing, the target process behaved linearly in most cases, at least when only two of the variables were excited simultaneously. However, some degree of nonlinearity was present in the variables.

Table 16. The results of the additivity testing of the dearomatization process.

Stepped input variables (changes)	DA1_BP_IBP	DA1_BP_FP	DA1_DIST_FC	DA1_TC	DA2_BP_FP
DA1_FEED_TC / DA1_FEED_ FC (5/5)	38 %	38 %	15 %	37 %	18 %
DA1_FEED_TC / DA1_FEED_ FC (5/-5)	17 %	15 %	24 %	11 %	19 %
DA1_FEED_TC / DA1_FEED_ FC (-5/5)	1 %	0 %	16 %	20 %	4 %
DA1_FEED_TC / DA1_FEED_ FC (-5/-5)	5 %	6 %	11 %	16 %	8 %
DA1_HEAT_TC / DA1_FEED_TC (5/5)	0 %	1 %	14 %	2 %	23 %
DA1_HEAT_TC / DA1_FEED_TC (5/-5)	19 %	16 %	8 %	18 %	434 %
DA1_HEAT_TC / DA1_FEED_TC (-5/5)	40 %	34 %	84 %	71 %	6 %
DA1_HEAT_TC / DA1_FEED_TC (-5/-5)	52 %	58 %	26 %	48 %	13 %
DA1_PC / DA1_HEAT_TC (5/5)	6 %	5 %	8 %	7 %	27 %
DA1_PC / DA1_HEAT_TC (5/-5)	5 %	4 %	10 %	2 %	12 %
DA1_PC / DA1_HEAT_TC (-5/5)	6 %	4 %	9 %	2 %	9 %
DA1_PC / DA1_HEAT_TC (-5/-5)	7 %	5 %	23 %	28 %	27 %
DA1_EA6_FEED_FC / DA1_PC (5/5)	9 %	10 %	6 %	**110 %**	10 %
DA1_EA6_FEED_FC / DA1_PC (5/-5)	3 %	1 %	1 %	14 %	2 %
DA1_EA6_FEED_FC / DA1_PC (-5/5)	4 %	3 %	2 %	10 %	5 %
DA1_EA6_FEED_FC / DA1_PC (-5/-5)	8 %	8 %	30 %	49 %	14 %
DA1_REFLUX_FC / DA1_EA6_FEED_FC (5/5)	8 %	10 %	**5221 %**	43 %	24 %
DA1_REFLUX_FC / DA1_EA6_FEED_FC (5/-5)	2 %	1 %	1 %	35 %	7 %
DA1_REFLUX_FC / DA1_EA6_FEED_FC (-5/5)	3 %	1 %	1 %	17 %	6 %
DA1_REFLUX_FC / DA1_EA6_FEED_FC (-5/-5)	11 %	16 %	57 %	**97 %**	**105 %**
DA2_FEED_ FC / DA1_REFLUX_FC (5/5)	21 %	30 %	**134 %**	74 %	1 %
DA2_FEED_ FC / DA1_REFLUX_FC (5/-5)	1 %	1 %	24 %	21 %	10 %
DA2_FEED_ FC / DA1_REFLUX_FC (-5/5)	3 %	2 %	78 %	57 %	0 %
DA2_FEED_ FC / DA1_REFLUX_FC (-5/-5)	17 %	8 %	9 %	59 %	7 %
DA2_EA7_FEED_FC / DA2_FEED_ FC (5/5)	5 %	2 %	65 %	50 %	11 %
DA2_EA7_FEED_FC / DA2_FEED_ FC (5/-5)	9 %	6 %	42 %	**259 %**	20 %
DA2_EA7_FEED_FC / DA2_FEED_ FC (-5/5)	4 %	1 %	**162 %**	71 %	4 %
DA2_EA7_FEED_FC / DA2_FEED_ FC (-5/-5)	9 %	6 %	72 %	12 %	21 %
DA1_FEED_ FC / DA2_EA7_FEED_FC (5/5)	1 %	1 %	42 %	60 %	81 %
DA1_FEED_ FC / DA2_EA7_FEED_FC (5/-5)	0 %	1 %	**107 %**	29 %	4 %
DA1_FEED_ FC / DA2_EA7_FEED_FC (-5/5)	10 %	8 %	51 %	30 %	27 %
DA1_FEED_ FC / DA2_EA7_FEED_FC (-5/-5)	12 %	10 %	36 %	9 %	76 %

7.1.2.3 Summary of the linearity testing results

Based on the invariance under scaling and the multiple input additivity testing, there was a degree of nonlinearity present in the target process, especially in the variable DA1_DIST_FC. However, in most cases the target process was sufficiently linear to be properly controlled by using a linear MPC. Even though there was a degree of nonlinearity present in the behaviour of the variable, the effect of nonlinearity on the performance of the MPC was relatively small due to the MPC feedback.

In order to counter the effects of the nonlinearity in DA1_DIST_FC, this variable is not directly controlled in the final FTMPC; instead, it is minimised by maximising the by-product yield. The maximisation of the by-product yield is transferred to the minimisation of the by-product flashpoint, DA2_BP_FP. When DA2_BP_FP is minimised, a maximum amount of distillate is fed back to the column through reflux, finally ending up as by-product, thereby maximising the by-product yield, minimising the by-product flashpoint and also minimising the overall distillate flow of the main column, DA1_DIST_FC.

Based on the linearity testing, the simulated target process had enough nonlinearity to successfully represent an actual process case. However, since the degree of nonlinearity was also small in general, it is possible to use a linear MPC for the control of the target dearomatization process.

7.1.3 Description of the MPC for the target dearomatization process

As the linearity of the target process has been tested, and the linear MPC has been found suitable for the control purposes, the linear MPC was next defined by acquiring the MPC model and defining the parameters for the MPC.

7.1.3.1 Modelling the target process for the MPC

Next, the linear model was formulated for the MPC. Based on the linearity testing, it was determined that a model composed of first order plus time delay (FOPTD) transfer functions would be sufficient for MPC purposes and the modelling could be based on a regular step testing procedure.

First, a steady-state was determined for the target process and a suitable process conditions were set based on the actual LARPO process. The step testing was then carried out by exciting each of the disturbance variables and manipulated variables by a 5% positive step change, which, according to the linearity testing, reflected the behaviour of the target process best. As a result of the step testing, the normalised (in relation to the standard deviation) step responses of the LARPO dearomatization process were acquired that are presented in Appendix D. Based on the results of the step testing, it was concluded that the first order transfer functions with time delay are sufficient to describe the dynamics of the process and could subsequently be used to construct the model for the MPC.

7.1.3.2 Parameters of the MPC

The MPC for the simulated LARPO process was constructed according to the recommendations of the preliminary simulation study of the industrial benchmark process, as well as process knowledge acquired in the control of the actual LARPO process. It became evident in the preliminary study that the MPC provided a flexible, straightforward and effective way of controlling the target process and, because an industrial-scale linear MPC is used to control the actual LARPO process, a Matlab-based MPC was used for the control of the simulated LARPO process.

The MPC parameters were adjusted according to the dynamics of the simulated dearomatization process. The control cycle for the MPC was set to one minute, since the changes in the process are relatively small and there is no need for faster control. The prediction horizon was set long enough to be able to react as early as possible to most situations in the simulated process. Since the total delays, including the analyser delays in the process varied between 0-40 minutes, the prediction horizon was set to 50 minutes. This means that while the prediction horizon is longer than the largest delay, it is not too long to keep the process under control. The control horizon was set to 40 minutes, which is a good compromise between efficiency and the required computation time.

The CV weights were set according to control preferences. The primary controlled variable (DA1_BP_IBP, DA1_BP_FP or DA1_TC) weights were set to 10 to indicate that the main column bottom product was to be kept at the setpoint at all times. The weight for the secondary variable DA2_BP_FP was set to 1 to indicate that the minimisation of the by-product flashpoint is not as important as keeping the main product within the defined specifications. No weight was set for DA1_DIST_FC as it is not controlled by the MPC.

The minimisation of the by-product flashpoint and the distillate flow rate was handled by setting the setpoint of DA2_BP_FP 0.2°C to less than the measured value during every time step. The value of the setpoint is lowered until its value is 0.5% higher than the minimum limit of DA2_BP_FP, after which the setpoint is kept at this value until the measured value rises above this limit.

The constraints for the CVs were set according to the product specifications; the minimum limits were based on the specification limits and the maximum limits are set to keep the MPC within control range. No limits were set for DA1_DIST_FC since it was not directly controlled; however, there were hard constraints set for this variable in the sub-level control system. The CV weights and the constraints for the CVs are presented in Table 17.

In order to minimise costs while keeping the product in specification, the setpoint for DA1_BP_FP was set 0.5% higher than the minimum limit, and for DA2_BP_FP the limit for minimisation was also set 0.5% higher than the minimum specification limit.

The maximum constraints for the MVs were set according to the mechanical limits of the target controller. The minimum constraints were set according to the operational limits; for instance, DA2_FEED_FC has a non-zero minimum value in order to ensure flow to the side stripper. Also, DA1_REFLUX_FC would need to have a minimum flow back to the column in order to keep the column separating capacity at moderate levels. DA1_EA6_FEED_FC has a minimum limit of 40% of the maximum limit since there is a minimum level of reboiling required for the separation procedure. Furthermore, if there would not be enough energy available, there would not be enough feed for side stripper DA2. DA2_EA7_FEED_FC needs to have a smaller relative minimum limit because the variation range for this variable is small and thus a higher limit would cause restrictions on the side stripper operation. In Table 17 and Table 18, the minimum constraints are presented in the absolute values for the CVs and in percentages of the maximum constraint for the MVs. The minimum value of the setpoint (of the minimum constraint) is also presented in Table 17.

The MV change rate constraints were set to -5% and +5% of the range of variation allowed for the controller. The weights for the input variables were set to 0, allowing full freedom for the input variables; in essence, this leaves the input variables out of the MPC objective function. The weights for the MV rates were set at 5. Selecting this value allows a relatively fast response time for each MV, the selection being based on the control performance. The constraints and weights for the manipulated variables are presented in Table 18.

Table 17. The constraints, weights and minimum setpoint values of the CVs.

CVs:	**Constraints** **% of the max limit**		**Weights**	**Min setpoint** (of the min limit)
	Min	Max		
DA1_BP_IBP	219.0	245.0	1	+0.5%
DA1_BP_FP	79.8	100.0	1	+0.5%
DA1_DIST_FC	-	-	-	-
DA1_TC	261.5	275.0	1	+0.5%
DA2_BP_FP	66.0	80.0	1	+0.5%

Table 18. The constraints and weights of the MVs.

MVs:	**Constraints** **% of the max limit**		**Rate constraints** **% of the range of variation**		**Weights**	**Rate weights**
	Min	Max	Min	Max		
DA1_REFLUX_FC	25.0 %	100.0 %	-5.00 %	5.00 %	0	5
DA1_EA6_FEED_FC	40.0 %	100.0 %	-5.00 %	5.00 %	0	5
DA2_FEED_FC	25.0 %	100.0 %	-5.00 %	5.00 %	0	5
DA2_EA7_FEED_FC	15.0 %	100.0 %	-5.00 %	5.00 %	0	5

7.2 Results of testing the nominal MPC for the target dearomatization process

The control performance of the MPC was next tested in order to verify the MPCs ability to control the target process with a sufficient level of performance. In addition, by determining the control performance of the nominal MPC, a baseline would be formed that can be used to compare the results with the integrated FTMPC. The performance of the nominal MPC was tested by introducing disturbances into the process and making setpoint changes to the reference trajectories of the CVs.

The performance of the nominal MPC was measured by calculating the deviation of the CVs from the target trajectory. In the first case, the disturbance variable DA1_FEED_TC (the DA1 feed temperature setpoint) was changed by +5%. In this case, the active controlled variables were DA1_BP_FP and DA2_BP_FP. The effect of the disturbances was recorded and the results are shown in Figure 26.

As can be seen from Figure 26, there was only a temporary effect of less than 1% on DA1_BP_FP, and less than a 2% temporary effect on DA2_BP_FP. In essence, the MPC handled the disturbance well and countered the effect of the disturbance efficiently, while keeping the CVs at their setpoint values.

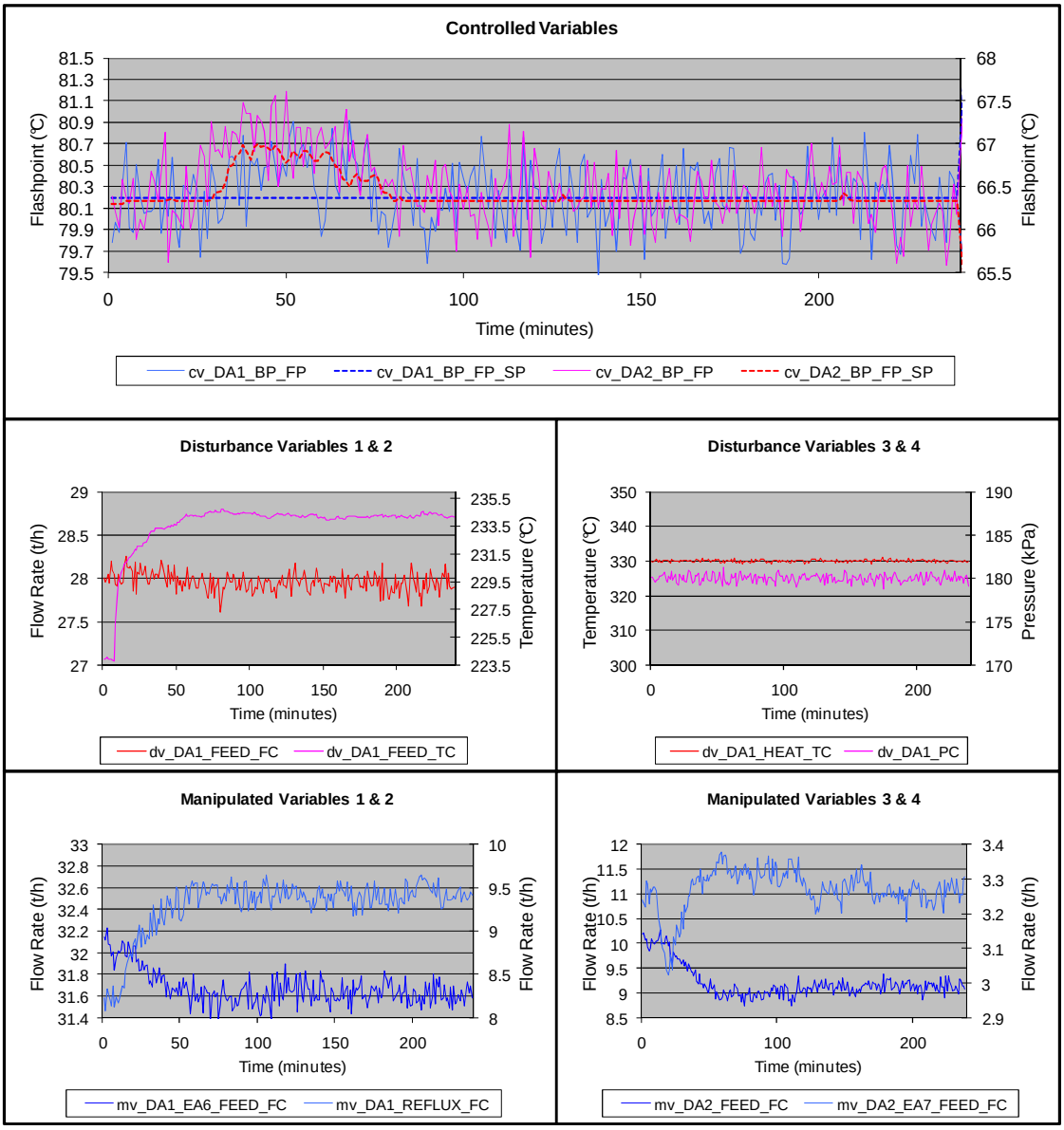

Figure 26. The effect of a +5% change in DV DA1_FEED_TC .

In the second control performance test, the setpoint of DA1_BP_FP was changed and the performance of the MPC was observed. The setpoint of DA1_BP_FP was changed by +1% of the current value at the time step 10 minutes. The response and effectiveness of the MPC was monitored and the results are shown in Figure 27:

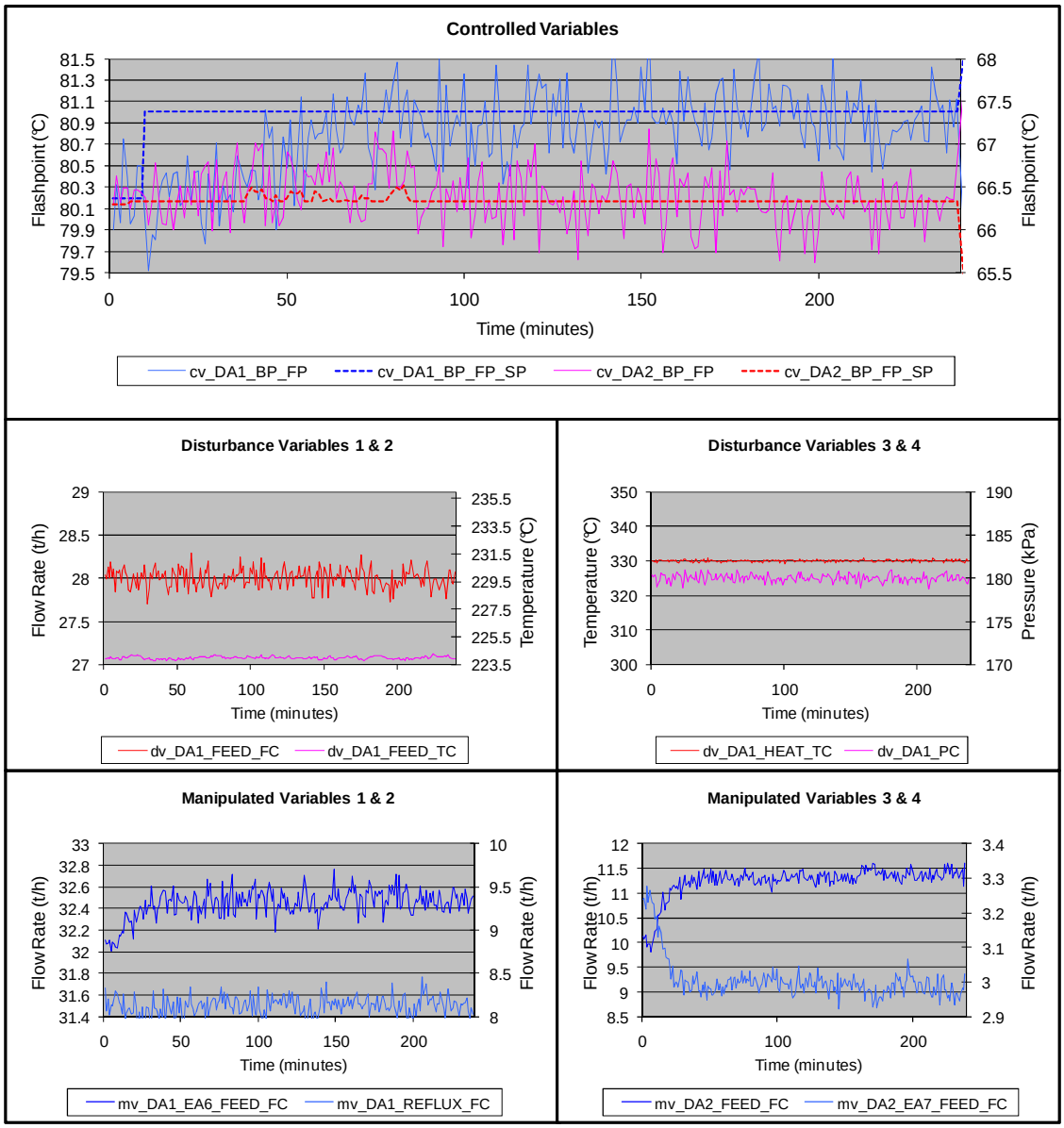

Figure 27. The effect of a +1% setpoint change in CV DA1_BP_FP.

As can be seen from the figure, the MPC followed satisfactorily the given setpoint changes: the target value was reached within 50 minutes and there was less than a 1% effect on the other CV, DA2_BP_FP.

The properties of the feedstock to the by-product stripper unit, DA2, change when the DA1 bottom product flashpoint is increased by increasing the feed rate of the stripper unit DA2. This increase causes the DA2 feedstock to become heavier, thus requiring more reboiling in order to keep the flashpoint requirements in the side stripper. This phenomenon causes nonlinearity in the side stripper control, which is transformed to delay and uncertainty in the control of the by-product flashpoint.

Based on the control testing, the performance of the MPC was satisfactory in normal conditions despite the nonlinearities present in the target process. The MPC was able to counter the effects of the disturbances and to follow the given reference trajectories. Therefore, it is concluded that the performance of the MPC is sufficient for the fault-tolerant control of the target process.

7.3 Validation of the of the integrated FTMPC performance

The performance of the FTMPC for the target dearomatization process was validated by introducing measurement and actuator faults and demonstrating the performance of the proposed FTC strategy. Generally, this validation with industrial process simulator is an important part of the FTMPC implementation process, as the performance of the proposed system has to be verified before moving on to the implementation of the FTMPC on the actual dearomatization process.

In this section, first the results of the FTMPC testing with bias and drift faults in the CV analysers and sensors are presented. Second, the results of the FTMPC testing are given with bias faults in the DV sensors. Third, the results of the bias faults in the MV sensors are described. Fourth, the results of testing the actuator faults in MVs are given and finally the results of the FTMPC validation are discussed.

7.3.1 Testing results of the active FTC strategy for the CV analyser and sensor faults

Sensor faults mostly affect the measurements and analysers considered as CVs in the MPC. When a CV sensor is affected by a fault, the MPC receives faulty information and adjusts the manipulated variable in the wrong direction. An FTC based on the FDD estimation is used to estimate the values of the CV analyser and sensor measurements.

The output variables for the FTC strategy for the CV analyser and sensor faults are presented in Table 7 and the input variables in Table 8 and Table 9. The structure of the PLS models used in the active data-based FTC strategy for the CV analyser and sensor faults is presented in Table 19 for the 1st set of PLS models, and in Table 20 for the 2nd set of PLS models. The first PLS is used for detecting faults, and the second one to identify the magnitude of the faults on the basis of delayed faultless data as introduced in Section 3.5.1.

Table 19. The structure of the 1st PLS model for the active data-based FTC strategy for the CV analyser and sensor faults.

Model	$PLS1_1$	$PLS1_2$	$PLS1_3$	$PLS1_4$	$PLS1_5$
Output	DA1_BP_IBP	DA1_BP_FP	DA1_DIST_FC	DA1_TC	DA2_BP_FP
Inputs	DA1_FEED_FC	DA1_FEED_FC	DA1_FEED_FC	DA1_FEED_FC	DA1_FEED_FC
	DA1_FEED_TC	DA1_FEED_TC	DA1_FEED_TC	DA1_FEED_TC	DA1_FEED_TC
	DA1_HEAT_TC	DA1_HEAT_TC	DA1_HEAT_TC	DA1_HEAT_TC	DA1_HEAT_TC
	DA1_PC	DA1_PC	DA1_PC	DA1_PC	DA1_PC
	DA1_REFLUX_FC	DA1_REFLUX_FC	DA1_REFLUX_FC	DA1_REFLUX_FC	DA1_REFLUX_FC
	DA1_EA6_FEED_FC	DA1_EA6_FEED_FC	DA1_EA6_FEED_FC	DA1_EA6_FEED_FC	DA1_EA6_FEED_FC
	DA2_FEED_FC	DA2_FEED_FC	DA2_FEED_FC	DA2_FEED_FC	DA2_FEED_FC
	DA2_EA7_FEED_FC	DA2_EA7_FEED_FC	DA2_EA7_FEED_FC	DA2_EA7_FEED_FC	DA2_EA7_FEED_FC
	DA1_BP_IBP(t-d_1)	DA1_BP_FP(t-d_1)	DA1_DIST_FC(t-d_1)	DA1_TC(t-d_1)	DA2_BP_FP(t-d_1)
	DA1_BP_IBP(t-d_2)	DA1_BP_FP(t-d_2)	DA1_DIST_FC(t-d_2)	DA1_TC(t-d_2)	DA2_BP_FP(t-d_2)

Table 20. The structure of the 2nd PLS model for the active data-based FTC strategy for the CV analyser and sensor faults.

Model	$PLS2_1$	$PLS2_2$	$PLS2_3$	$PLS2_4$	$PLS2_5$
Output	DA1_BP_IBP	DA1_BP_FP	DA1_DIST_FC	DA1_TC	DA2_BP_FP
Inputs	DA1_FEED_FC	DA1_FEED_FC	DA1_FEED_FC	DA1_FEED_FC	DA1_FEED_FC
	DA1_FEED_TC	DA1_FEED_TC	DA1_FEED_TC	DA1_FEED_TC	DA1_FEED_TC
	DA1_HEAT_TC	DA1_HEAT_TC	DA1_HEAT_TC	DA1_HEAT_TC	DA1_HEAT_TC
	DA1_PC	DA1_PC	DA1_PC	DA1_PC	DA1_PC
	DA1_REFLUX_FC	DA1_REFLUX_FC	DA1_REFLUX_FC	DA1_REFLUX_FC	DA1_REFLUX_FC
	DA1_EA6_FEED_FC	DA1_EA6_FEED_FC	DA1_EA6_FEED_FC	DA1_EA6_FEED_FC	DA1_EA6_FEED_FC
	DA2_FEED_FC	DA2_FEED_FC	DA2_FEED_FC	DA2_FEED_FC	DA2_FEED_FC
	DA2_EA7_FEED_FC	DA2_EA7_FEED_FC	DA2_EA7_FEED_FC	DA2_EA7_FEED_FC	DA2_EA7_FEED_FC
	DA1_BP_IBP(t-d_3)	DA1_BP_FP(t-d_3)	DA1_DIST_FC(t-d_3)	DA1_TC(t-d_3)	DA2_BP_FP(t-d_3)
	DA1_BP_IBP(t-d_4)	DA1_BP_FP(t-d_4)	DA1_DIST_FC(t-d_4)	DA1_TC(t-d_4)	DA2_BP_FP(t-d_4)

The NIPALS algorithm presented in 3.4.1 was used for the iterative training of the PLS models. PLS for CV analyser and sensor faults has been trained by using a data set consisting of 600 minutes of process data. This data set has been generated under MPC control, while manipulating the DVs and the CV reference trajectories in order to create sufficient excitation to capture the closed-loop behaviour of the target process for the data-based FDD methods. These training data are presented in Appendix E.

The number of the latent variables was determined using the knee-in-the-plot method, in which the selection of the latent variables is based on the largest drop in the captured variance of the latent variables. The cumulative variances for the input vector X and the output vector Y and the number of latent variables for each PLS model is presented in Table 21.

Table 21. The cumulative variances for X and Y and the number of the LVs for the PLS for the CV analyser and sensor faults.

PLS model	Cumulative variance of *X*	Cumulative variance of *Y*	Number of latent variables
$PLS1_1$	88	99	5
$PLS1_2$	89	99	5
$PLS1_3$	89	97	5
$PLS1_4$	94	99	5
$PLS1_5$	88	99	5
$PLS2_1$	86	99	5
$PLS2_2$	89	99	5
$PLS2_3$	83	91	5
$PLS2_4$	93	99	5
$PLS2_5$	84	92	5

As can be seen from the cumulative variances, the first set of the models captured the variance slightly better than the second set of the models. This is because the past values of the CV in the second set are further back in the past, and therefore there was a lower correlation between the old CV value and the current, thereby resulting slightly less accurate estimations of the CV value. However, the correlations for the estimations are sufficiently high for fault estimation purposes. The more accurate set of the models, the 1^{st} set, was used for fault detection purposes, which is a more time-critical function of the active data-based FTC strategy for the CV analyser and sensor faults.

The active data-based FTC strategy for the CV analyser and sensor faults was then tested by introducing bias- or drift-shaped faults into the analyser outputs and measurements, and analysing the active data-based FTC strategy performance based on the measured outputs.

7.3.1.1 Bias fault in the analyser output

First, an upward bias-shaped fault with a magnitude of 5% of the nominal value of the DA1_BP_FP was introduced into the DA1 bottom product flashpoint analyser output during the time step T_1 = 15 minutes without the active data-based FTC strategy. The fault lasted for 90 minutes until the time step T_2 = 105 minutes, after which the fault was removed from the process. The FDD part of the active data-based FTC strategy for the CV analyser and sensor faults was turned on but no FTC actions were carried out. The PLS-based prediction and the effect of the fault can be seen in Figure 28.

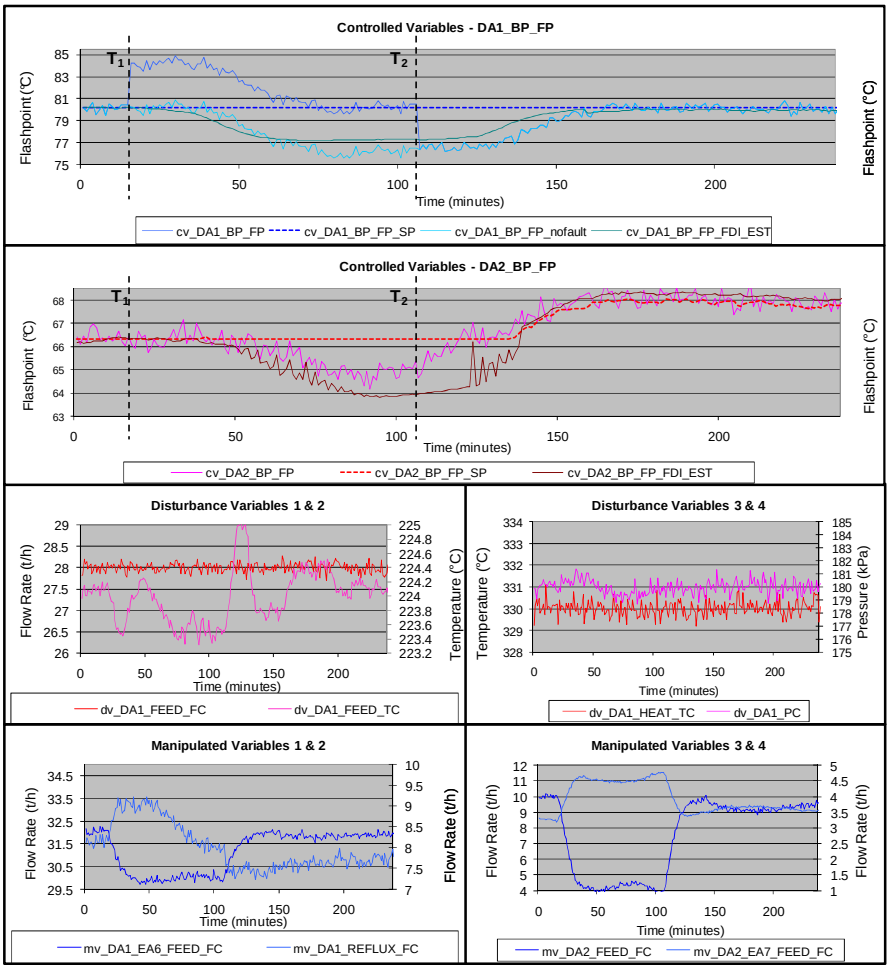

Figure 28. The effects of a +5% bias fault in CV DA1_BP_FP during t = 15 -105 minutes, without the active data-based FTC strategy for the CV analyser and sensor faults.

As can be seen from Figure 28, the +5% upward fault caused an opposite effect on CV DA1_BP_FP; the measurement value was changed by -5% and then returned back to the original value as soon as the effect of the fault ended. The value of DA2_BP_FP was also changed by -3% and, after the effect of the fault ended, the value of the DA2 bottom product flashpoint was increased to +2% of the original value due to the correction to DA1_BP_FP. Since DA2_BP_FP was set to minimisation, the value slowly decreased back afterwards to the minimum limit over time. The PLS was able to predict the actual value of the measurement effectively; there was about a 1% maximum difference between the prediction and the actual measurement value, even though the faulty value was relayed to FDD and affects the performance of the FDD.

Overall, the fault had the effect that both DA1_BP_FP and DA2_BP_FP were off the specification limits for 90 minutes.

Next, the previous fault scenario with a +5% bias-shaped fault affecting DA1_BP_FP was tested with the active data-based FTC strategy for the CV analyser and sensor faults.

An upward bias-shaped fault with a magnitude of 5% of the nominal value of the DA1_BP_FP was introduced into the output of the DA1 bottom product flashpoint analyser during the time step T_1 = 15 minutes with the FTC turned on. As before, the fault lasted for 90 minutes until the time step T_2 = 105 minutes, after which the fault was removed from the process. As can be seen from the PLS fault detection values in Figure 29, the FTC actions were engaged at the time step T_d = 34 minutes, 19 minutes after the fault started to affect the process variable. Also, there was no interference in another CV, DA2_BP_FP, and there were no false alarms during the test run.

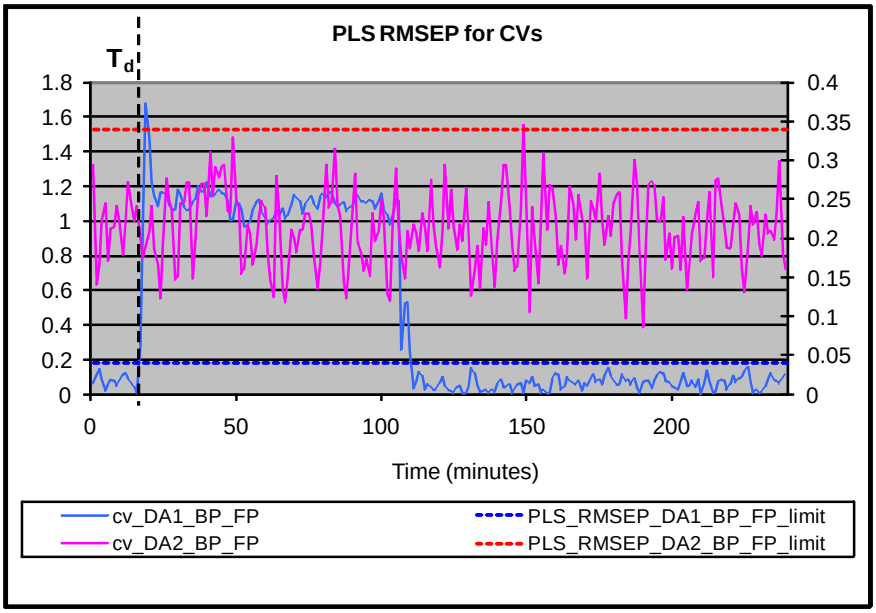

Figure 29. The PLS RMSEP values for a +5% bias fault in CV DA1_BP_FP during t = 15 - 105 minutes with the active data-based FTC strategy for the CV analyser and sensor faults.

As can be seen from Figure 30, with the active data-based FTC strategy for the CV analyser and sensor faults, the +5% bias fault had almost no effect at all on the controlled variables. The PLS was able to predict the actual value of the measurement accurately, and there was clearly less than 1% difference between the measured and predicted value. With the active data-based FTC strategy for the CV analyser and sensor faults enabled, DA1_BP_FP was be off spec for 10 minutes. In general, both DA1_BP_FP and DA2_BP_FP remained within the specification limits despite the fault, thus improving the reliability of the control system and providing savings in off-spec production.

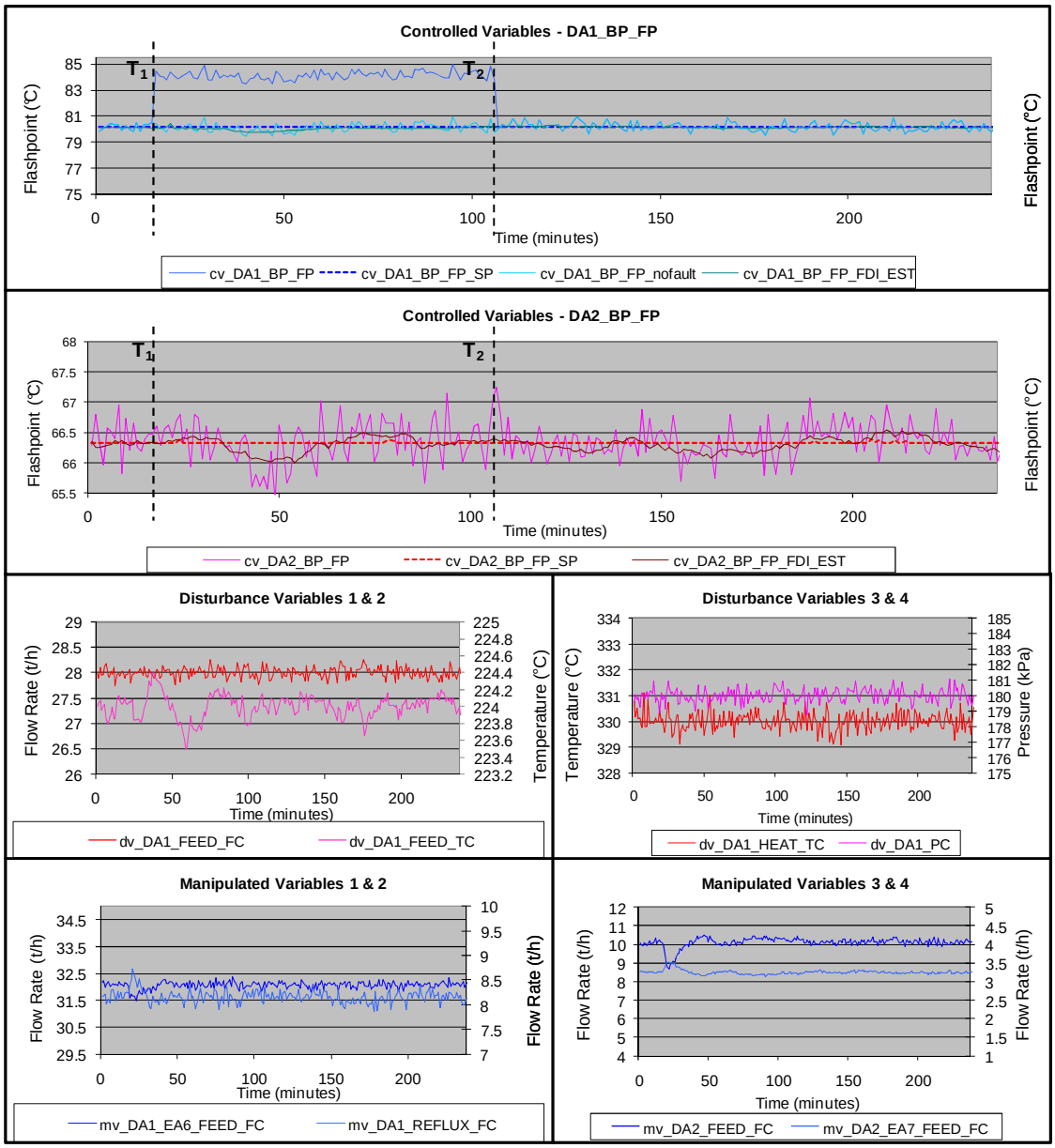

Figure 30. The effects of a +5% bias fault in CV DA1_BP_FP during t = 15 - 105 minutes, with the active data-based FTC strategy for the CV analyser and sensor faults.

7.3.1.2 Drift fault in the analyser output

In the second case, the effect of a drift-shaped fault was tested with and without the active data-based FTC strategy for the CV analyser and sensor faults.

First, an upward drift-shaped gradually-increasing fault with a final magnitude of 5% of the nominal value of the DA1_BP_FP was introduced into the DA1 bottom product flashpoint analyser output. This fault started at the time step T_1 = 15 minutes, and the testing was carried out without the active data-based FTC strategy being active. The fault lasted for 90 minutes until the time step T_2 = 105 minutes, after which the fault was removed from the process. Again, only the FDD part of the active data-based FTC strategy for the CV analyser and sensor faults was turned on; however, no FTC actions were made. The PLS-based prediction and the effect of the fault can be seen in Figure 31.

As can be seen from Figure 31, the upward fault caused the value of DA1_BP_FP to decrease by a maximum of -4% of the nominal value, and then the value returned back to the nominal level as soon as the effect of the fault ended. The value of the DA2_BP_FP was also changed by -2% and, after the effect of the fault ended, the value of the DA2 bottom product flashpoint was increased to +2% of the original value due to the correction to DA1_BP_FP. Again, the value of DA2_BP_FP then decreased slowly back to the minimum limit over time due to the minimisation. Also in this case with a drift fault, the PLS was able to predict the actual value of the measurement effectively; there was less than a maximum difference of 1% between the prediction and the actual measurement value for both DA1_BP_FP and DA2_BP_FP, even though the faulty value was relayed to FDD and affects the performance of the FDD component. Overall, the drift fault had the effect that both DA1_BP_FP and DA2_BP_FP were off the specification limits for 90 minutes. Next, the previous fault scenario with a +5% drift-shaped fault affecting DA1_BP_FP was tested with the active data-based FTC strategy for the CV analyser and sensor faults turned on.

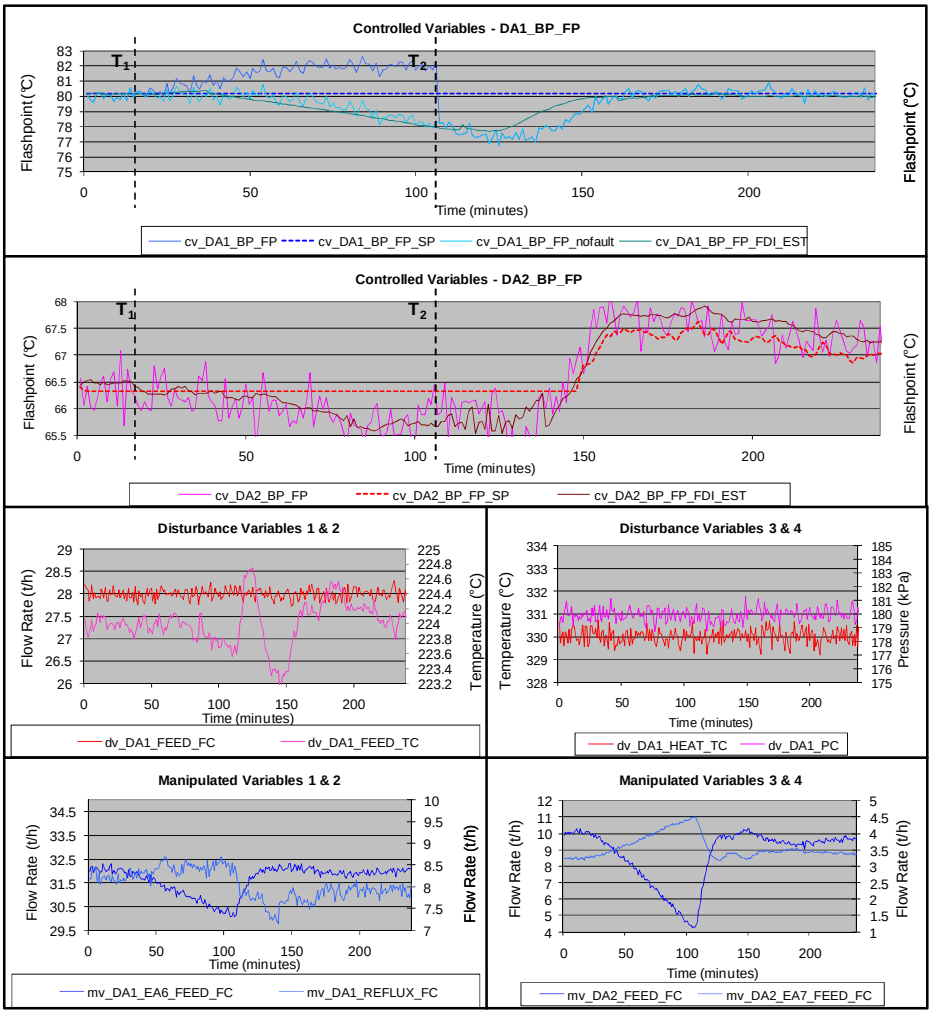

Figure 31. The effects of a +5% drift fault in CV DA1_BP_FP during t = 15 - 105 minutes, without the active data-based FTC strategy for the CV analyser and sensor faults.

An upward drift-shaped fault with a final magnitude of 5% of the nominal value of DA1_BP_FP was introduced into the DA1 bottom product flashpoint analyser output during the time step T_1 = 15 minutes, with the active data-based FTC strategy for the CV analysers and sensors turned on. The fault lasted for 90 minutes until the time step T_2 = 105 minutes, after which the fault was removed from the process. As can be seen from the PLS fault detection values in Figure 32, the FTC actions were engaged at the time step T_d = 34 minutes, 19 minutes after the fault started to affect the process. There was also no interference with DA2_BP_FP and there were no false alarms during the test run.

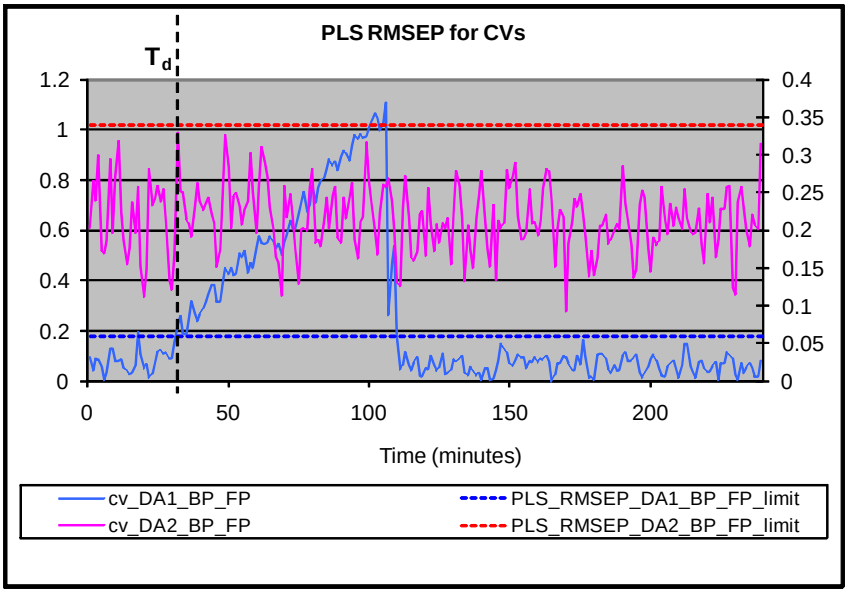

Figure 32. The PLS RMSEP values for a +5% drift fault in CV DA1_BP_FP during t = 15 - 105 minutes, with the active data-based FTC strategy for the CV analysers and sensors.

As can be seen from Figure 33, with the active data-based FTC strategy for the CV analyser and sensor faults, the +5% drift fault had an effect of less than 0.5% on the controlled variables. The PLS was able to predict the actual value of the measurement accurately, and there was clearly a difference of less than 1% between the measured and predicted value. Both DA1_BP_FP and DA2_BP_FP remained within the specification limits despite the fault, thus improving the reliability of the control strategy and saving costs by reducing the amount of off-spec production.

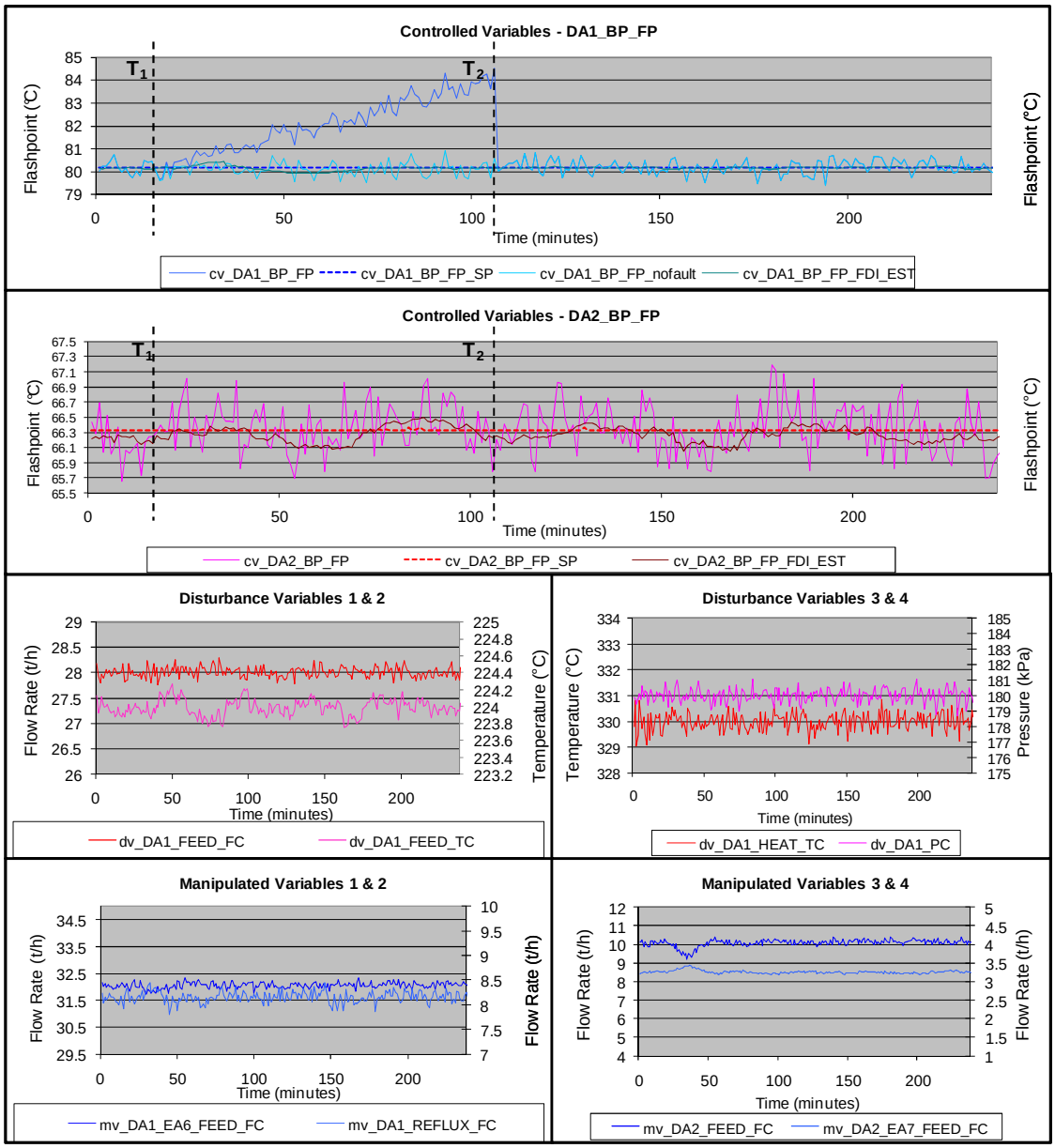

Figure 33. The effects of a +5% drift fault in CV DA1_BP_FP during t = 15 - 105 minutes, with the active data-based FTC strategy for the CV analyser and sensor faults.

7.3.2 Testing results of the active FTC strategy for the DV sensor faults

Sensor faults can also affect the sub-level controller measurements, such as flow or temperature measurements. As stated above, the most typical faults in sensors are bias and drift-shaped faults, and this also applies to the flow or temperature measurements. When a DV sensor is affected by a sensor fault, the MPC receives faulty information and adjusts the manipulated variable most probably in the wrong direction. For instance, if an upward bias fault affects a DV, the MPC detects an increase in DV value and adjusts the MVs to counter the effect accordingly. As an effect of the adjustment, the value of the CVs changes due to the false correction and the MPC adjusts the MVs again based on the feedback. In essence, a sensor faults in DVs do not cause a permanent deviation in the CV values, but rather a disturbance in the MPC behaviour, causing delay and a short-lasting deviation between CVs and the CV setpoint values. In this case, an FTC based on the FDD estimation was used to estimate the values of the DV sensors in the past. The input measurements of the FTC strategy for the DV sensor faults are presented in Table 22; the structure of the 1st PLS model used for the fault detection in Table 23; and the 2nd PLS model used for the fault estimation in Table 24.

Table 22. The inputs of the active data-based FTC strategy for the DV sensor faults.

Variable name	Variable description	Unit
DA1_TEMP_1	DA1 top/overhead temperature	*°C*
DA1_TEMP_3	DA1 temperature, tray 13	*°C*
DA1_TEMP_4	DA1 temperature, tray 21	*°C*
DA1_OVHD_FLOW_FC	DA1 overhead gas flow rate	*t/h*
DA2_DIST_FC	DA2 overhead gas flow rate	*t/h*

Table 23. The structure of the 1st PLS model for the active data-based FTC strategy for the DV sensor faults.

Model	**DV_PLS1_1**	**DV_PLS1_2**	**DV_PLS1_3**	**DV_PLS1_4**
Output	DA1_FEED_FC	DA1_FEED_TC	DA1_HEAT_TC	DA1_PC
Inputs	DA1_TEMP_1	DA1_TEMP_1	DA1_TEMP_1	DA1_TEMP_1
	DA1_TEMP_2	DA1_TEMP_2	DA1_TEMP_2	DA1_TEMP_2
	DA1_TEMP_3	DA1_TEMP_3	DA1_TEMP_3	DA1_TEMP_3
	DA1_OVHD_FLOW_FC	DA1_OVHD_FLOW_FC	DA1_OVHD_FLOW_FC	DA1_OVHD_FLOW_FC
	$DA1\_FEED\_FC(t-d_{max}-d_1)$	$DA1\_FEED\_TC(t-d_{max}-d_1)$	$DA1\_HEAT\_TC(t-d_{max}-d_1)$	$DA1\_PC(t-d_{max}-d_1)$
	$DA1\_FEED\_FC(t-d_{max}-d_2)$	$DA1\_FEED\_TC(t-d_{max}-d_2)$	$DA1\_HEAT\_TC(t-d_{max}-d_2)$	$DA1\_PC(t-d_{max}-d_2)$

Table 24. The structure of the 2nd PLS model for the active data-based FTC strategy for the DV sensor faults.

Model	**DV_PLS2_1**	**DV_PLS2_2**	**DV_PLS2_3**	**DV_PLS2_4**
Output	DA1_FEED_FC	DA1_FEED_TC	DA1_HEAT_TC	DA1_PC
Inputs	DA1_TEMP_1	DA1_TEMP_1	DA1_TEMP_1	DA1_TEMP_1
	DA1_TEMP_2	DA1_TEMP_2	DA1_TEMP_2	DA1_TEMP_2
	DA1_TEMP_3	DA1_TEMP_3	DA1_TEMP_3	DA1_TEMP_3
	DA1_OVHD_FLOW_FC	DA1_OVHD_FLOW_FC	DA1_OVHD_FLOW_FC	DA1_OVHD_FLOW_FC
	$DA1\_FEED\_FC(t-d_{max}-d_3)$	$DA1\_FEED\_TC(t-d_{max}-d_3)$	$DA1\_HEAT\_TC(t-d_{max}-d_3)$	$DA1\_PC(t-d_{max}-d_3)$
	$DA1\_FEED\_FC(t-d_{max}-d_4)$	$DA1\_FEED\_TC(t-d_{max}-d_4)$	$DA1\_HEAT\_TC(t-d_{max}-d_4)$	$DA1\_PC(t-d_{max}-d_4)$

The NIPALS algorithm presented in 3.4.1 was used for the iterative training of the PLS models, and the amount of latent variables was determined using the knee-in-the-plot method. PLS for the DV sensor faults was trained by using a data set consisting of 600 minutes of process data. This data set was generated under MPC control, while manipulating the DVs and the CV reference trajectories in order to create sufficient excitation to capture the closed-loop behaviour of the target process for the data-based FDD methods. This training data is presented in Appendix E.

The cumulative variances for the input vector X and the output vector Y, and the number of cumulative latent variables for each PLS model are presented in Table 25:

Table 25. The cumulative variances for X and Y and the number of the LVs for the PLS for the DV sensor faults.

PLS model	Cumulative variance of *X*	Cumulative variance of *Y*	Number of latent variables
DV_PLS1$_1$	81	98	3
DV_PLS1$_2$	83	99	2
DV_PLS1$_3$	99	99	2
DV_PLS1$_4$	99	99	2
DV_PLS2$_1$	81	98	3
DV_PLS2$_2$	83	99	2
DV_PLS2$_3$	99	100	2
DV_PLS2$_4$	99	99	2

Next, the active data-based FTC strategy for the DV sensor faults was tested with the bias fault in a DV sensor. The drift fault was not tested because it has small or no effect at all on the process.

A downward bias-shaped fault with a magnitude of 5% of the nominal value of DA1_FEED_FC was introduced into the DA1 feed flow measurement during the time step T_1 = 15 minutes, with FTC turned off. The fault lasts for 90 minutes until the time step T_2 = 105 minutes, after which the fault was removed from the target process. The FDD part of the active data-based FTC strategy for the DV sensor faults was turned on, but no FTC actions were made. The PLS-based prediction and the effect of the fault can be seen in Figure 34.

As can be seen from Figure 34, the -5% downward fault caused a downward effect on both DA1_BP_FP and DA2_BP_FP. Immediately after the effects started to appear in the CVs, the feedback control system started to compensate for the deviance from the setpoint value, thus correcting the error in the measurement. The PLS was able to predict the actual value of the DV measurement effectively. Overall, the fault had the effect that both DA1_BP_FP and DA2_BP_FP were off the specification limits for 90 minutes. The overall effect of the DV sensor fault was much lower than a fault in the CVs.

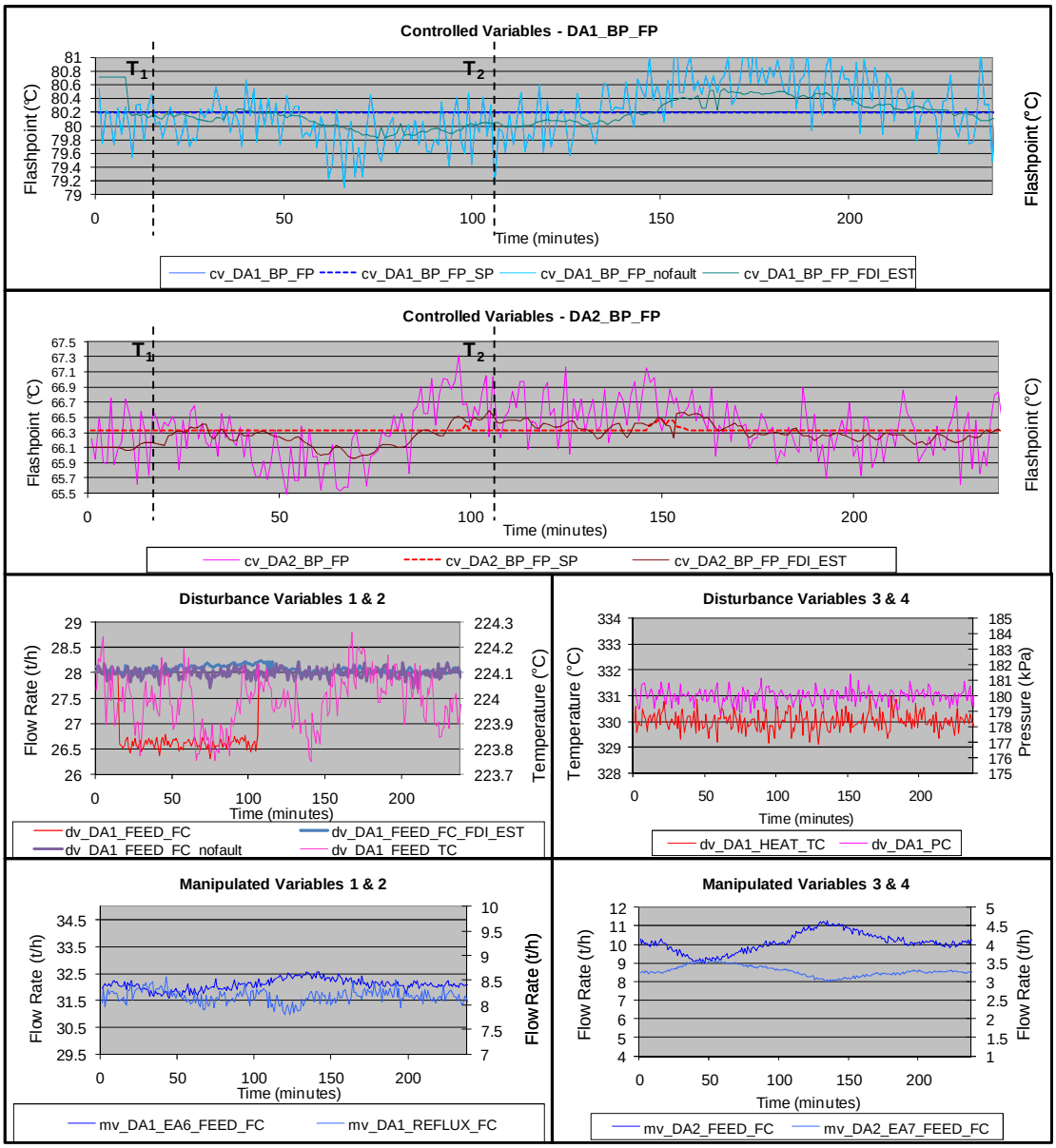

Figure 34. The effects of a -5% bias fault in DV DA1_FEED_FC during t = 15 - 105 minutes, without the active data-based FTC strategy for the DV sensor faults.

Next, the previous fault scenario with a -5% bias-shaped fault affecting DA1_FEED_FC was tested with the active data-based FTC strategy for the DV sensors.

A downward bias-shaped fault with a magnitude of 5% of the nominal value of the DA1_FEED_FC was introduced into the DA1 feed flow measurement during the time step T_1 = 15 minutes, with the active data-based FTC strategy for the DV sensor faults turned on. As before, the fault lasted for 90 minutes until the time step T_2 = 105 minutes, after which the fault was removed from the process. As can be seen from the PLS fault detection values in Figure 35, the FTC actions were engaged at the time step T_d = 34 minutes, 19 minutes after the fault starts to affect the process. The delay in the detection was caused by the backward prediction from the measurement values. There were no false alarms during this test run.

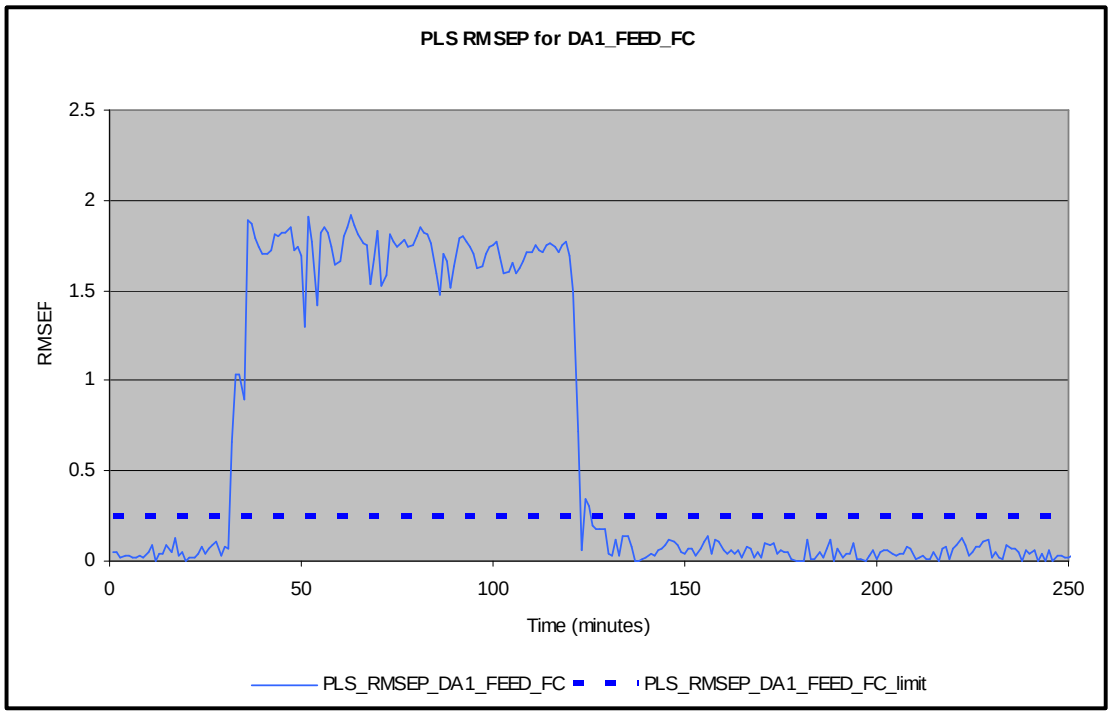

Figure 35. The PLS RMSEP values for a -5% bias fault in DV DA1_FEED_FC during t = 15 - 105 minutes, with the active data-based FTC strategy for the DV sensor faults.

As can be seen from Figure 36, with the active data-based FTC strategy for the DV sensor faults, the -5% bias fault had a considerably smaller effect on the controlled variables; this time DA_BP_FP was off-spec for only 25 minutes. In this case, there was virtually no effect on DA2_BP_FP due to the active data-based FTC strategy. The PLS was able to predict the actual value of the measurement accurately despite the spiking caused by the dynamic input to the FDD. In general, both DA1_BP_FP and DA2_BP_FP remained more closely within the specification limits despite the fault, thus improving the reliability of the control system and reducing off-spec production.

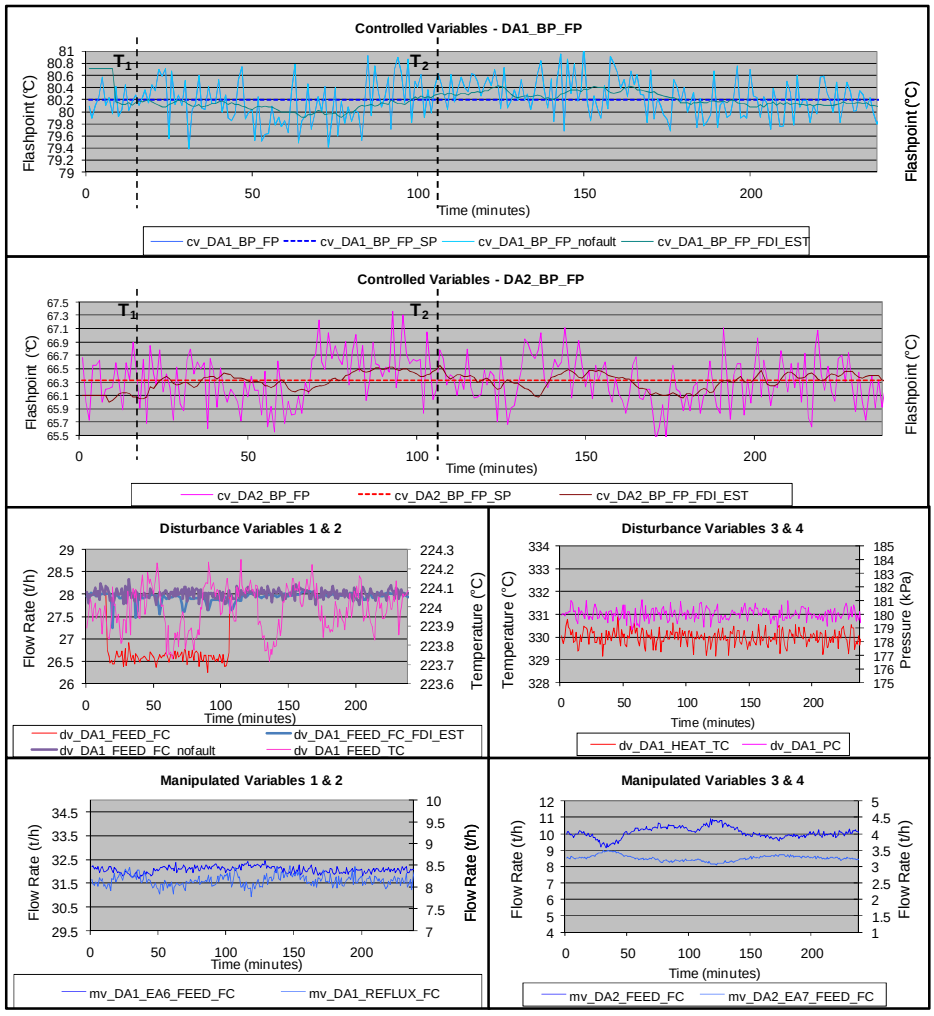

Figure 36. The effects of a -5% bias fault in DV DA1_FEED_FC during t = 15 - 105 minutes, with the active data-based FTC strategy for the DV sensor faults.

7.3.3 Testing results of the active FTC strategy for the MV sensor faults

The sensor faults for MVs cause a deviation in the MV value and a disturbance in MPC behaviour: a downward fault in an MV causes an elevating effect on the actual value, which is increased by the magnitude of the fault. This again causes deviation in the CV values from the CV setpoint values; however, as is the case with DV faults, this deviation is rapidly removed through feedback. The drift faults were not tested in this study because the effect of a drift-shaped fault was easily handled by the feedback and therefore an abrupt bias fault caused the most disturbances in the CV values. PLS-based FDD and controller reconfiguration methods were used in the case of the active data-based FTC strategy for MV sensors in such a way that as soon as the fault was detected by the FDD, opposite steps change was made to the faulty measurement and the faulty measurement was disabled until the fault was removed.

The inputs for the active data-based FTC strategy for the MV sensor faults are presented in Table 26, and the structure of the PLS model in Table 27.

Table 26. The inputs for the active data-based FTC strategy for the MV sensor faults.

Variable name	Variable description	Unit
DA1_TEMP_1	DA1 top/overhead temperature	*°C*
DA1_TEMP_2	DA1 temperature, tray 5	*°C*
DA1_TEMP_3	DA1 temperature, tray 13	*°C*
DA1_TEMP_4	DA1 temperature, tray 21	*°C*
DA1_TEMP_5	DA1 temperature, tray 41	*°C*
DA1_TEMP_6	DA1 bottom product temperature	*°C*
DA1_OVHD_FLOW_FC	DA1 overhead gas flow rate	*t/h*
DA1_BP_FC	DA1 bottom product flow rate	*t/h*
DA2_DIST_FC	DA2 overhead gas flow rate	*t/h*
DA2_PC1	DA2 upper pressure measurement	*bar*
DA1_FEED_EA_FC	DA1 feed heat exchanger hot fluid flow	*t/h*
DA2_BP_TC	DA2 bottom product temperature	*°C*
DA2_BP_FC	DA2 bottom product flow rate	*t/h*

Table 27. The structure of the PLS model for the active data-based FTC strategy for the MV sensor faults.

Model	MV_PLS1_1	MV_PLS1_2	MV_PLS1_3	MV_PLS1_4
Output	DA1_REFLUX_FC	DA1_EA6_FEED_FC	DA2_FEED_FC	DA2_EA7_FEED_FC
Inputs	DA1_TEMP_1	DA1_TEMP_1	DA1_TEMP_3	DA1_TEMP_2
	DA1_TEMP_2	DA1_TEMP_2	DA1_TEMP_4	DA2_DIST_FC
	DA1_TEMP_3	DA1_TEMP_3	DA1_TEMP_5	DA2_BP_TC
	DA1_TEMP_4	DA1_TEMP_4	DA1_TEMP_6	DA2_BP_FC
	DA1_OVHD_FLOW_FC	DA1_TEMP_5	DA1_BP_FC	
	DA2_DIST_FC	DA1_TEMP_6	DA2_BP_TC	
		DA1_OVHD_FLOW_FC	DA2_BP_FC	
		DA1_BP_FC		
		DA1_FEED_EA_FC		
		DA2_BP_TC		
		DA2_BP_FC		

As before, the NIPALS algorithm presented in 3.4.1 was used for the iterative training of the PLS models, and the number of latent variables was determined using the knee-in-the-plot method. PLS for the MV sensor faults was trained by using a data set consisting of 600 minutes of process data. This data set was generated under MPC control, while manipulating the DVs and the CV reference trajectories in order to create sufficient excitation to capture the closed-loop behaviour of the target process for the data-based FDD methods. These training data are presented in Appendix E. The cumulative variances for the input vector X and the input vector Y and the number of cumulative latent variables for each PLS model is presented in Table 28.

Table 28. The cumulative variances for X and Y and the number of the LVs for the PLS for the MV sensor faults.

PLS model	Cumulative variance of X	Cumulative variance of Y	Number of latent variables
MV_PLS1_1	98	69	5
MV_PLS1_2	93	87	5
MV_PLS1_3	99	99	3
MV_PLS1_4	90	85	3

The active data-based FTC strategy for the MV sensor faults was next tested with a bias fault in the MV sensor. A downward bias-shaped fault with a magnitude of 10% of the nominal value of DA1_REFLUX_FC was introduced into the DA1 reflux flow measurement during the time step T_1 = 15 minutes, without the active data-based FTC strategy. The fault lasted for 90 minutes until the time step T_2 = 105 minutes, after which the fault was removed from the process. The FDD part of the active data-based FTC strategy for the MV sensor faults was turned on, but no FTC actions were made. The PLS-based prediction and the effect of the fault can be seen in Figure 37.

As can be seen from Figure 37, the -10% downward fault caused a downward effect on both DA1_BP_FP and DA2_BP_FP. Immediately after the effects started to appear in the CVs, the feedback control system started to compensate for the deviance from the setpoint value, thus correcting the error in the measurement. PLS was able to predict the actual value of the DV measurement effectively. Overall, the fault had the effect that both DA1_BP_FP and DA2_BP_FP were off the specification limits for 40 minutes. The overall effect of the MV sensor fault was much lower than a fault in the CVs.

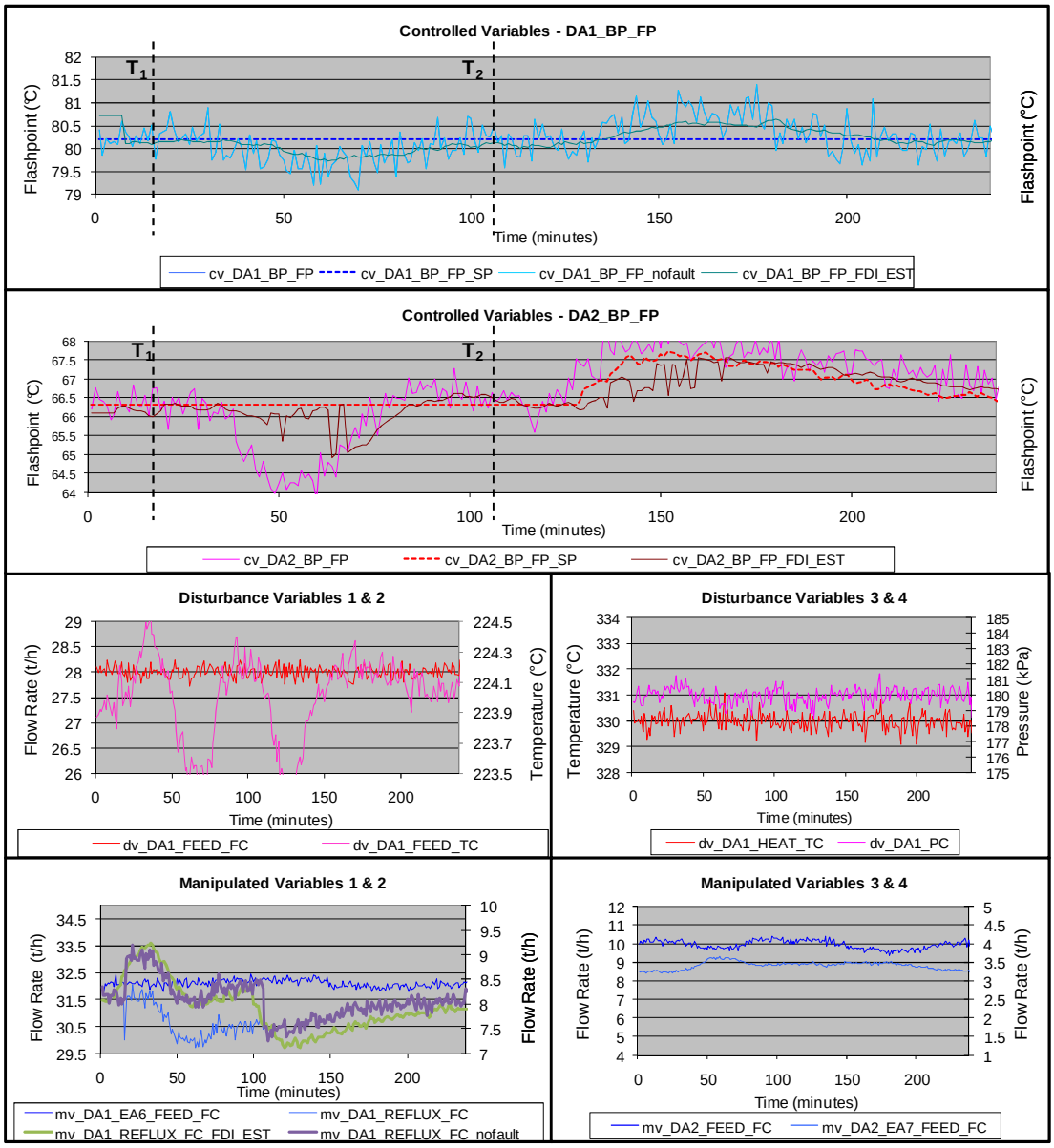

Figure 37. The effects of a -10% bias fault in MV DA1_REFLUX_FC during t = 15 - 105 minutes, without the active data-based FTC strategy for the MV sensor faults.

Next, the previous fault scenario with a -10% bias-shaped fault affecting DA1_REFLUX_FC was tested with the active data-based FTC strategy for the MV sensors.

A downward bias-shaped fault with a magnitude of 10% of the nominal value of DA1_REFLUX_FC was introduced into the DA1 reflux flow measurement during the time step T_1 = 15 minutes, with the active data-based FTC strategy for the MV sensor faults. As before, the fault lasted for 90 minutes until the time step T_2 = 105 minutes, after which the fault was removed from the target process. As can be seen from the PLS fault detection values in Figure 38, the FTC actions were engaged at the time step T_d = 27 minutes, 12 minutes after the fault was introduced. At this time, an opposite step change with an estimated fault magnitude was made to the faulty MV, after which the MV was disabled until the fault has been removed. The delay was caused by the estimation based on the current measurement values. There were no false alarms during this test run.

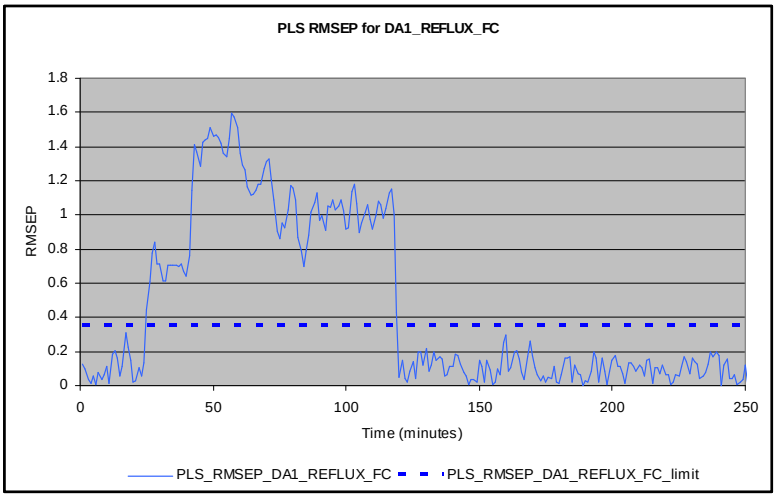

Figure 38. The PLS RMSEP values for a -10% bias fault in MV DA1_REFLUX_FC during t = 15 - 105 minutes, with the active data-based FTC strategy for the MV sensor faults.

As can be seen from Figure 39, with the active data-based FTC strategy for the MV sensors, the -10% bias fault had a considerably smaller effect on the controlled variables, thus keeping the product within the specification limits. The effect was also smaller for DA2_BP_FP. The FDD was able to predict the actual value of the measurement with reasonable accuracy. In general, both DA1_BP_FP and DA2_BP_FP remained more closely within the specification limits despite the fault, thus improving the reliability of the control system and reducing off-spec production.

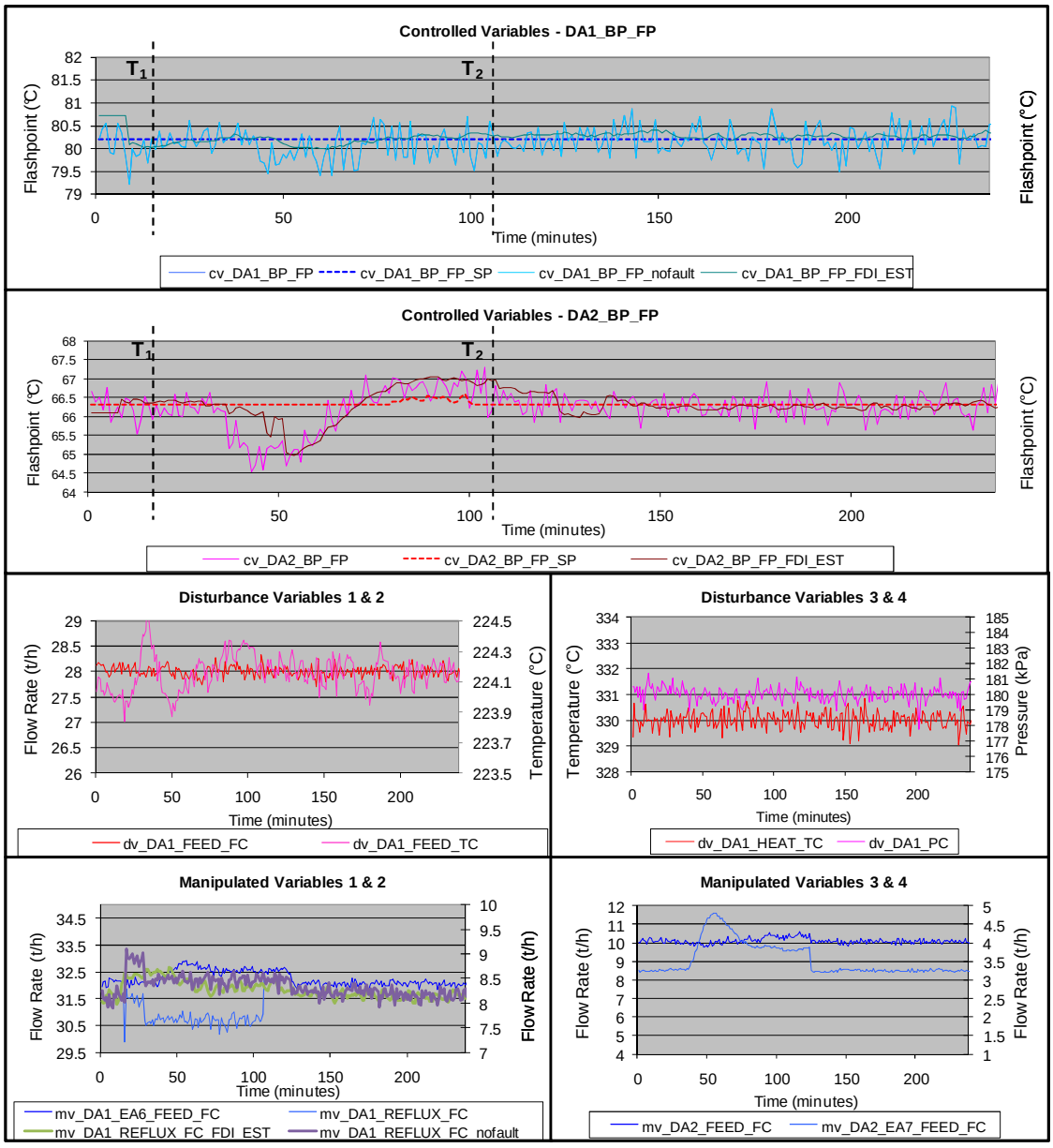

Figure 39. The effects of a -10% bias fault in MV DA1_REFLUX_FC during t = 15 - 105 minutes, the active data-based FTC strategy for the MV sensor faults.

7.3.4 Testing results of the active FTC strategy for the MV actuator faults

As stated by Bao et al. (2003), one of the most common faults in sub-level controllers, such as flow controllers, is a stuck valve fault. In this kind of fault, a valve is stuck in a certain position and the performance of the actuator can be severely decreased. The performance decrease can be so bad that it may not be used for control and thus lowering the performance of the overall control strategy. The cause of the fault can be sudden fouling (a large particle stuck in the valve), slowly progressive fouling (accumulation of material in the valve) or a broken valve. Under steady state conditions, the stuck valve fault is not detectable; however, if a disturbance or a setpoint change occurs, the fault prevents the valve being operated, effectively lowering the overall performance of the control system.

The FDD component in this case is very straightforward: the fault is detected if there is a difference between the control signal and the actuator measurement. A stuck valve fault was introduced into the DA2 feed flow measurement during the time step T_1 = 10 minutes. At the same time, a setpoint change of +1% was issued to the DA1 bottom product flashpoint, DA1_BP_FP. The FDD part of the active FTC strategy for the MV actuator faults was turned on but the FTC part was turned off. The effect of the fault can be seen in Figure 40.

As can be seen from Figure 40, the fault caused a delay in the MPC response, since the MPC could not use the primary controller to change the CV value; eventually, due to the feedback, other MVs had to be used to compensate for the stuck MV. Without a fault the MPC reached the given setpoint within 75 minutes, as can be seen in Figure 27. However, with a stuck valve fault in DA2_FEED_FC, the setpoint was reached within 200 minutes, causing a delay of 125 minutes due to a stuck valve fault in the critical actuator.

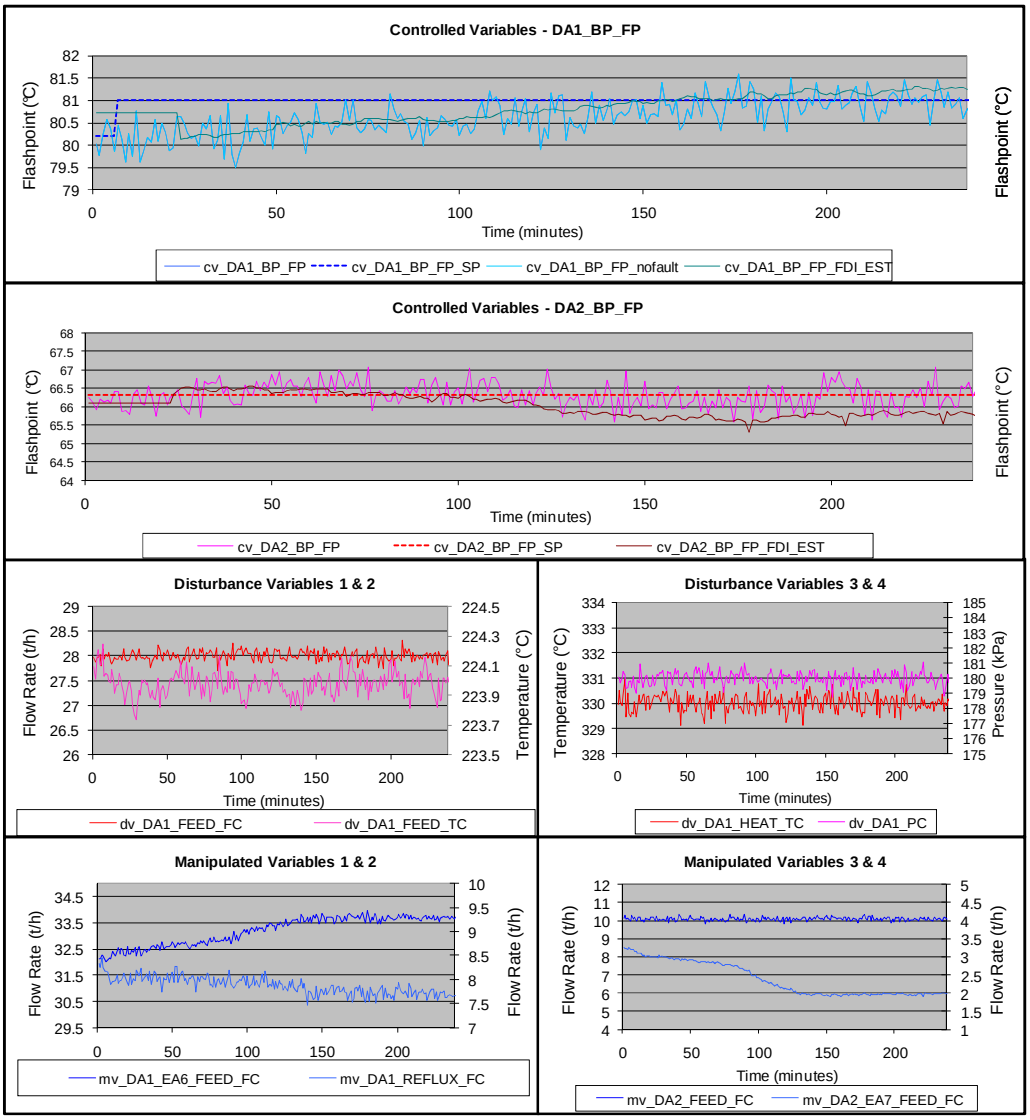

Figure 40. The effects of a stuck valve fault in MV DA2_FEED_FC while a +1% step change is made to the CV DA1_BP_FP setpoint and with the active FTC strategy for the MV actuator faults.

Next, the previous fault scenario was repeated with the active FTC strategy for the MV actuator faults. As can be seen from Figure 41 representing the root-mean square error (RMSE) value of DA2_FEED_FC, the fault was detected within three minutes of the occurrence of the fault. Once the fault had been detected, the MPC is reformulated and an auxiliary MV, DA1_FEED_TC, was activated instead of the faulty MV, which was switched off.

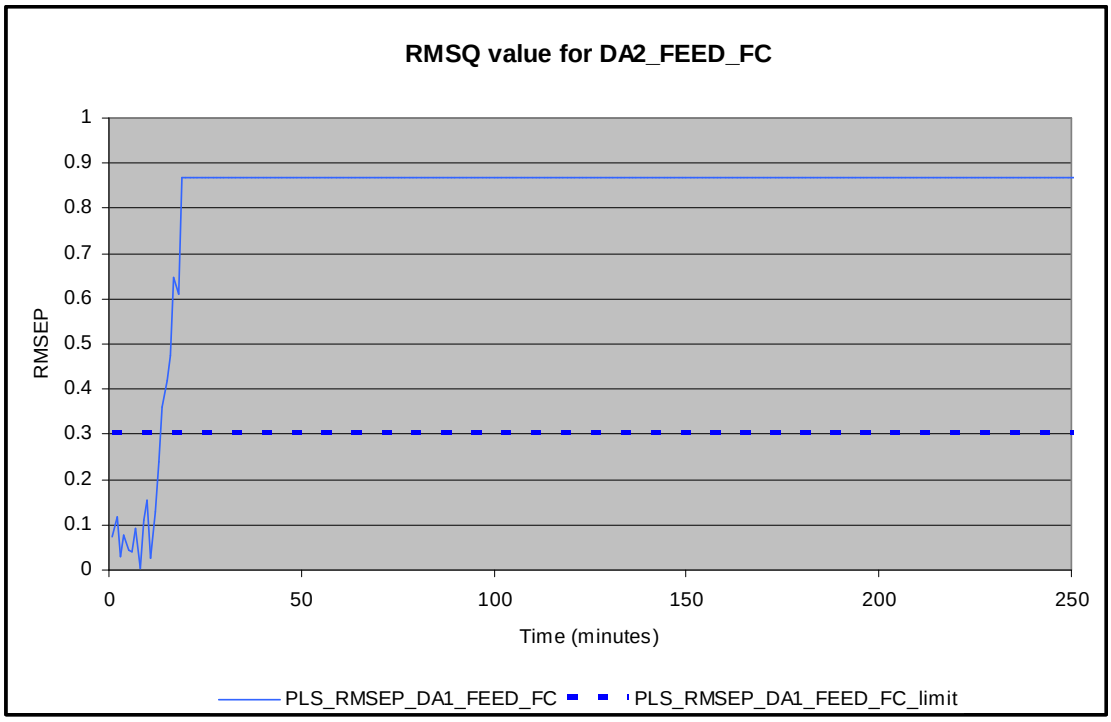

Figure 41. The RMSQ values of the stuck valve fault in MV DA2_FEED_FC representing the fault detection of the stuck valve fault.

This time, because the faulty MV was excluded from the MPC MV inputs, the MPC response time was much better; the target setpoint value was reached within 100 minutes after the setpoint change, which was 25 minutes slower than with the case without a stuck valve fault. Therefore, the active FTC strategy for the MV actuator faults had improved the response time by 100 minutes. The results of testing the MV actuator faults are presented in Figure 42.

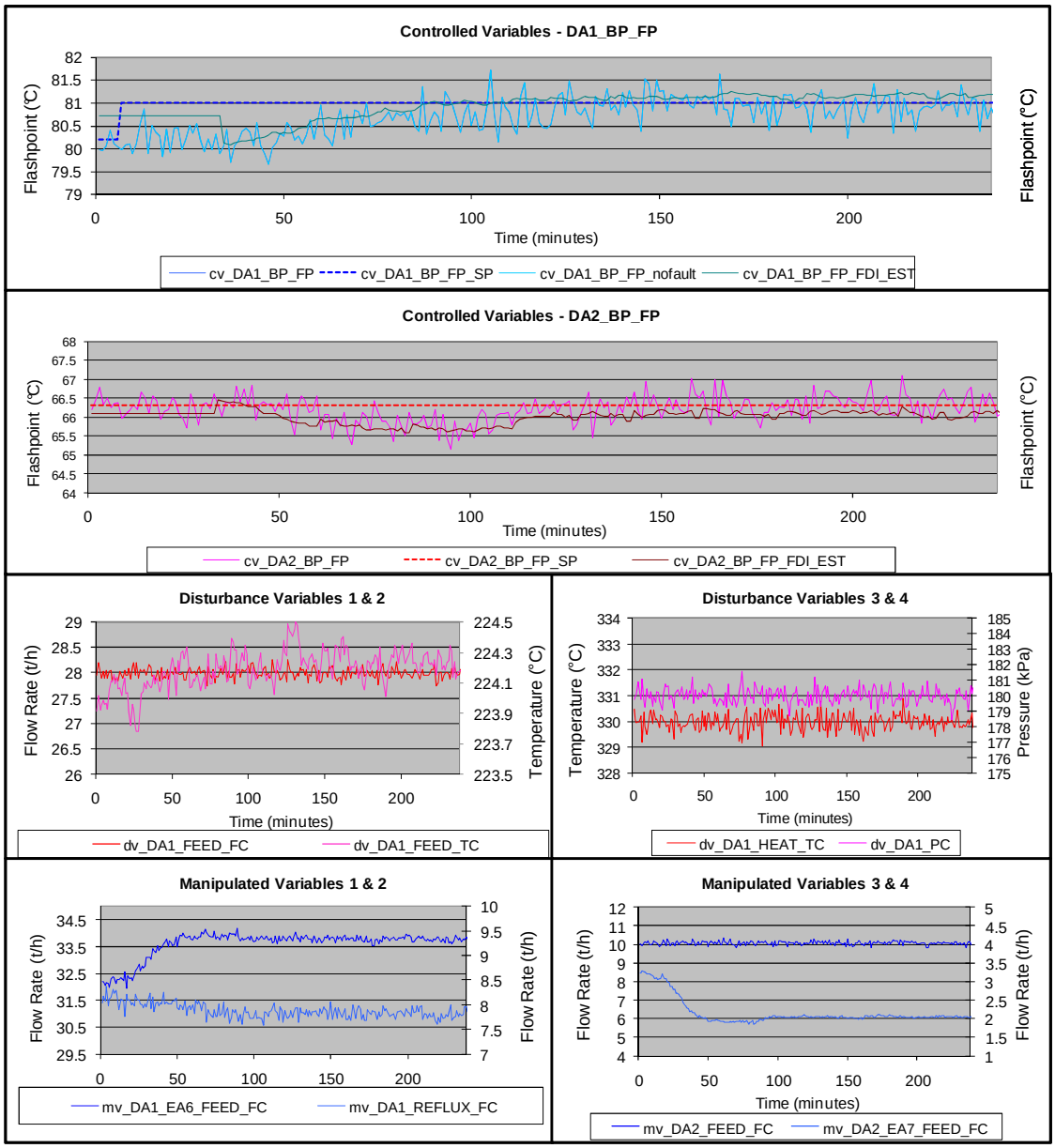

Figure 42. The effects of a stuck valve fault in MV DA2_FEED_FC while a +1% step change is made to the CV DA1_BP_FP setpoint and with the active FTC strategy for the MV actuator faults.

7.3.5 Summary and discussion of validating the performance of the integrated FTMPC for the target dearomatization process

In order to validate the performance of the integrated FTMPC, a testing was carried out with different fault types affecting the target process. In all the fault cases, the integrated FTMPC significantly improved the resistance and response time of the control system against the effects of the faults. With the integrated FTMPC, the off-spec production was considerably reduced; the performance of the control system when affected by a fault was improved; and the overall reliability was considerably better than with the nominal MPC.

The results of different FTC tests are presented with reaction times to different fault types in Table 29 for periods when the bottom product flashpoint is off the specification limit with and without the integrated fault-tolerant MPC. The ISE values are calculated for DA1_BP_FP and DA2_BP_FP in order to compare the results. For a case without any fault, the average ISE for both DA1_BP_FP and DA2_BP_FP is 30. The ISE values for different fault cases, with and without the integrated fault-tolerant MPC, are presented in Table 30.

*Table 29. Results of the testing of the integrated fault-tolerant MPC with different fault types (*compared to a case without a fault).*

Tested fault type	Fault type	Detection time	Product off spec, without FTC	Product off spec, with FTC
CV Sensor fault	+5% Bias	*19 minutes*	*Fault duration*	*10 minutes*
CV Sensor fault	+5% Drift	*19 minutes*	*Fault duration*	*0 minutes*
DV Sensor fault	-5% Bias	*20 minutes*	*Fault duration*	*25 minutes*
MV Sensor fault	-10% Bias	*16 minutes*	*40 minutes*	*10 minutes*
MV actuator fault	Stuck valve	*3 minutes*	*125 minutes**	*25 minutes**

Table 30. ISE values of the target process with and without the integrated fault-tolerant MPC and the percentages of improvement with the nominal ISE level of 30.

Tested fault type	DA1_BP/DA2_BP ISE, without FTC	DA1_BP/DA2_BP ISE, with FTC	Improvement
CV Sensor fault (+5% bias)	1223 / 114	*27 / 30*	*98 / 74%*
CV Sensor fault (+5% drift)	396 / 57	*23 /27*	*94 / 51%*
DV Sensor fault (-5% bias)	48 / 38	*32 /38*	*43 / 0%*
MV Sensor fault (-10% bias)	46 / 147	*30 / 66*	*35 / 66%*
MV actuator fault (stuck valve)	75 / 30	*64 / 30*	*15 / 0%*

As can be seen from Tables 29 and 30, the off-spec production was reduced as a result of fast detection and compensation of the faults, and the performance of the MPC was considerably improved with the integrated fault-tolerant MPC when compared to the nominal ISE level of approximately 30. Based on these results, it can be concluded that although the CV faults had longer lasting and more severe effects, the lower level controller faults also had an effect on the overall performance of the control system. Therefore, usage of the integrated FTMPC that also takes into account faults in DVs and MVs has a definitive effect on the performance of the control system.

7.4 Economic evaluation of the integrated FTMPC

In this chapter, the economic benefits for the integrated fault-tolerant MPC are calculated based on the FTMPC testing results presented in the previous section, actual fault occurrence probabilities in the dearomatization process presented in Section 6.2, approximated product prices as well as expert knowledge of the target process. In the calculations, the following assumptions are made:

- The price of a bottom product loss in the column DA1 is the price difference between the solvent product and the bulk product using the same feedstock type (for instance, diesel or gasoline). The price for the bottom product loss in this case can be estimated to be approximately USD 100 /t.

- The feed level to the unit is 28 t/h; the average bottom product flow rate 17 t/h; the average side product flow rate 9 t/h; and the average overhead distillate flow rate 2 t/h.

- If the product FP goes below the specification limit, it needs to be corrected by preparing over-quality bottom product for an equivalent time. The quality of the bottom product can be increased by 1°C by increasing the overhead distillate flow by an average of 2 t/h; or alternatively by decreasing the unit feed by 2 t/h on average. In essence, an increase in the overhead distillate flow rate or a decrease in the feed flow rate causes the unit to lose capacity of 2 t/h on average for 1°C of FP. At the same time, the bottom product flow rate also decreases by 2 t/h. We assume 1°C of FP correction is used for all cases.

- The side product flow rate is assumed to be at a maximum, which forces an increase in the overhead flow rate or a decrease in the feed rate in order to correct the off spec batch.

- The over-quality of the final product has the effect that in order to produce over-quality product, the overhead distillate flow rate has to be increased and the bottom product flow rate reduced, essentially losing capacity of the unit by 2 t/h for 1°C of FP over-quality in the final product.

As an example, if the bottom product has been -1^{o}C off specifications for 10 hours, a total 17 t/h * 10 h = 170 tons of off-spec product have been produced. In order to correct this back to specifications, the unit has to operate with +1°C quality for 170 t / (17 t/h -2 t/h) = 11 h. During this time, the unit loses capacity 2 t/h *11 h = 22 t and this capacity has a value of 22 t * USD 100 /t = USD 2,200. Alternatively, the correction can be made with a smaller FP value. In this case, although the correction time is much longer, the losses are smaller due to the higher overall feed rate. In practice, there is not much time available to finish the product, and therefore the corrections need to be made with higher losses in order to prepare the product in time before delivery to the customers.

7.4.1 Economic evaluation of the sensor faults in the CVs and in the DVs

As stated in Section 6.2, during 2008 - 2009 3% off spec and 3% over-quality was produced due to faults in the analyser readings, in which case the analyser measurement were either higher or lower than the laboratory measurements by 2.8°C.

If it is assumed that the 3% of off-spec production causes at least eight hours of off-spec production, and each 1°C in FP causes 2 t/h losses, then a total of 750 t of total unit capacity is lost during one year due to the off spec production. In total, this means 750 t/year * USD 100 /t = USD 75,000 /year in off spec losses for this one specific grade only in the case of analyser failures.

If it is assumed that the 3% of over-quality production caused at least eight hours of over-quality production, and each 1°C in FP caused 2 t/h losses, then a total of 630 t of capacity was lost during one year due to the over-quality of the final product. In total, this means losses of 600 t/year * USD 100 /t = USD 60,000 /year in over-quality for this one specific grade only in the case of analyser failure.

The DV fault losses cannot accurately be calculated since there is no alternate measurement with which to compare the flow or temperature measurements. However, the combined probability of the DV and MV faults occurring can be estimated to be approximately the same as for the analyser faults (6%), as the number of faulty components in the maintenance logs was the same as the analyser faults, as discussed in Chapter 6. In this case, the DV faults would then occur in at least 3% of the total number of analyses made out of the main product in a year, which would be approximately eight faults per year.

In the case of DV faults, the fault lasted only for about 90 minutes with -5% and -10% faults, as can be seen from Table 29. The duration and magnitude of the effect of the fault depends on the magnitude of the fault. After 90 minutes, the MPC compensated for the fault and control of the CVs was restored. If the product was off spec for 1°C for approximately 90 minutes, this would cause an average loss of 3.4 t of production/fault. In total, this would cause approximately a 30 t loss of capacity each year, which would cost 30 t/year * USD 100 /t = USD 3,000 /year for the heavy grade alone.

In total, USD 141,000 is lost on average due to malfunctioning sensor or analyser measurements in CVs or DVs each year for this specific grade alone.

7.4.2 Economic evaluation of the sensor faults in the MVs

The probability of the MV sensor faults is assumed to be the same as with the DVs (3%), and the total number of MV sensor faults would approximately be eight faults per year.

As with the DV sensor faults, the MV fault lasted for about 90 minutes with -5% and -10% faults. The duration and magnitude of the effect of the fault depends on the magnitude of the fault. After 90 minutes, the MPC compensated for the fault and control of the CVs is restored. If the product was off spec for 1°C for approximately 90 minutes due to the MV sensor fault, this would cause an average loss of 3.4 t of production/fault. In total, this would cause approximately a 30 t loss of capacity each year, which would cost 30 t/year * USD 100 /t = USD 3,000 /year for the heavy grade alone.

7.4.3 Economic evaluation of the actuator faults in the MVs

Although the stuck valve losses cannot be precisely calculated, an estimation of stuck valve fault effects can be calculated using the probability of a valve fault. Stuck valve faults on actuators permanently decrease the performance of the control system, and thus can cause long-lasting performance problems unless the faulty actuator is repaired or replaced. However, as stated in Chapter 6 and based on the refinery maintenance logs, the occurrence of a stuck valve fault was only 16% of the total number of control system component faults, whereas the analyser and measurement device faults each account for 42%. Therefore, the probability of a stuck valve fault was approximately 30% lower than that for analyser or sensor faults. This means that stuck valve faults occurs on approximately 2% of the sampling times during a period of one year for the heavy grade.

In the case of actuator faults, the effect of a fault depends on whether there is a disturbance or a setpoint change, during which the stuck valve fault effects appear. In the example case in Table 29 with a stuck valve fault occurring during a setpoint change, the bottom product was off specifications for 125 minutes, which was 100 minutes less than with the FTC set on. If the product was off specifications by 1°C for approximately 100 minutes due to a DV or MV sensor fault, this would cause an average loss of production of 3.8 t/fault, which is equal to approximately 20 t of the capacity loss to the unit in one year, which would cost 20 t/h * USD 100 /t = USD 2,000 for the heavy grade alone.

7.4.4 Summary of the economic evaluation

Overall, it is estimated that the integrated fault-tolerant MPC has the potential to produce, at a maximum, savings of some USD 148,000 during one year in the case of the heavy grade alone. Over 90% of the savings would be achieved by more optimal operation by reducing the effect of analyser faults through the use of fault accommodation. Less than 10% of the savings would be achieved with the active data-based FTC strategy on the DV and MV sensor fault accommodation and controller reconfiguration methods for stuck valve faults.

In general, based on industrial experience of project costs and cost estimates, it could be estimated that an industrial-scale version of the integrated fault-tolerant MPC without an MPC implementation would cost approximately USD 50,000 - 100,000. Therefore, the integrated fault-tolerant MPC like this would have a repayment period of 4 - 8 months, thereby making an investment of this magnitude highly profitable in normal economic conditions. In addition, if an integrated fault-tolerant MPC would be implemented in a process without an MPC already in place, the profits would be even higher due to better optimisation of the target process and lower overall costs, since the implementation could be carried out in connection with the installation of an MPC allowing the full design of the integrated fault-tolerant MPC.

8 Conclusions

In this thesis, an integrated FTMPC reducing the effects of the faults in the analyser, flow, temperature and pressure measurements, and in the actuators has been developed for an industrial dearomatization process. First, the results of a literature study of state-of-the-art in FTC for the target process were presented and the most suitable FTC components and design schemes were determined. Second, based on these schemes and the FTMPC user requirements, the integrated FTMPC containing three parallel-running FTC strategies was developed. These three strategies contain fault accommodation- and controller reconfiguration-based FTC strategies and an FDD component based on the recursive PLS. Third, three data-based FDD methods and the fault accommodation-based FTC strategy were tested and the FDD methods compared on a recognised preliminary testing process. Based on the preliminary testing results, the most suitable FDD method, recursive PLS, was selected as the FDD method for the final application. Fourth, the performance of the nominal MPC was determined and the developed integrated fault-tolerant MPC with three FTC strategies was validated with the simulated dearomatization process with faults in the CV, DV and MV sensors and MV actuators. Finally, based on the validation results, the profitability of the integrated FTMPC was evaluated by using the estimated price of the end product and faults in the actual dearomatization process located in the Naantali refinery.

The hypotheses presented in Chapter 1 are: (1) The integration of the data-based FDD methods and the fault accommodation and the controller reconfiguration FTC methods provide the control system of a dearomatization process with the tools needed to overcome the typical process and measurement disturbances and faults in the dearomatization process environment; and (2) The availability and profitability of the dearomatization process are enhanced by the compensation of the critical faults using the fault accommodation and the controller reconfiguration FTC methods. These hypotheses have been verified by the results acquired in testing the proposed integrated fault-tolerant MPC with the simulated dearomatization process in Section 7.3, and with the economic evaluation in Section 7.4.

Based on the results of the thesis, the integrated fault-tolerant MPC was able to reduce the effect of the typical faults in the target process. Therefore, it could be estimated that the reliability of the dearomatization process is enhanced if the integrated fault-tolerant MPC would be implemented in the actual dearomatization process. Based on the economic evaluation of just one feed grade, the integrated FTMPC was found to be highly profitable; the annual estimated savings would be a maximum of USD 143,000, thereby the integrated FTMPC would pay for itself in less than one year. It can therefore be estimated that the integrated FTMPC would provide considerable savings in off-spec production, energy consumption and, in general, improvement of the unit operation due to faster detection and prevention of the fault effects.

The next task in the industrial FTMPC development would be to verify the accuracy of the FTMPC models by using the actual plant data. This verification would be carried out by comparing the FDD estimated values with the plant measurement values. After the accuracy of the PLS prediction has been verified, it would be beneficial to implement the integrated FTMPC directly in the software environment of the existing MPC in the actual plant. This maximises the data transfer rate, minimises errors and makes the integrated FTMPC as easy as possible to maintain and control through the existing graphical user interfaces (GUI). After the implementation, the accuracy of the FDD models should be verified during a long testing period by monitoring the difference between the FDD estimations and the measurements in different operation points without activating the FTC components. Next, when the accuracy of the FDD models has been found sufficient, the testing of the FTC strategies would be carried out. Finally, after the FTMPC performance has been fully verified under different operating conditions, it would be possible to take the FTMPC in normal plant operational use.

References

Abdi, H. (2010). Partial least squares regression and projection on latent structure regression (PLS Regression), Wiley Interdisciplinary Reviews: Computational Statistics, 2(1), 97–106.

Bao, J., Zhang, W.Z. & Lee, P.L. (2003). Decentralized fault-tolerant control system design for unstable processes, Chemical Engineering Science, 58(22), 5045–5054.

Bars, R., Colaneri, P., de Souza, C.E., Dugard, L., Allgöwer, F., Kleimenov, A. & Scherer, C. (2006). Theory, algorithms and technology in the design of control systems, Annual Reviews in Control, 30(1), 19–30.

Bemporad, A., Borrelli, F. & Morari, M. (2003). Min–max Control of Constrained Uncertain Discrete-Time Linear Systems. IEEE Transactions on Automatic Control, 48(9), 1600–1606.

Bemporad, A., Morari, M. & Ricker N.L. (2007). Matlab Model Predictive Control Toolbox 2 – User's Guide, http://www.mathworks.com/access/helpdesk/help/pdf_doc /mpc/mpc_ug.pdf, Mahworks 2007, 16.4.2007.

Bitmead R.R., Gevers M. & Wertz V. (1990). Adaptive optimal control: the thinking man's GPC, Prentice-Hall, New York, 244 p.

Blanke, M., Izadi-Zamanabadi, R., Bogh, R. & Lunau, Z.P. (1997). Fault-tolerant control systems – A holistic view, Control Engineering Practice, 5(5), 693–702.

Blanke, M., Kinnaert, M, Lunze, J. & Staroswiecki, M. (2003). Diagnosis and Fault-Tolerant Control. Springer-Verlag, Berlin, 566 p.

Buffington, J.M. & Enns, D.F. (1996). Lyapunov Stability Analysis of Daisy Chain Control Allocation, Journal of Guidance, Control and Dynamics, 19(6), 1226–1230.

Camacho, E.F. & Bourdons, C. (2004). Model Predictive Control, the 2nd edition, Springer-Verlag, London, 280 p.

Campo, P.J. & Morari, M. (1987). Robust Model Predictive Control, In proceedings of 6th American Control Conference, Edgar, T.F. (Editor), American Automatic Control Council, Minneapolis, 1021–1026.

Cannon, M. (2004). Efficient nonlinear model predictive control algorithms, Annual Reviews in Control, 28(2), 229–237.

Deshpande, A.P., Patwardhan, S.C. & Narasimhan, S.S. (2009). Intelligent state estimation for fault tolerant nonlinear predictive control, Journal of Process Control, 19(2), 187–204.

Dunia, R., Qin, S.J., Edgar, T.F. & McAvoy, T. (1996). Identification of Faulty Sensors Using Principal Component Analysis, AIChE Journal, 42(10), 2797–2812.

Frank, P.M., Ding, S.X. & Marcu, T. (2000). Model-based fault diagnosis in technical processes, Transactions of the Institute for Measurement and Control, 22(1), 57–101.

Gani, A., Mhaskar, P. & Christofides, P.D. (2007). Fault-tolerant control of a polyethylene reactor, Journal of Process Control, 17(5), 439–451.

Gerlach, R.W., Kowalski, B.R., & Wold, H. (1979). Partial least squares modelling with latent variables, Analytica Chimica Acta, 112(4), 417–421.

Gertler, J.J. (1998). Fault detection and diagnosis in engineering systems, Marcel Dekker Inc., New York, 484 p.

Griffin, G, & Maybeck, P. (1997). MMAE/MMAC control for bending with multiple uncertain parameters, IEEE Transactions on Aerospace and Electronic Systems, 33(3), 903–911.

Hotelling, H. (1933). Analysis of a complex of statistical variables into principal components , Journal of educational psychology, 24, 417–441.

Hotelling, H. (1947). Multivariate Quality Control, In Techniques of Statistical Analysis, Eisenhart, C., Hastay, M.W. & Wallis, W.A. (Editors), McGraw-Hill, New York, 111–184.

Huang, R., Patwardhan, S.C. & Biegler, L.T. (2009). Multi-Scenario-Based Robust Nonlinear Model Predictive Control with First Principle Models, Computer-Aided Chemical Engineering, Alves, R., Nascimento C. & Biscaia, E. Jr. (Editors), Elsevier, Amsterdam, 1293–1298.

Hyötyniemi, H. (2001). Multivariate regression – Techniques and tools, Espoo, Helsinki University of Technology, 125 p.

Isermann, R. & Ballé, P. (1997). Trends in the application of model-based fault detection and diagnosis of technical processes, Control Engineering Practice, 5(5), 709–719.

Jackson, J.E. & Mudholkar, G.S. (1979). Control Procedures for Residuals Associated With Principal Component Analysis, Technometrics, 21(3), 341–349.

Jackson, J.E. (1991). User's Guide to Principal Components, New York, Wiley Interscience, 592 p.

Jalali, A.A. & Nadimi, V. (2006). A Survey on Robust Model Predictive Control from 1999-2006, In proceedings of International Conference on Computational Intelligence for Modelling Control and Automation and International Conference on Intelligent Agents, Web Technologies and Internet Commerce (CIMCA-IAWTIC'06), Mohammadian, M. (Editor), IEEE Computer Society, Sydney, 207–213.

de Jong, S. (1993). SIMPLS: an alternative approach to partial least squares regression, Chemometrics and Intelligent Laboratory Systems, 18(3), 251–263.

Kanev, S. & Verhaegen, M. (2000). Controller reconfiguration for non-linear systems, Control Engineering Practice, 8(11), 1223–1235.

Keerthi S.S., Gilbert E. G. (1988). Optimal, infinite horizon feedback laws for a general class of constrained discrete time systems: Stability and moving-horizon approximations, Journal of Optimization Theory and Application, 57(2), 265–293.

Kettunen, M. & Jämsä-Jounela, S.-L. (2006a). Fault tolerant MPC with an embedded FDI system, In proceedings of Nordic Process Control Workshop (NPCW ‘06), Jørgensen, S.B. (Editor), Nordic Process Control Group, Lyngby, (poster).

Kettunen, M. & Jämsä-Jounela, S.-L. (2006b). Fault tolerant MPC with an embedded FDI system, In Proceedings of 1st Workshop on Application of Large scale systems (ALSIS ’06), Filip, F., Yliniemi, L. & Leiviskä K. (Editors), Finnish Automation Society, Helsinki/Stockholm.

Kettunen, M., Zhang, P. & Jämsä-Jounela, S-L. (2008). Embedded Fault Detection, Isolation, Accommodation System in a Model Predictive Controller for an Industrial Benchmark Process, Computers & Chemical Engineering, 32(12), 2966–2985.

Kettunen, M. & Jämsä-Jounela S-L. (2010). Data-based, fault-tolerant model predictive control of a complex dearomatization process, Industrial and engineering chemistry research, submitted for review.

Koivisto, K., Kettunen, M., Sourander, M., Liikala, T., Léger, J.-B. & Sauter, D. (2008). Fault-tolerant control protects processes and products, Hydrocarbon processing, 87(10), 51–61.

Kothare, M., Balakrishnan, V. & Morari, M. (1996). Robust constrained model predictive control using Linear Matrix Inequalities, Automatica, 32(10), 1361–1379.

Lazar, M., Muñoz de la Peña, D., Heemels, W.P.M.H. & Alamo, T. (2008). On input-to-state stability of min–max nonlinear model predictive control. Systems & Control Letters, 57(1), 39–48.

Lee, J.H. & Cooley, B. (1997). Recent advances in model predictive control and other related areas, In Proceedings of the Fifth Conference on Chemical Process Control (CPC V) Assessment and New Direction for Research, vol. 93, AIChE Symposium Series No. 316, 201–216.

Liikala, T. (2005). The use of fault detection in model predictive control of a refinery process unit, Master's Thesis, Helsinki University of Technology, Espoo, 133 p.

Luyben, W.L., (1990). Process Modeling, Simulation and Control for Chemical Engineers, McGraw-Hill, New York, 752 p.

Maciejowski, J.M. (1998). The Implicit Daisy-Chaining Property of Constrained Predictive Control, Applied mathematics and Computer Science, 8(4), 101–117.

Maciejowski, J.M. (2002). Predictive Control with Constraints, Prentice Hall, London, 352 p.

Mahmoud, M.M., Jiang, J. & Zhang, Y.M. (2003). Active fault tolerant control systems: Stochastic analysis and synthesis, Lecture notes in control and information sciences (Vol. 287), Springer-Verlag, Berlin, 207 p.

Manuja, S., Narasimhan, S. & Patwardhan, S. (2008). Fault diagnosis and fault tolerant control using reduced order models, The Canadian Journal of Chemical Engineering, 86(4), 791–803.

Marlin, T. (1995). Process Control: Designing Processes and Control Systems for Dynamic Performance, McGraw-Hill International Editions, Chemical Engineering Series, New York, 1056 p.

Mayne D.Q. & Michalska H. (1990). Receding Horizon Control of Non-Linear Systems, IEEE Transactions on Automatic Control, 35(5), 814–824.

McAvoy, T., Jämsä-Jounela, S-L., Patton, R., Perrier, M., Weber, H., & Georgakis, C. (2004). Milestone report for area 7 industrial applications, Control Engineering Practice, 12(1), 113–119.

McFarlane, R.C., Reneman, E.C., Bartee, J.F. & Georgakis, C. (1993). Dynamic simulator for a model IV fluid catalytic cracking unit, Computational Chemistry, 17(3), 275–300.

Mendonca, L.F., Sousa, J. & Sa da Costa, J.M.G. (2008). Fault accommodation of an experimental three tank system using fuzzy predictive control, In Proceedings of Fuzzy Systems FUZZ-IEEE 2008 (IEEE World Congress on Computational Intelligence), Feng, G.G. (Editor), IEEE, Hong Kong, 1619–1625.

Mhaskar, P., Gani, A., McFall, C., Christofides, P.D. & Davis, J.F. (2007). Fault-tolerant control of nonlinear process systems subject to sensor faults, AIChE Journal, 53(3), 654–668.

Mhaskar, P. & Kennedy, A.B. (2008). Robust model predictive control of nonlinear process systems: Handling rate constraints, Chemical Engineering Science, 63(2), 366–375.

Morari, M. & Lee, J.H. (1999). Model predictive control: past, present and future, Computers and Chemical Engineering, 23(4–5), 667–682.

Muske, K.R. & Rawlings, J.B. (1993). Model Predictive Control with Linear Models, AIChE Journal, 39(2), 262–287.

Narasimhan, S.H. & Mah, R.S.H. (1988). Generalized Likelihood Ratios for Gross Error Identification in Dynamic Processes, AIChE Journal, 34(8), 1321–1331.

Patwardhan, S.C., Manuja, S., Narasimhan, S., & Shah, S.L. (2006). From data to diagnosis and control using generalized orthonormal basis filters. Part II: Model predictive and fault tolerant control, Journal of Process Control, 16(2), 157–175.

Pearson, K. (1901). On lines and planes of closest fit to systems of points in space, Philosophical magazine series, 6(2), 559–572.

Prakash, J., Patwardhan, S.C. & Narasimhan, S.A. (2002). Supervisory Approach to Fault-Tolerant Control of Linear Multivariable Systems, Industrial & Engineering Chemistry Research, 41(9), 2270–2281.

Pranatyasto, T.N. & Qin, S.J. (2001). Sensor validation and process fault diagnosis for FCC units under MPC feedback, Control Engineering Practice, 9(8), 877–888.

Prett, D.M. & Morari, M. (1987). Shell Process Control Workshop, Butterworth Publishers, Stoneham, 369 p.

Qin, S.J. & Badgwell, T.A. (2003). A survey of industrial model predictive control technology, Control Engineering Practice, 11(7), 733–764.

Raimondo, D.M., Limon, D., Lazar, M., Magni, L. & Camacho, E.F. (2009). Min–max model predictive control of nonlinear systems: A unifying overview on stability, European Journal of Control, 15(1), 1–17.

Ralhan, S. & Badgwell, T.A. (2000). Robust Model Predictive Control for Integrating Linear Systems with Bounded Parameters, Industrial & Engineering Chemistry Research, 39(8), 2981–2991.

Ray, W.H. (1989). Advanced Process Control, Butterworth Publishers, Boston, 376 p.

Rawlings, J.B. (2000). Tutorial overview of model predictive control, IEEE Control systems magazine, 20(3), 38–52.

Richards, A. (2005). Robust Model Predictive Control for Time-Varying Systems, In Proceedings of the 44th IEEE Conference on Decision and Control, and the European Control Conference 2005, Camacho, E.F. (Editor), IEEE, Seville, 3747–3752.

Rodrigues, M., Theilliol, D., Aberkane, S. & Sauter D. (2007). Fault Tolerant Control Design for Polytopic LPV Systems, International Journal of Applied Mathematics and Computer Science, 17(1), 27–37.

Staroswiecki, M. & Gehin, A-L. (2001). From control to supervision, Annual Reviews in Control, 25, 1–11.

Theilliol, D., Noura, H. & Ponsart J.C. (2002). Fault diagnosis and accommodation of a three-tank system based on analytical redundancy, ISA Transactions, 41(3), 365–382.

Vatanski, N., Vermasvuori, M., Ylinen, R., Jämsä-Jounela, S-L., Sourander, M., Leger, J-B. & Rondeau, E. (2005). Definitions of the user needs and the functional architecture for the NeCST system, Project report of Networked Control Systems Tolerant to Faults (NeCST) EU IST-2004-004303.

Venkatasubramanian, V., Rengaswamy, R. & Kavuri, S.N. (2003a). A review of process fault detection and diagnosis. Part I: Quantitative model-based methods, Computers & Chemical Engineering, 27(3), 293–311.

Venkatasubramanian, V., Rengaswamy, R., Kavuri, S.N. & Yin K. (2003b). A review of process fault detection and diagnosis: Part III: Process history based methods, Computers & Chemical Engineering, 27(3), 327–346.

Vermasvuori, M., Vatanski, N. & Jämsä-Jounela, S-L. (2005). Data-based fault detection of the online analysers in a dearomatization process, In Proceedings of 1st NeCST workshop on Networked Control Systems & Fault Tolerant Control, Sauter, D., Rondeau, E. & Noura, H. (Editors), NeCST, EU-IST-2004-004303, Ajaccio, 219–224.

Vermasvuori, M. (2008). Methodology for utilising prior knowledge in constructing data-based process monitoring systems with an application to dearomatization process, Doctoral dissertation, Helsinki University of Technology, Espoo, 212 p.

Wang, D. & Romagnoli J.A. (2003). Robust model predictive control design using a generalized objective function, Computers and Chemical Engineering, 27(7), 965–982.

Willsky, A.S. & Jones, H.L. (1976). A Generalized Likelihood Ratio Approach to the Detection and Estimation of Jumps in Linear Systems, IEEE Transactions on Automatic Control, 21(1), 108–112.

Witsenhausen, H.S. (1968). A min–max control problem for sampled linear systems, IEEE Transactions on Automatic Control, 13(1), 5–21.

Wold H. (1973). Nonlinear Iterative Partial Least Squares (NIPALS) modeling: some current developments. In Krishnaiah, PR (Editor). Multivariate Analysis, Academic Press, New York, 383–407.

Wold, S., Martens, H. & Wold, H. (1983). The multivariate calibration problem in chemistry solved by the PLS method, in Proceedings of Conference Matrix Pencils, Ruhe A. & Kågstørm, B. (Editors), Lecture Notes in Mathematics, Springer-Verlag, Heidelberg, 286–293.

Wu, F. (2001). LMI-based robust model predictive control and its application to an industrial CSTR problem, Journal of Process Control, 11(6), 649–659.

Zhang, Y.M. & Jiang, J. (2008). Bibliographical review on reconfigurable fault-tolerant control systems, Annual Reviews in Control, 32(2), 229–252.

Zheng, Z.Q. & Morari, M. (1993). Robust stability of constrained model predictive control, In Proceedings of American Control Conference 1993, 379–383.

Zhou, K. & Ren, Z. (2001). A new controller architecture for high performance, robust, and fault-tolerant control, IEEE Transactions on Automatic Control, 46 (10), 2688–2693.

Appendices

Appendix A Description of the integrated fault-tolerant model predictive controller procedures

A.1 Procedure of the FTC strategy for the faults in the sensors of the CVs and DVs by using fault accommodation

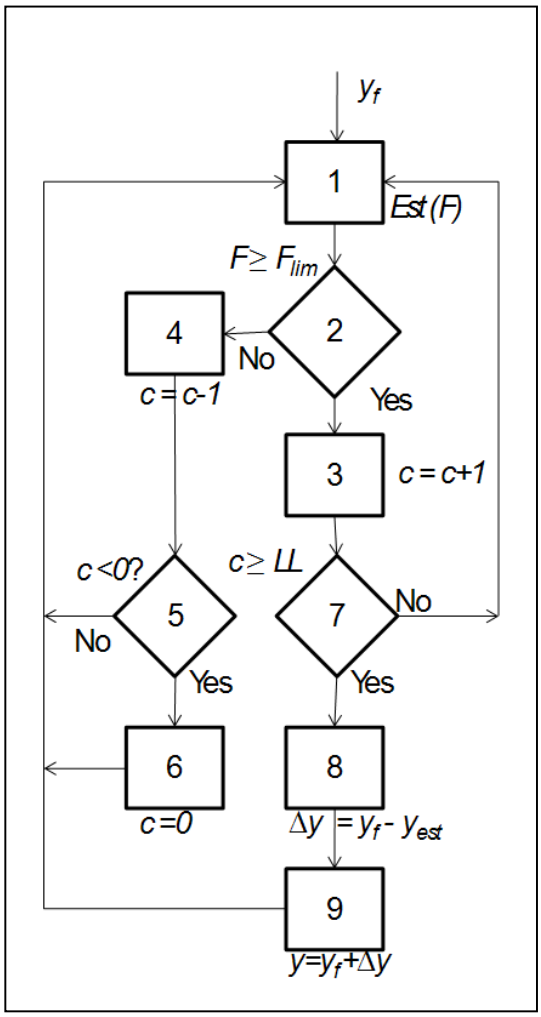

1. Detect and isolate faults by using the PLS-based FDD and determine the value of the fault detection index F

2. Determine if $F \geq F_{lim}$,, if this is true, go to Step 3; if this is untrue, go to Step 4

3. Increase the fault detection delay counter c by one and go to Step 7

4. Decrease the fault detection delay counter c by one and go to back to Step 1

5. If value of the counter c is less or equal to 0, go to Step 6; otherwise go back to Step 1

6. Set the counter c value to 0 and go back to Step 1

7. If value of the counter c is equal or greater than the low limit LL, go to Step 6; otherwise go back to Step 1

8. Estimate the correction value Δy by using the PLS-based FDD, scale the correction values according to the delay counter value (the magnitude of the correction is increased according to the value of c), $\Delta y = y_f - y_{est}$

9. Accommodate the faulty measurement y_f : $y=y_f+\Delta y$, where $\Delta y = y_f - y_{est}$, then go back to Step 1

A.2 Procedure of the FTC strategy for the faults in the sensors of the MVs by using fault accommodation and controller reconfiguration

1. Detect and isolate faults by using the PLS-based FDD and determine the value of the fault detection index F

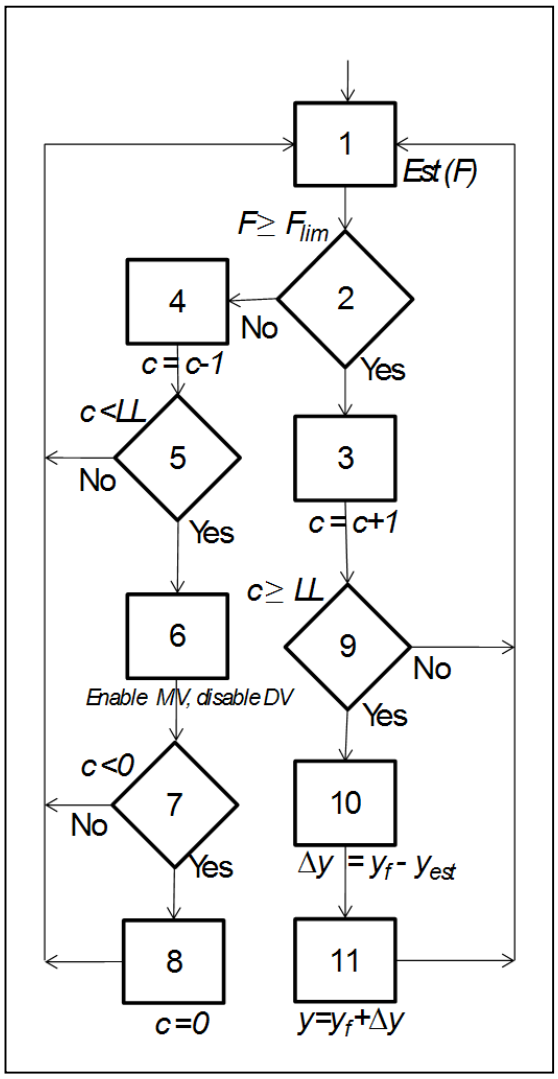

2. Determine if $F \geq F_{lim}$,, if this is true, go to Step 3; if this is untrue, go to Step 4

3. Increase the fault detection delay counter c by one and go to Step 7

4. Decrease the fault detection delay counter c by one and go to Step 5

5. If value of the counter c is below the low limit LL go to Step 6

6. Enable (previously) faulty MV and assign the (previously) activated DV back as a DV, then go back to Step 1

7. If value of the counter c is less or equal to 0, go to Step 8; otherwise go back to Step 1

8. Set the counter c value to 0 and go back to Step 1

9. If value of the counter c is equal or greater than the low limit LL, go to Step 10; otherwise go back to Step 1

10. Estimate the non-faulty measurement values and the correction value $\Delta y = y_f - y_{est}$

11. Move MV to the opposite direction of the fault by the magnitude of Δy, disable the faulty MV (set it as a disturbance variable), and activate one of the DVs as an MV, then go back to Step 1

A.3 Procedure of the FTC strategy for the faults in the actuators of the MVs by using controller reconfiguration

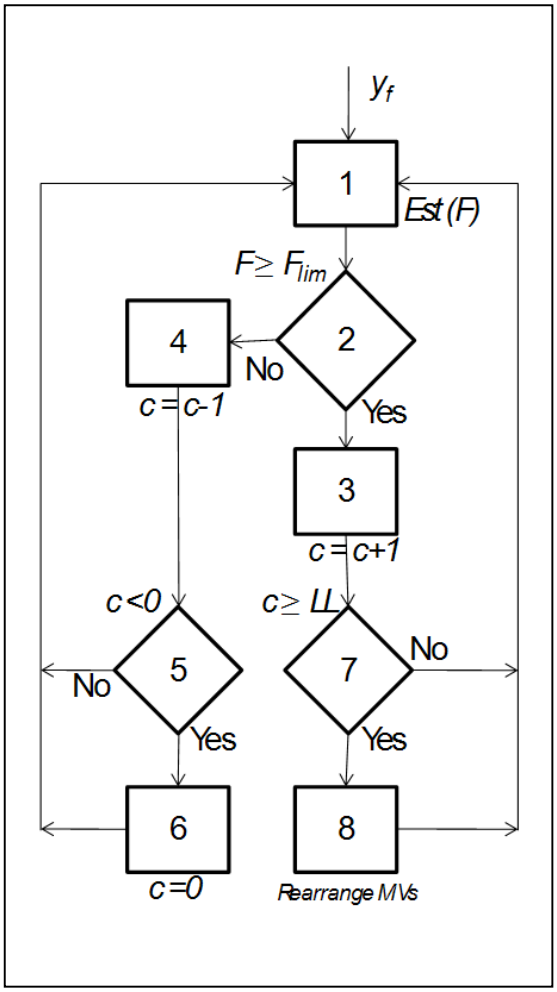

1. Detect and isolate faults by using the residual between the flow measurement value and the MPC setpoint and determine the value of the fault detection index F

2. Determine if $F \geq F_{lim}$,, if this is true, go to Step 3; if this is untrue, go to Step 4

3. Increase the fault detection delay counter c by one and go to Step 7

4. Decrease the fault detection delay counter c by one and go to Step 5

5. If value of the counter c is less or equal to 0, go to Step 6; otherwise go back to Step 1

6. Set the counter c value to 0 and go back to Step 1

7. If value of the counter c is equal or greater than the low limit LL, go to Step 8; otherwise go back to Step 1

8. Disable the MV (set it as a disturbance variable), and activate one of the DVs to become as an MV, then go back to Step 1

Note: Once the MV has been reassigned due to the actuator fault, it needs to be manually set back active if the fault is corrected. This is due to the detection mechanism, which is based on the residual between the setpoint set by the MPC (which is not available if the MV is disabled) and the measurement.

Appendix B Graphical representation of the fault accommodation-based FTC strategy testing on the benchmark process

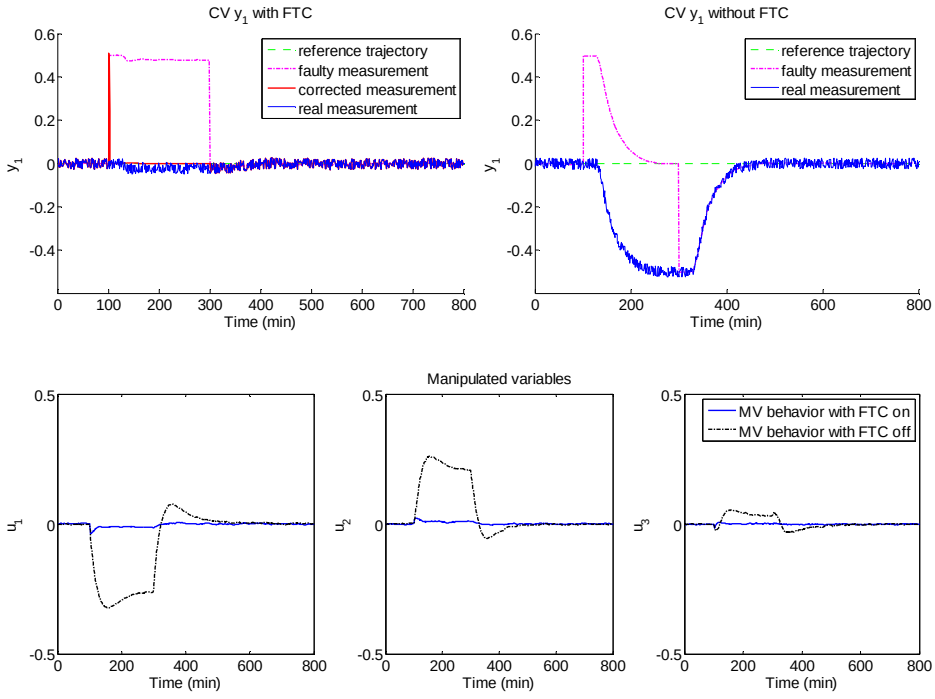

Figure A - 1. The performance of the active fault accommodation-based FTC strategy with the PLS-based FDD in the case of a bias fault in y_1 of the industrial benchmark process.

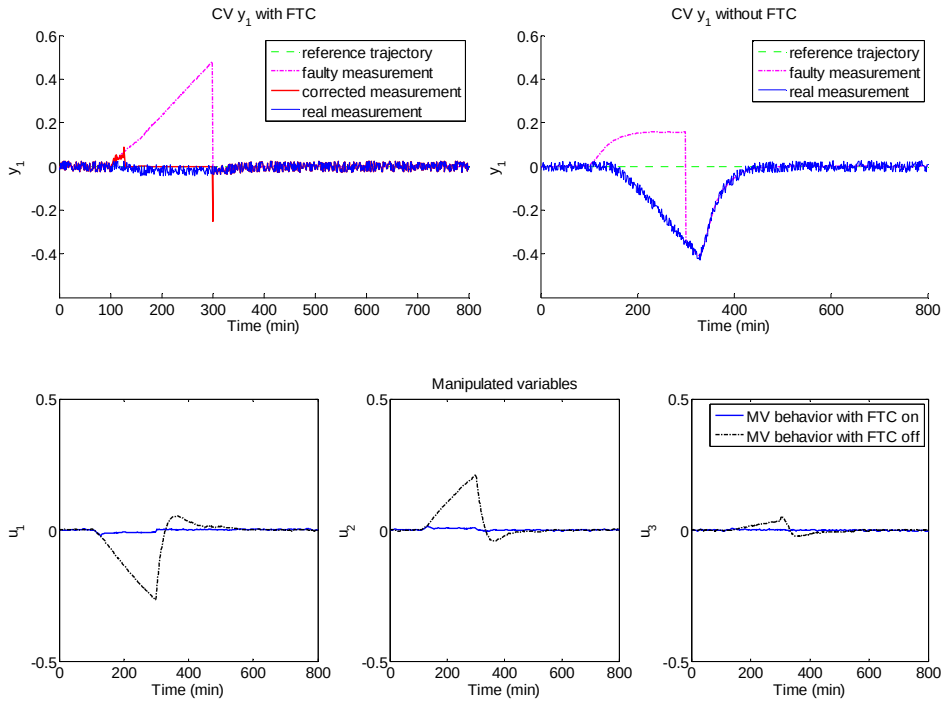

Figure A - 2. The performance of the active fault accommodation-based FTC strategy with the PLS-based FDD in the case of a drift fault in y_1 of the industrial benchmark process.

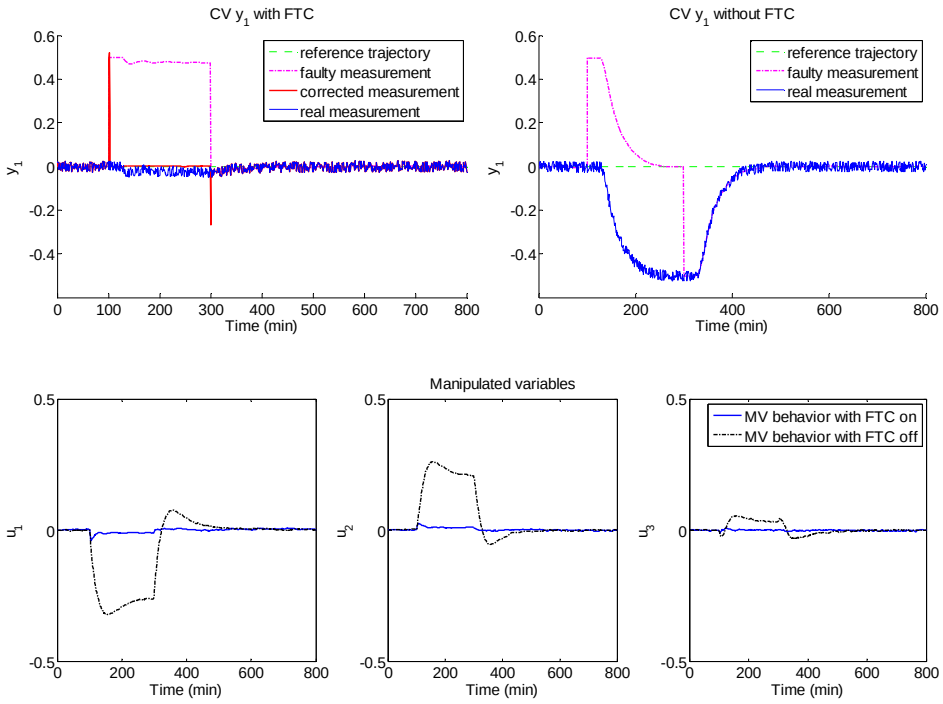

Figure A - 3. The performance of the active fault accommodation-based FTC strategy with the PCA-based FDD in the case of a bias fault in y_1 of the industrial benchmark process.

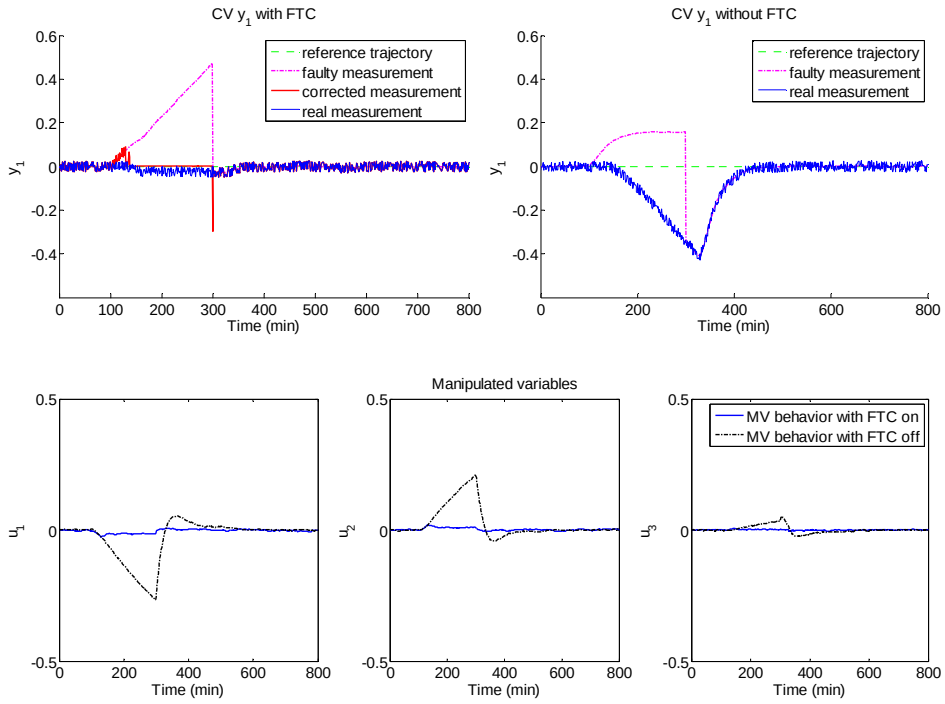

Figure A - 4. The performance of the active fault accommodation-based FTC strategy with the PCA-based FDD in the case of a drift fault in y_1 of the industrial benchmark process.

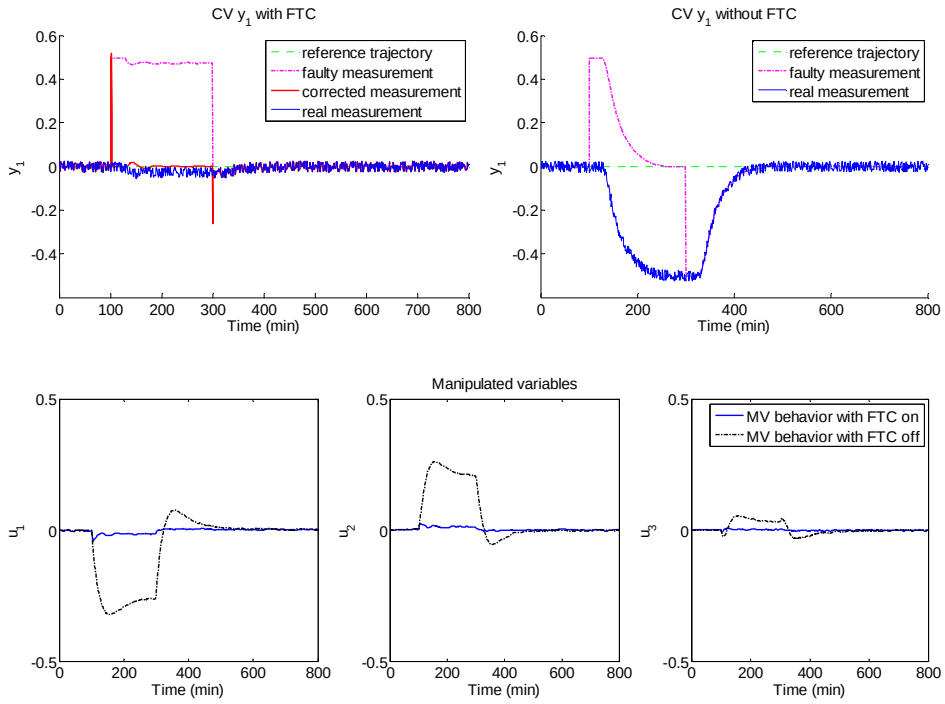

Figure A - 5. The performance of the active fault accommodation-based FTC strategy with the SMI-based FDD in the case of a bias fault in y_1 of the industrial benchmark process.

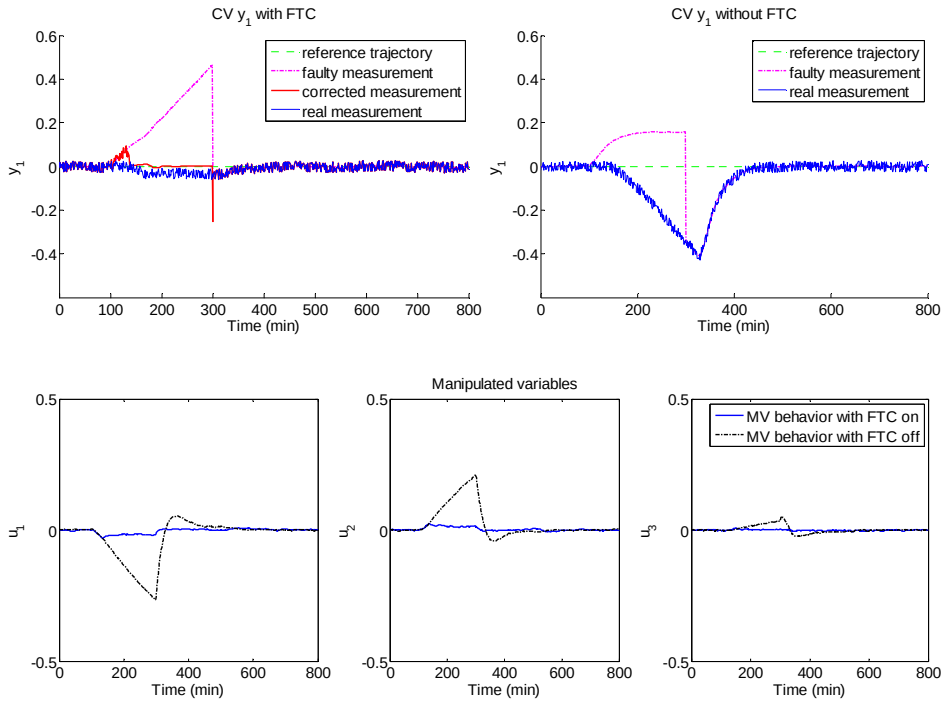

Figure A - 6. The performance of the active fault accommodation-based FTC strategy with the SMI-based FDD in the case of a drift fault in y_1 of the industrial benchmark process.

Appendix C Responses of the ±1%, ±5% and ±10% changes in the inputs (normalised in relation to the standard deviation)

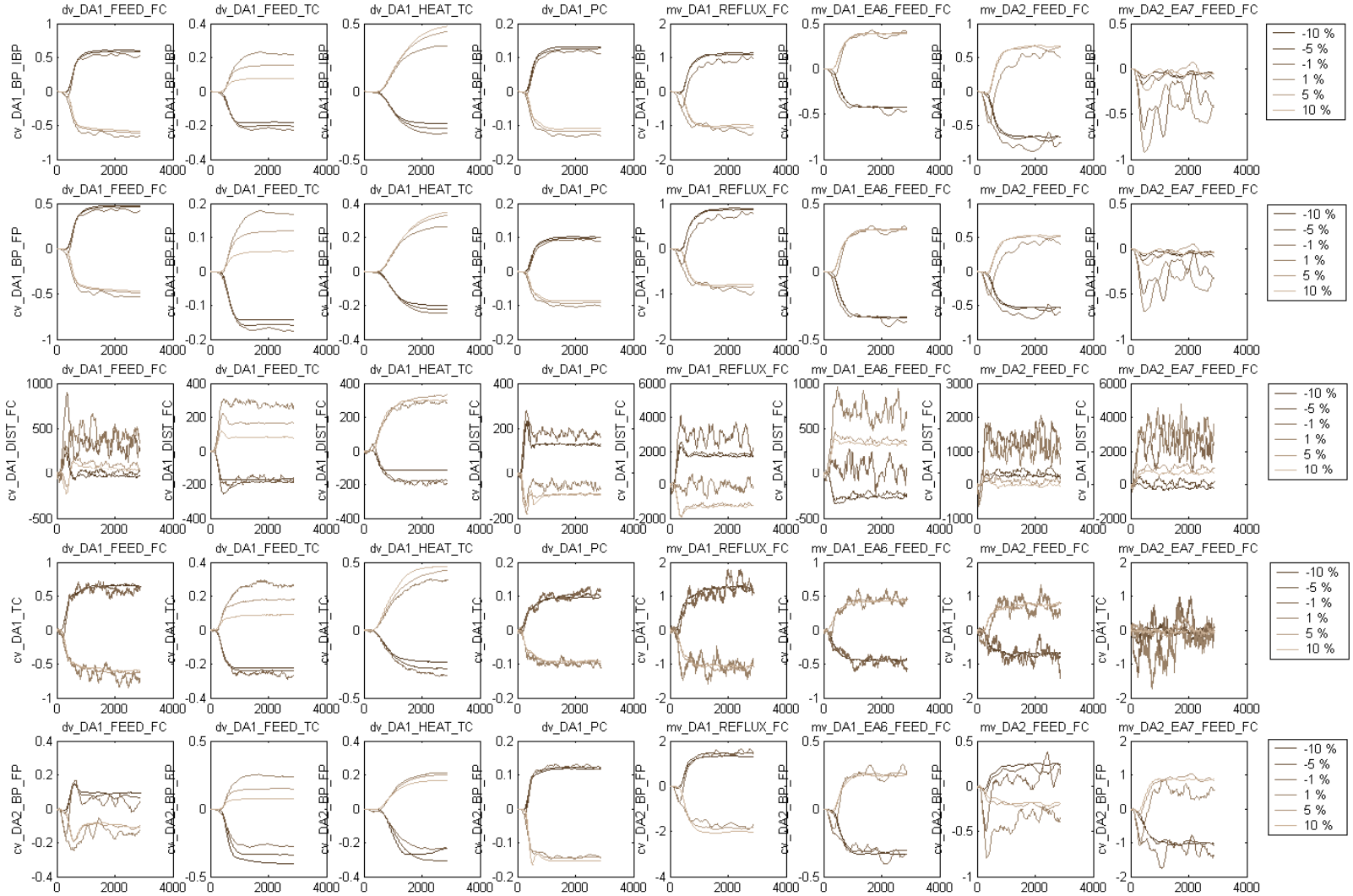

Appendix D Step responses of 5% step changes in the inputs (normalised in relation to the standard deviation)

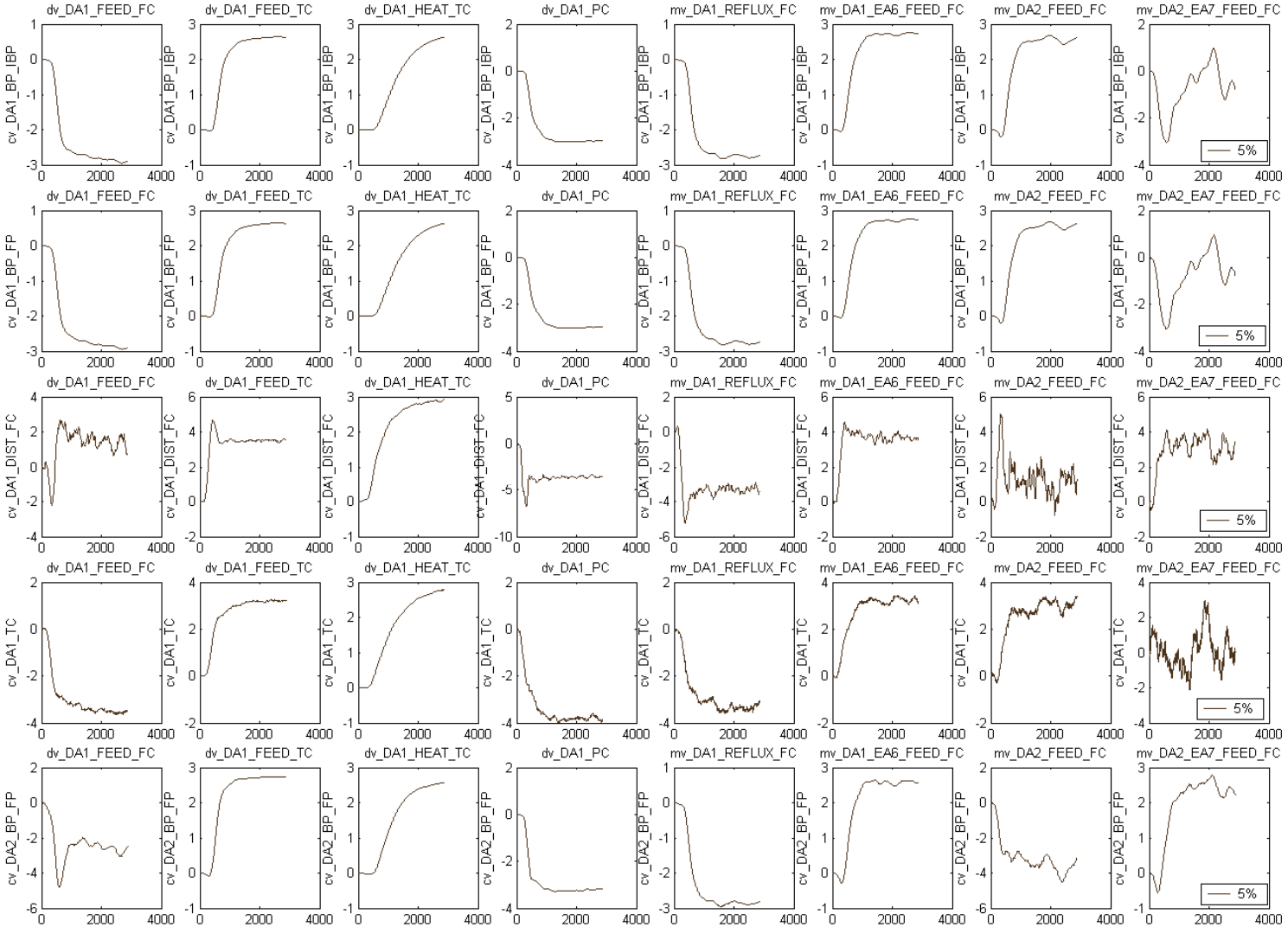

Appendix E Training data for the PLS-based FDD

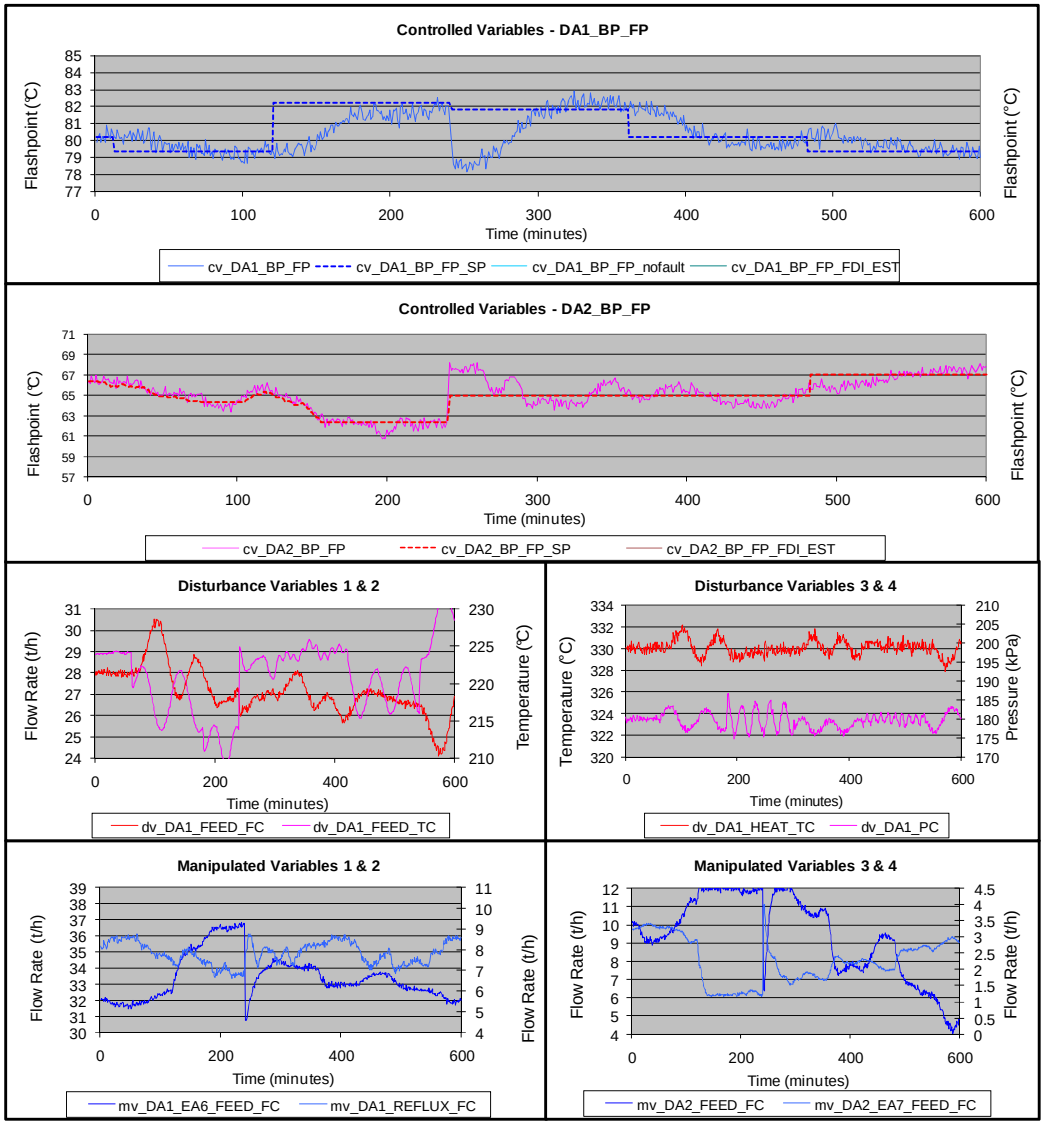

Figure A - 7. The training data for the PLS-based FDD.

ISBN 978-952-60-3200-9
ISBN 978-952-60-3201-6 (PDF)
ISSN 1795-2239
ISSN 1795-4584 (PDF)